

**DEVELOPMENT OF GROUTING METHODOLOGY USING NUMERICAL  
MODELING TO OPTIMIZE RESERVOIR SEEPAGE REDUCTION,  
SPRING HOLLOW DAM, ROANOKE, VIRGINIA**

**ARTHUR LAKES LIBRARY  
COLORADO SCHOOL OF MINES  
GOLDEN, CO 80401**

**by**

**Rose M. Zeiler**

ProQuest Number: 10796655

All rights reserved

INFORMATION TO ALL USERS

The quality of this reproduction is dependent upon the quality of the copy submitted.

In the unlikely event that the author did not send a complete manuscript and there are missing pages, these will be noted. Also, if material had to be removed, a note will indicate the deletion.



ProQuest 10796655

Published by ProQuest LLC (2019). Copyright of the Dissertation is held by the Author.

All rights reserved.

This work is protected against unauthorized copying under Title 17, United States Code  
Microform Edition © ProQuest LLC.

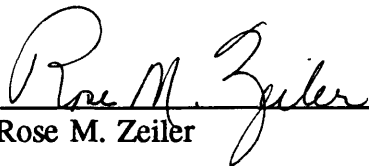
ProQuest LLC.  
789 East Eisenhower Parkway  
P.O. Box 1346  
Ann Arbor, MI 48106 – 1346

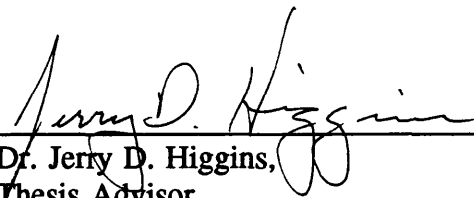
T-4763

A thesis submitted to the Faculty and Board of Trustees of the Colorado School of Mines in partial fulfillment of the requirements for the degree of Doctor of Philosophy (Geological Engineering).

Golden, Colorado

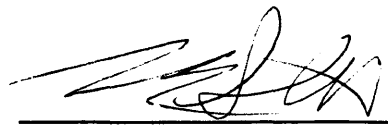
Date 11/13/95

Signed:   
Rose M. Zeiler

Approved:   
Dr. Jerry D. Higgins,  
Thesis Advisor

Golden, Colorado

Date 11/14/95

  
Dr. Roger E. Slatt  
Head, Department of Geology  
and Geological Engineering

## ABSTRACT

Construction of the 12,400 acre-foot capacity Spring Hollow Dam was completed in January, 1994. The reservoir was constructed in Roanoke County, Virginia to meet the drinking water needs of the residents. The site of the dam and reservoir is located within a complex geologic terrain of folded and thrustured Paleozoic carbonates, shales, and siltstones. The reservoir valley, Spring Hollow, is one of several north-south trending valleys which carry water to the Roanoke River.

The carbonates in the area display solution features consistent with karst topography. The fractured and solutioned carbonate beds, striking perpendicular to the valley trend, provide a hydraulic connection between valleys. Initial site investigations indicated that Spring Hollow was a discharge zone. Construction of the reservoir was expected to disturb the hydrogeologic regime, reversing the ground-water gradient and allowing seepage out of the reservoir through the solutioned carbonates along the valley walls. Estimates of seepage out of the reservoir at maximum capacity indicated that a grouting program would be necessary to mitigate seepage losses.

The purpose of this research was to develop a grouting methodology that was based on the use of numerical modeling as a tool. It's applicability is demonstrated in the karst terrain of the site of the Spring Hollow Dam and Reservoir. As an approach to

the grouting program, a grout optimization methodology was developed. This was accomplished by identifying zones of potentially high seepage rates using geological, hydrological, and geomorphological analyses, and numerically simulating the hydrogeologic regime. Numerical modeling was used as a tool to evaluate the potential for seepage from the reservoir, to evaluate grouting alternatives to optimize grouting, to evaluate the effectiveness of the grout, and to predict seepage rates through the reservoir at maximum capacity. Additionally, the numerical modeling methodology includes a performance assessment of the grout curtain under reservoir conditions, and provides a means of evaluating remedial designs.

As demonstrated with field data collected after the partial filling of the reservoir, a grouting methodology using numerical modeling as a tool can be effectively implemented. The grout optimization and seepage reduction objectives of the methodology are validated by the success of the selective grouting program in reducing seepage to an acceptable level under reservoir conditions. Additionally, the reliability, not only of the model, but also of the method, is borne out by the ability of the model to accurately simulate reservoir conditions.

## TABLE OF CONTENTS

	Page
ABSTRACT	iii
LIST OF APPENDICES	ix
LIST OF FIGURES	x
LIST OF TABLES	xiv
LIST OF PLATES	xv
ACKNOWLEDGEMENTS	xvi
Chapter 1. INTRODUCTION .....	1
Chapter 2. PURPOSE AND OBJECTIVES .....	4
Chapter 3. TECHNICAL APPROACH .....	5
3.1 Evaluation of Seepage Potential .....	5
3.2 Evaluation of Grouting Alternatives .....	7
3.3 Evaluation of Grout Effectiveness .....	8
3.4 Prediction of Post-Reservoir Seepage .....	8
3.5 Performance Assessment and Evaluation of Remedial Designs .....	8
Chapter 4. PREVIOUS WORK .....	9
Chapter 5. SITE LOCATION .....	14
Chapter 6. EVALUATION OF SEEPAGE POTENTIAL .....	17
6.1 Site Characterization .....	17
6.1.1 Geology .....	17

6.1.1.1 Lithologies .....	22
6.1.1.2 Soils .....	25
6.1.1.3 Structure .....	26
6.1.2 Site Hydrology .....	27
6.1.2.1 Stream Flow Measurements .....	27
6.1.2.2 Water Budget of Spring Hollow .....	39
6.1.3 Geomorphologic Interpretation .....	42
6.1.3.1 Processes and Climate .....	42
6.1.3.2 Landforms .....	42
6.1.3.3 Drainage Analysis .....	46
6.1.3.4 Vegetation .....	48
6.1.3.5 Anthropogenic Activities .....	50
6.1.3.6 Extension of Geologic Units .....	50
6.1.4 Site Hydrogeology .....	53
6.1.4.1 Aquifer Description .....	53
6.1.4.2 Pre-Grout Ground-water and Surface-Water Interaction .....	54
6.1.4.3 Conceptual Model .....	57
6.2 Delineation of Zones with Seepage Potential .....	60
6.3 Estimation of Seepage Rates .....	67
6.3.1 Analytical Estimate of Seepage Rates .....	67
6.3.2 Numerical Estimate of Seepage Rates .....	72
6.3.2.1 Model Setup and Input Parameters .....	72
6.3.2.2 Calibration and Results .....	76
6.3.2.3 Grout-Effectiveness Piezometers .....	78
<b>Chapter 7. EVALUATION OF GROUTING ALTERNATIVES .....</b>	<b>80</b>
7.1 Test-Grout Program .....	81
7.1.1 Grouting Results .....	81
7.1.2 Ground-Water and Surface-Water Monitoring .....	84

7.2 Evaluation of Grout Impact on Seepage . . . . .	87
7.2.1 Ground-Water and Surface-Water Monitoring . . . . .	89
7.2.2 Numerical Simulation and Prediction . . . . .	91
7.2.2.1 Model Setup and Input Parameters . . . . .	91
7.2.2.2 Calibration and Results . . . . .	94
7.3 Development of Grouting Alternatives . . . . .	95
Chapter 8. EVALUATION OF GROUT EFFECTIVENESS . . . . .	99
8.1 Reservoir-Wide Grouting Program . . . . .	101
8.1.1 Grout and Concrete Volumes . . . . .	101
8.1.2 Ground-Water Monitoring . . . . .	108
8.1.3 Geologic Mapping . . . . .	110
8.2 Effectiveness of Grout . . . . .	116
8.2.1 Qualitative Approach . . . . .	119
8.2.1.1 Ground-Water Monitoring . . . . .	119
8.2.1.1.1 Pre-Grout Monitoring Wells . . . . .	120
8.2.1.1.2 Post-Grout Monitoring Wells . . . . .	124
8.2.1.2 Post Grout Water Table . . . . .	130
8.2.2 Quantitative Approach . . . . .	130
8.2.2.1 Assumptions, Limitations, and Simplifications . . . . .	132
8.2.2.2 Grid Size and Boundary Conditions . . . . .	132
8.2.2.3 Input Parameters . . . . .	137
8.2.2.3.1 Aquifer Depth . . . . .	137
8.2.2.3.2 . . . . .	138
8.2.2.3.3 Anisotropy . . . . .	140
8.2.2.3.4 Recharge . . . . .	141
8.2.3 Pre-Grout Simulation . . . . .	142



8.2.3.1 Calibration Targets . . . . .	142
8.2.3.2 Calibration and Results . . . . .	143
8.2.3.3 Violation of Darcy’s Law . . . . .	148
8.2.4 Post-Grout Simulation . . . . .	151
8.2.4.1 Calibration Targets . . . . .	152
8.2.4.2 Results . . . . .	154
8.2.5 Evaluation of Grout Effectiveness . . . . .	154
Chapter 9. PREDICTION OF POST-RESERVOIR SEEPAGE . . . . .	157
Chapter 10. PERFORMANCE ASSESSMENT . . . . .	159
Chapter 11. SUMMARY OF METHODOLOGY . . . . .	163
11.1 Evaluation of Seepage Potential . . . . .	163
11.2 Evaluation of Grouting Alternatives . . . . .	164
11.3 Evaluation of Grout Effectiveness . . . . .	165
11.4 Prediction of Post-Reservoir Seepage . . . . .	165
11.5 Performance Assessment and Evaluation of Remedial Designs . . . . .	166
Chapter 12. CONCLUSIONS . . . . .	167
Chapter 13. REFERENCES . . . . .	169

LIST OF APPENDICES

	Page
Appendix A. Structural Data . . . . .	172
Appendix B. Data . . . . .	176
Appendix C. Input Files for Numerical Models . . . . .	184
Appendix D. Hydrographs of Selected Wells . . . . .	186

LIST OF FIGURES

	Page
Figure 1. Location of Spring Hollow Dam and Reservoir . . . . .	3
Figure 2. North-South Trending Valleys of the Research Area . . . . .	15
Figure 3. Roller-Compacted-Concrete, Spring Hollow Dam . . . . .	16
Figure 4. Location of Research Area Within Valley and Ridge Physiographic Province . . . . .	18
Figure 5. Stratigraphic Column of Roanoke County, Virginia . . . . .	20
Figure 6. Cross-Section of a Portion of the Upper Roanoke River Valley Area Near the Research Area . . . . .	21
Figure 7. Detailed Geologic map of the Research Area . . . . .	23
Figure 8. Vertical Strata Striking East-West Along the East Dam Abutment . . . .	24
Figure 9. Stream-Bed Elevations Along Dry, Spring, and Cove Hollows . . . . .	28
Figure 10. Sinking Point of Dry Hollow in October, 1992 . . . . .	31
Figure 11. Summary of Weir, Flume, and Rainfall Data for Spring Hollow . . . . .	33
Figure 12. Large Sinkhole Along East Rim of Reservoir . . . . .	43
Figure 13. Schematic of Blankenship Cave in Dry Hollow . . . . .	45
Figure 14. Drainage Analysis of Research Area . . . . .	47
Figure 15. Vegetation Analysis of Research Area . . . . .	49
Figure 16. Bedrock Map of the Reservoir Area Based on Geomorphologic Analysis . . . . .	51

Figure 17. Water Table of the Research Area Reflecting Pre-Grout and Post-Grout Conditions . . . . . 55

Figure 18. Hydrologic System of the Research Area . . . . . 59

Figure 19. Zonation of the Reservoir Based on Gradient Reversal Under Conditions of the Reservoir at Maximum Capacity . . . . . 62

Figure 20. Zonation of the Reservoir Based on the Presence of Karst Features . . . . . 63

Figure 21. Zonation of the Reservoir Based on the Degree of Drainage Dissection . . . . . 65

Figure 22. Seepage Potential Map of the Reservoir . . . . . 66

Figure 23. Cross-Section Through the High-Solution Zone From Spring Hollow to Dry Hollow . . . . . 68

Figure 24. Geology of the High-Solution Zone Modeled for an Estimate of Seepage . . . . . 71

Figure 25. Model Grid Used For a Numerical Estimate of Seepage Rate Through the High-Solution Zone . . . . . 74

Figure 26. Simulated Pre-Grout and Post-Grout Heads of the High-Solution Zone . . . . . 77

Figure 27. Locations of Grout Holes at the Test-Grout Site . . . . . 82

Figure 28. Area of the Test-Grout Program . . . . . 83

Figure 29. Geologic Cross-Section of the Test-Grout Program Area . . . . . 85

Figure 30. Hydrologic and Grout Data Recorded During the Test-Grout Program . . . . . 90

Figure 31. Test-Grout Program Numerical Model Grid and Boundary Conditions . . . . . 92

Figure 32. Selected Grout Zones for Reservoir-Wide Grout Program . . . . . 100

Figure 33. Grout Volumes in Grout Zone 1 .....	102
Figure 34. Grout Volumes in Grout Zone 2 .....	104
Figure 35. Grout Volumes in Grout Zone 3 .....	105
Figure 36. Grout Volumes in Grout Zone 4 .....	106
Figure 37. Grout Volumes in the Pond Spring Grout Zone .....	107
Figure 38. Pre-Grout Water Table of the Research Site .....	109
Figure 39. Geologic Cross-Section A .....	111
Figure 40. Geologic Cross-Section B .....	112
Figure 41. Geologic Cross-Section C .....	113
Figure 42. Geologic Map Produced During the Reservoir-Wide Grout Program .....	114
Figure 43. Photograph Along the East Dam Abutment Displaying Fracture Set J-6 .....	117
Figure 44. Base of Colluvial/Residual Material in Dry Hollow .....	118
Figure 45. Hydrographs of Wells R3 and G1 .....	121
Figure 46. Hydrographs of Wells R1 and R2 .....	122
Figure 47. Hydrographs of Well B20 and the Doyle Well .....	123
Figure 48. Hydrograph of Wells G4 and G5 .....	125
Figure 49. Hydrograph of Wells G6 and G7 .....	126
Figure 50. Hydrograph of Wells P2 and P3 .....	128
Figure 51. Hydrograph of Wells P4 and P5 .....	129

Figure 52. Water-Table Map Reflecting the Rise in Water Levels Related to the 1992 and 1993 Reservoir-Wide Grouting Activities .....	131
Figure 53. Reservoir-Wide Numerical Model Grid and Boundary Conditions for Layer 1 .....	133
Figure 54. Reservoir-Wide Numerical Model Grid and Boundary Conditions for Layer 2 .....	134
Figure 55. Pre-Grout Simulated Water-Table Map .....	146
Figure 56. Calibrated Hydraulic Conductivity Zones for Layer 2 .....	147
Figure 57. Post-Grout Simulated Water-Table Map .....	155

## LIST OF TABLES

	Page
Table 1. Boreholes and Wells Located Within the Research Area . . . . .	10
Table 2. 1985 Stream and Spring Flow Data for the Research Area . . . . .	29
Table 3. 1987 Stream and Spring Flow Data for the Research Area . . . . .	34
Table 4. 1989 Stream and Spring Flow Data for the Research Area . . . . .	35
Table 5. Estimation of Potential Evapotranspiration Using the Modified Thornwaite Method . . . . .	40
Table 6. Grout Volumes per Grouthole, Test-Grout Program . . . . .	86
Table 7. Seepage Through Carbonates A, B, and C at Various Grout Curtain Hydraulic Conductivities with the Reservoir at the 1410-Foot Elevation . . . . .	97
Table 8. Comparison of Pre-Grout Target Heads with Simulated Heads . . . . .	144
Table 9. Reynold's Number Calculations for Determination of Flow Conditions . . . . .	150
Table 10. Comparison of Post-Grout Target Heads with Simulated Heads . . . . .	153
Table 11. Comparison of 1275-Foot Reservoir Target Heads with Simulated Heads . . . . .	160

LIST OF PLATES

Plate 1. Features Map of the Research Site, Spring Hollow  
    Dam and Reservoir ..... Pocket



## ACKNOWLEDGEMENTS

The author wishes to express heartfelt gratitude to her husband, Rick Johnson, and her children, Tazwell and Johanna, for the love and support that saw her through this long process, and for their unwavering faith in her ability. Gratitude goes also to Mal Johnson, for the fabulous Blue Lightning that made modeling runs alot faster.

The author thanks Dr. Gordon Matheson, a member of her committee, whose efforts were responsible for the modeling methodology remaining a part of the Spring Hollow Dam and Reservoir project, and whose technical support was invaluable in the completion of this research. The author also wishes to thank Dr. Matheson for the memorable trips by small aircraft which he piloted to and from the site.

The author expresses gratitude to Dr. Jerry Higgins for first piquing her interest in geological engineering through two excellent courses on the subject, and who encouraged her to seek an advanced degree in geological engineering. Gratitude is also expressed to Dr. Higgins for serving as her advisor, for providing counsel throughout her graduate years, and for his efforts in seeking financial assistance. The author thanks Colorado School of Mines for financial support, including a Colorado Fellowship, a research assistantship and a teaching assistantship.

The author extends appreciation to Dr. Karl Nelson who served on her committee and whose interest and technical support was much appreciated; Dr. Ken Kolm who served on her committee and who took the time to provide guidance during the course of this research; and Dr. Ron Cohen who served on her committee.

The author thanks Dr. Anne Clift and Judith Schenk for their support and encouragement. The author also acknowledges Schnabel Engineering Associates, Inc. for opportunities to visit the site, and access to data.

## Chapter 1

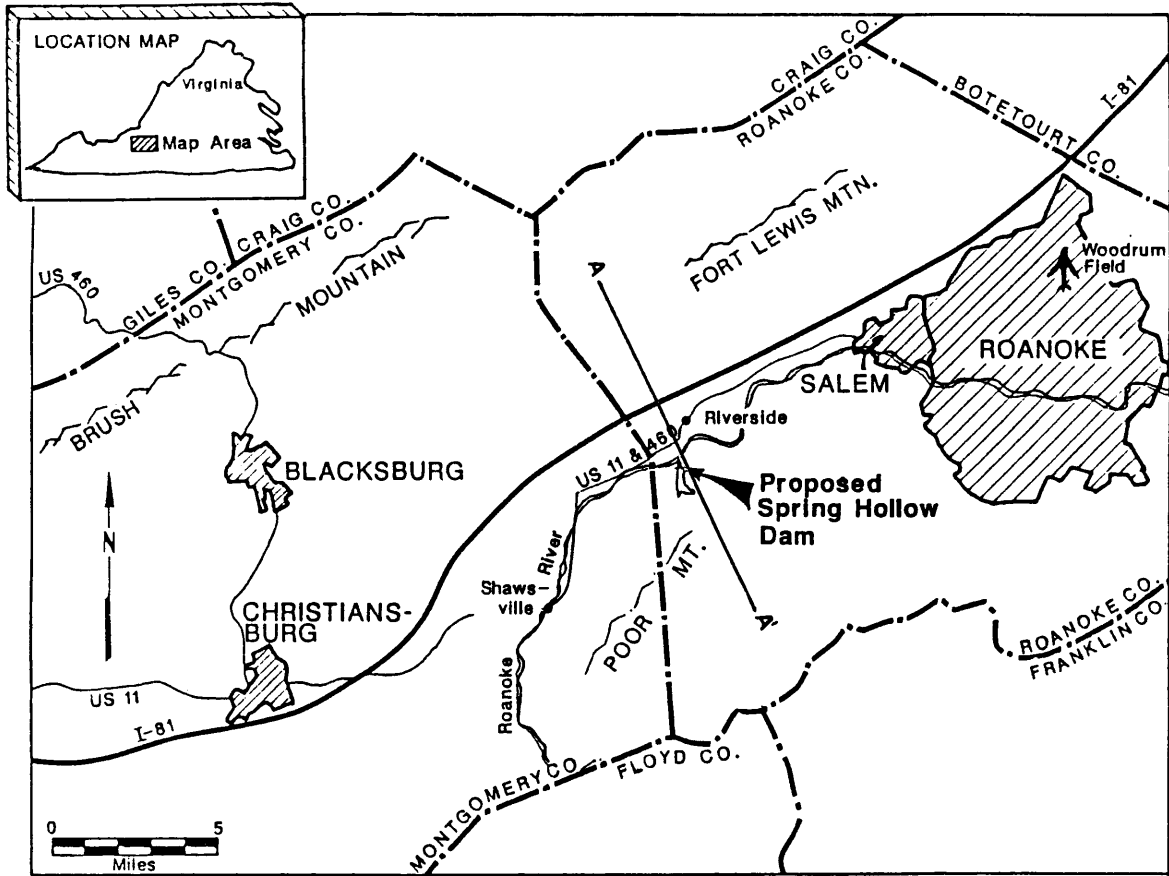
### INTRODUCTION

To meet the water supply needs of the people of Roanoke County, Virginia, the Spring Hollow dam and reservoir, a pump storage facility, was constructed in Spring Hollow, Roanoke County (Figure 1). Construction of the 243-foot high roller-compacted-concrete dam was completed in September, 1993. The reservoir was designed to hold up to 12,400 acre-feet of water.

The Spring Hollow Reservoir, by virtue of its location in an area known to contain karst features, was expected to be subject to significant seepage losses. Seepage occurs in all reservoirs, however, if the seepage is excessive, the reservoir may not hold water at the design capacity. Grouting is often used to reduce seepage. Grouting in carbonates with solution features, such as sinkholes and caves, may be extensive, since large volumes of grout may be required to fill the cavities in the rock. Additionally, solution features in carbonates occur at random along fractures. For these reasons, grouting in karst terrain is an expensive and uncertain undertaking. A method of grout optimization, seepage prediction and remedial evaluation is desirable.

Estimates of potential seepage rates from the Spring Hollow Reservoir at maximum reservoir pool elevation were unacceptably large indicating the necessity for

preventive measures. In order to reduce the potential seepage, a grouting program was carried out in phases from 1991 through 1993. A method of identifying optimal grouting alternatives and assessing the effectiveness of the grouting program in reducing reservoir seepage losses was developed.



(From SEA, 1989)

Figure 1

Location of Spring Hollow Dam and Reservoir

## Chapter 2

### PURPOSE AND OBJECTIVES

The purpose of this research was to develop a grouting methodology that is based on the use of numerical modeling as a tool. Its applicability is demonstrated in the karst terrain of the Spring Hollow Dam and Reservoir site. More specifically, this methodology is described by the following objectives:

- 1) Evaluate the potential for seepage from the reservoir;
- 2) Evaluate grouting alternatives to reduce reservoir seepage while optimizing grouting;
- 3) Evaluate grout effectiveness;
- 4) Predict post-reservoir seepage; and
- 5) Develop a working model for use as a performance-assessment and remedial-design tool.

The contribution of this research is the demonstration that numerical modeling can be used to establish whether the magnitude of potential seepage warrants a grouting program, to assess the effectiveness of a grouting program, and to optimize a grouting program. The results of the research is the development of guidelines for the utilization of numerical modeling as a design tool to predict reservoir seepage losses and evaluate seepage minimization strategies. An additional benefit of this research is the

demonstration that numerical modeling can be used to help design monitoring well locations for installation during the grouting program. It will be shown that strategically placed monitoring wells can be used in place of grout curtain drilling and packer testing to analyze the effectiveness of the grout curtain and can provide guidance when sufficient grouting has been completed.

## Chapter 3

### TECHNICAL APPROACH

#### 3.1 Evaluation of Seepage Potential

A review of the literature relating to grouting practices and approaches was undertaken. Additionally, a review of literature pertaining to the site was conducted including unpublished literature generated during the characterization of the site and the construction of the dam and reservoir.

The site was characterized geologically, hydrologically, and geomorphologically to develop a hydrogeological conceptual model using available data, including that collected by Schnabel Engineering Associates (SEA) during a series of field activities. The available data included borehole and well logs, geologic maps, aerial photography, stream and spring flow measurements, and monitoring well water-level measurements. The products of this characterization were a conceptual model of the hydrogeologic regime and a geologic map of the area surrounding the reservoir valley, which was based on an integration of the geomorphological interpretation and the previously mapped Spring Hollow geology (SEA, 1989). The map represents an extension of the lithologic units from the reservoir valley into the adjacent valleys.

Using analytical and numerical models, the post-reservoir seepage rates along the perimeter of the reservoir with the highest occurrence of solution features were estimated.



These estimates were used to evaluate whether seepage losses would be great enough to warrant mitigation through grouting. The numerical model was used also to predict post-grout heads for optimal placement of upgradient piezometers.

The site was classified according to seepage potential. Using the components of the site characterization and a series of overlays, a rating system for seepage potential was developed, and the site was zoned according to potential for high, medium, and low seepage rates. The product of the zonation was a seepage potential classification map of the reservoir and reservoir perimeter.

### 3.2 Evaluation of Grouting Alternatives

Grouting alternatives were evaluated through a numerical simulation of two zones of highest seepage potential. This second, simplified model was based on data collected during a test-grout program conducted by SEA in 1991 (SEA, 1991a) and included most of the eastern half of the reservoir. The model was used to simulate the impact of the grout curtain at various effective hydraulic conductivities. The impact of grouting was related to percent reduction in seepage and zones for grouting were selected to achieve an acceptable seepage rate while minimizing grouting (SEA, 1991b). This evaluation provided a basis for development of a reservoir-wide grouting plan. All supporting data were provided by the author, however the plan itself was prepared by SEA.

### 3.3 Evaluation of Grout Effectiveness

A three-dimensional numerical model of the reservoir valley and the adjacent valleys was developed to evaluate the effectiveness of the grouting program. Pre-grout conditions were simulated, and the model was calibrated to pre-grout ground- and surface-water data. Post-grout conditions were then simulated, and model verification was performed. The effect of the grout curtain on the hydrogeologic regime was evaluated.

### 3.4 Prediction of Post-Reservoir Seepage

Based on the calibrated site-wide model, a working model was developed that was used to predict seepage at various elevations of the grouted reservoir. The reservoir was simulated at elevations of 1375 feet, 135 feet below the ultimate reservoir elevation, and 1410 feet, the maximum reservoir pool elevation. Seepage rates were predicted for these two scenarios.

### 3.5 Performance Assessment and Evaluation of Remedial Designs

Although the reservoir has not yet been filled to capacity, a preliminary performance assessment was conducted to reflect conditions through the first half of 1994 reflecting an average reservoir pool elevation of 1275 feet. Additionally, the working model can be used to evaluate remedial designs, as necessary, prior to implementation.

## Chapter 4

### PREVIOUS WORK

Several field investigations of the site were carried out by SEA beginning in 1984 during the development stages and continuing through the construction of the dam and reservoir in 1993. The researcher was associated with SEA from 1988 to the present and was involved with the reservoir and dam project throughout that time.

In 1984 and 1985, SEA conducted a preliminary geotechnical investigation of the site in order to characterize its suitability for a dam and reservoir (SEA, 1985). During this investigation monitoring wells were installed, and exploratory boreholes drilled. Details of these boreholes and monitoring wells are presented in Table 1. The locations are shown on Plate 1. An outcrop map was produced from preliminary geologic mapping of the site. Additionally, some ground-water and surface-water monitoring was conducted.

A second field study expanding on the first was undertaken by SEA in 1986 and 1987 (SEA, 1987, Martin and Milner, 1988). For the purpose of detecting subsurface solution features and their impact on the hydrology of the system, stream and spring flows were recorded, a fracture-trace analysis was performed, additional boreholes were drilled

Table 1  
Well and Borehole Data of the Research Area

Well Borehole	Year of Drilling/ Installation	Elevation (Feet)	Total Depth		Unconsolidated Material to Depth Below GS (Feet)	Screened Interval Elevation (Feet)	Lithology	RQD %	Recovery %	Type of Aquifer
			Below GS (Feet)	GS to Bottom (Feet)						
B1	1984	1185.1	110.9	1134.1-1154.1	Ls	90	100	100	Flowing Artesian	
B2, B2A-E	1984	1419.7	26.5	C:26.5	NA	NA	NA	NA	NA	
B3	1984	1219.6	87.6	R:4.5	NA	NA	NA	NA	NA	
B4	1985	1211.8	50	R:9.1	Standpipe to 1162	Dolo/Ls	32-76	93-100	Water Table	
B5	1984	1240.3	60.1	R:60.1	Standpipe to 1180	R	NA	NA	Water Table	
B6	1984	1273.4	50	R: 2.2	1223.4-1233.4	Dolo	80-100	96-100	WT/Perched	
B7	1984	1441	206	C:130.1, R:206	Standpipe to 1334?	R	NA	NA	WT/Perched	
B8, B8A	1985	1475.8	105	C/R:100.6	Standpipe to 1375	RC/Siltst	0	53-59	Dry	
B9	1985	1306.5	67.4	R:7.9	1258.5-1268.5	Dolo	0	4	Water Table	
B10	1985	1320.3	49.2	R:5.0	1271.7-1281.7	Ls	25-100	47-100	Artesian	
B11	1985	1252.2	50	R:4.0	Open	Ls/Dolo	0-94	98-100	Water Table	
B12	1985	1370.5	40.7	R:2.9	1340.5-1360.5	Siltst	14-66	33-100	Flowing Artesian	
B13	1985	1351.5	67.3	R:11.1	1284.5-1314.5	Dolo/Ls	0-57	21-87	Perched	
B14	1985	1406.7	55.2	R:4.5	Standpipe to 1378.9	Dolo	0-28	25-90	Perched	
B15	1985	1325	100.7	R:13	NA	NA	NA	NA	NA	
B16	1985	1272.6	100	R:16	Standpipe to 1172.6	Mar Sh	97	Apr-00	Water Table	
BRW1	1985	1475.8	32.5	R:32.5	NA	NA	NA	NA	NA	
BRW2	1985	NA	35.5	R:35.5	NA	NA	NA	NA	NA	
BRW3	1985	NA	14.1	R:14.1	NA	NA	NA	NA	NA	
BRW4	1985	NA	45.5	R:45.5	NA	NA	NA	NA	NA	
BRW5	1985	NA	14.5	C:9.0, R:14.5	NA	NA	NA	NA	NA	
BRW6	1985	NA	14	C:14.0	NA	NA	NA	NA	NA	

(continued)

Table 1 (continued)

Well Borehole	Year of Drilling/ Installation	Elevation (Feet)	Total Depth		Unconsolidated Material to Depth Below GS (Feet)	Screened Interval Elevation (Feet)	Lithology	RQD %	Recovery %	Type of Aquifer
			Below GS (Feet)	GS to Bottom						
BRW7	1985	NA	15.5	NA	C:15.5	NA	NA	NA	NA	NA
BRW8	1985	NA	5.3	NA	R:5.3	NA	NA	NA	NA	NA
BRW9	1985	NA	3.3	NA	R:3.3	NA	NA	NA	NA	NA
B16ABC	1986	1250	133	NA	R/C:8.0	NA	NA	NA	NA	NA
B14A	1989	1407	200	1207-1237	R:18	Var/Mar Sh	75-100	100	Water Table	Water Table
B16D	1989	1275.9	100	1175.9-1205.9	R/C:10.0	Sh/Ls	62-100	82-100	Water Table	Water Table
B17A	1989	1394.4	200	1184.4-1214.4	R:0, C:0	Ls	60-95	100	Water Table	Water Table
B18	1989	1454.6	57.2	R:2.2	R:2.2	Standpipe to 1417.1	Dolo/Ls	0-4	15-95	Perched?
B19	1989	1270.8	100	R:5.0	R:5.0	1170.8-1200.8	Var Sh	60-100	100	Water Table
B20	1989	1315	120	R:10.0	R:10.0	1195-1225	Ls	100	100	Water Table
R1	1989	1593.1	375	R:20.0	R:20.0	1263.1-1283.1	Ls	NA	NA	Water Table
R2	1989	1501	385	R:20.0	R:20.0	1116-1136	Ls	NA	NA	Water Table
R3	1989	1650	405	NA	NA	1227.5-1247.5	Ls	NA	NA	Water Table
DH1	1989	1401	70	A:32, R:52	A:32, R:52	1331-1351	Sh	NA	NA	Water Table
Q1	1989	1246	50	R:5.0	R:5.0	1196-1216	Ls	44-70	100	Water Table
G1	1991	1442.3413	201	R:4.0	R:4.0	1239.4-1259.4	Mar Sh/Dol	31-56	100	Water Table
G2	1991	1453.4139	215	R:14.0	R:14.0	1238.1-1258.1	Sh/Ls	"6-83	100	Perched?
G3	1991	1440.3955	201	R:7.3	R:7.3	1239.4-1259.4	Sh	98	100	Perched?
G4	1992	1515.1	327	R:8.0	R:8.0	1188.1-1224.1	Dolo	NA	NA	Water Table
G5	1992	1470.2	337	R/C:105	R/C:105	1133.2-1230.2	Dolo	NA	NA	Water Table
G6	1992	1462.1	287	C:70	C:70	1176.1-1226.1	Sh	NA	NA	Water Table
G7	1992	1415	NA	NA	NA	NA	NA	NA	NA	NA
G8	1992	1415	NA	NA	NA	NA	NA	NA	NA	NA
P1	1993	1576.68	375	NA	NA	NA	Sh	NA	NA	Perched

(continued)

Table 1 (continued)

Well Borehole	Year of Drilling/ Installation	Elevation (Feet)	Total Depth		Unconsolidated		Elevation (Feet)	Lithology	RQD %	Recovery %	Type of Aquifer
			Below GS (Feet)	GS to Depth (Feet)	Material to Depth Below GS (Feet)	Screened Interval					
P2	1993	1518.19	265	NA	NA	NA	Sh	NA	NA	NA	Water Table
P3	1993	1612.81	425	NA	NA	NA	NA	NA	NA	NA	Water Table ?
P4	1993	1499.08	291	C:271	NA	NA	C/Sh	NA	NA	NA	Water Table
P5	1993	1459.86	240	C:190	NA	NA	C/Sh	NA	NA	NA	Water Table
P6	1993	1640.28	325	NA	NA	NA	Sh	NA	NA	NA	Water Table
NA: Not Available or GS: Ground Surface C: Colluvium Sh: Shale Ls: Limestone R: Residuum A: Alluvium Mar: Maroon Dolo: Dolomite Siltst: Siltstone											

(Table 1, Plate 1), and water-pressure tests, tracer tests, and an electromagnetic survey were conducted.

A third field investigation in 1989 was carried out by SEA (SEA, 1989) as part of the design phase. A number of water-level monitoring wells were installed and boreholes drilled (Table 1, Plate 1). In addition, in situ permeability tests, rock mass modulus, and point-load strength tests, geophysical borehole logging, installation of surface-water monitoring equipment, geologic mapping, geotechnical investigatory drilling, and ground-water and surface-water monitoring were conducted. A revised geologic map of Spring Hollow was produced.

In 1991, a test-grout program was conducted (SEA, 1991a). In 1992, SEA supervised the grouting of the reservoir and the construction of the roller-compacted-concrete dam (SEA, 1992a, 1992b, 1992c, 1992d, 1992e). The construction of the dam was completed in 1993, and additional grouting along the reservoir perimeter was performed in late 1993 (SEA, 1994a).

## Chapter 5

### SITE LOCATION

The reservoir valley, Spring Hollow, is situated along the Roanoke River in west central Roanoke County, west central Virginia (Figure 1). The research area, shown in Figure 2, contains three north-south trending valleys with streams that flow to the Roanoke River. The topography contains karst features, is rugged and heavily forested, with elevations ranging from 1160 feet to almost 1700 feet in the immediate area. The drainage basin of Spring Hollow, the reservoir valley, is approximately 540 acres.

The 243-foot-high RCC dam, pictured in Figure 3, at maximum capacity will hold the reservoir at elevation 1410 feet circumscribing an area of 158 acres, and holding 3.2 billion gallons of water. Five pumps have the capacity to pump 80 million gallons per day (mgd) into the reservoir from the Roanoke River.



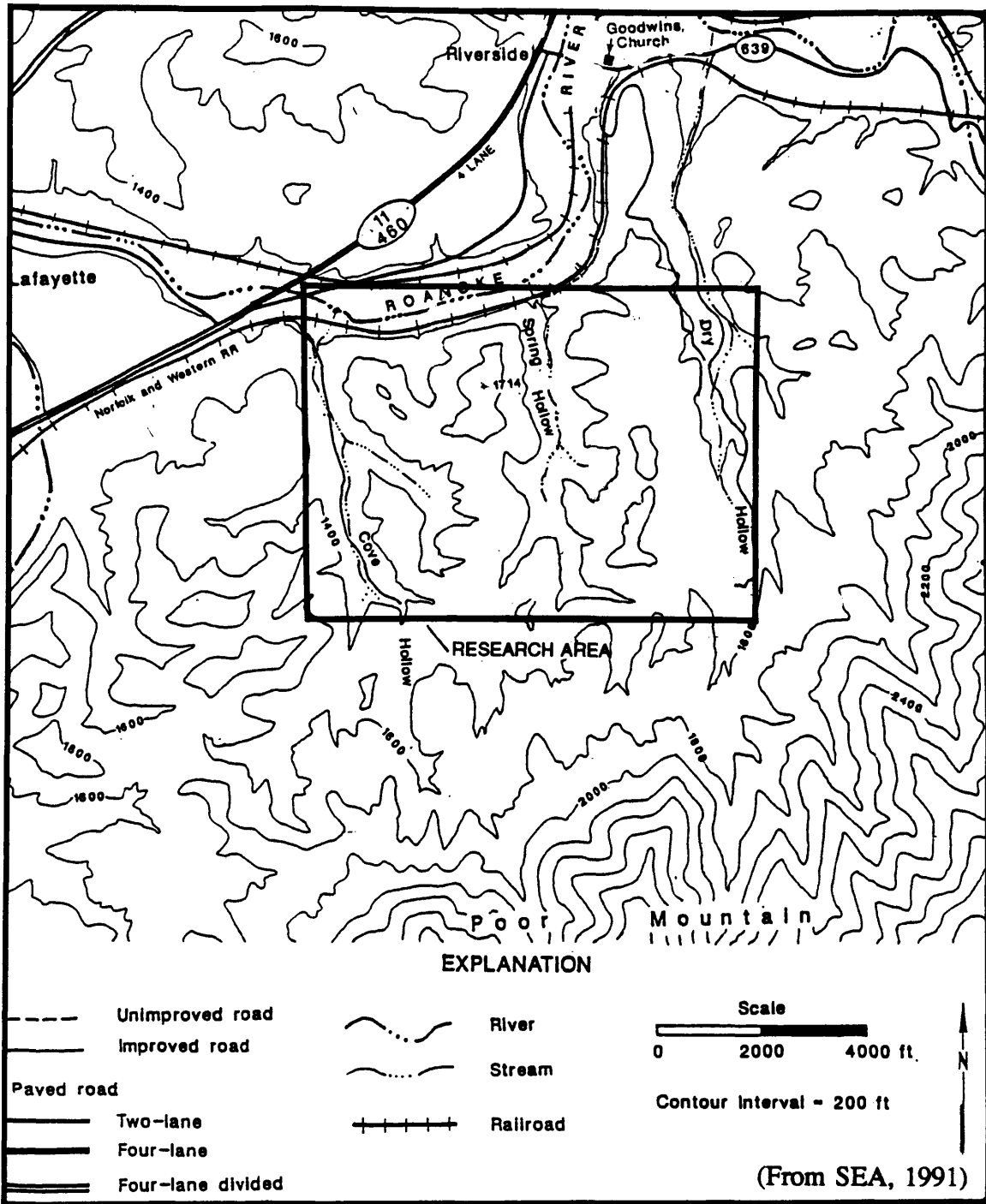


Figure 2

North-South Trending Valleys of the Research Area



Figure 3  
Roller-Compacted-Concrete Spring Hollow Dam

## Chapter 6

### EVALUATION OF SEEPAGE POTENTIAL

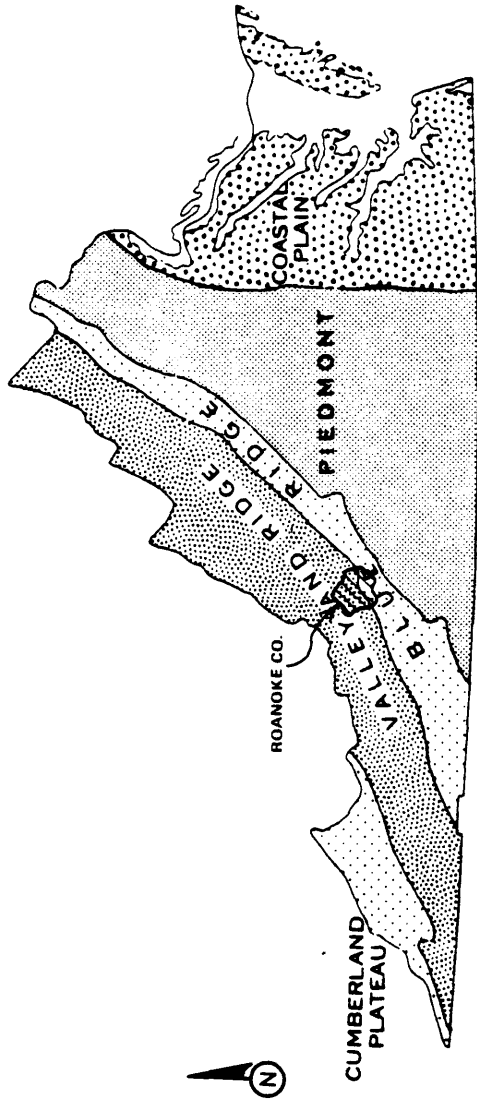
The major obstacle to the successful construction of a dam and reservoir in karst terrain is excessive seepage. In order to determine whether potential seepage losses presented a significant risk, an evaluation of the seepage potential of Spring Hollow was completed. The evaluation included hydrogeological conceptualization through site characterization, and an estimate of post-reservoir seepage rates based on the results of analytical and numerical models of an area of the reservoir with the highest occurrence of solution features.

#### 6.1 Site Characterization

The research area includes the reservoir valley and extends to the two adjacent streams, Cove Hollow and Dry Hollow (Figure 2, Plate 1). In order to build a conceptual model, the site was characterized geologically, hydrologically, and geomorphologically.

##### 6.1.1 Site Geology

Roanoke County is within the Valley and Ridge Physiographic Province at the hinge point between the southern and northern Appalachians (Figure 4) and is dominated by the compressive tectonics characteristic of this region. The site is within the upper



(From Breeding and Dawson, 1976)

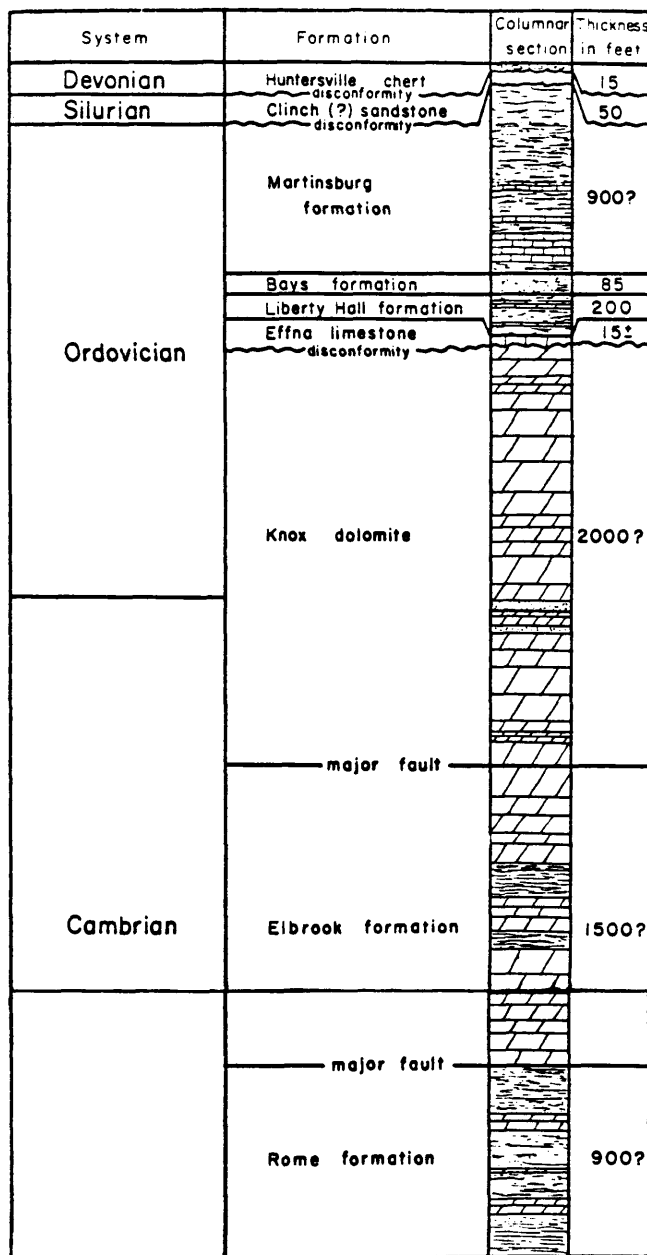
Figure 4

Location of Research Area Within the Valley and Ridge Physiographic Province of Virginia

Roanoke River Valley Area, which was mapped in 1959 (Edwards, 1959). The lithologies of the area include Lower Paleozoic carbonates and shales with some sandstone (Figure 5). Although not shown in Figure 5, pre-Rome formations include Lower and Middle Cambrian clastic and carbonate rocks, and PreCambrian metamorphic rocks (Edwards, 1959). A cross-section (Breeding and Dawson, 1976), shown in Figure 6, indicates that the area contains a number of major thrust faults that have displaced stratigraphy, thrusting younger rocks on top of older.

The research site is located on the Max Meadows Thrust Fault, a sheet comprised solely of the Cambrian Rome Formation (Figure 6). It is comprised of drag folds and minor thrust faults (Edwards, 1959, Amato, 1974), which repeat the section. Underlying the Max Meadows Thrust sheet is the Salem Thrust sheet, comprised of the Cambrian Elbrook Formation, a younger, predominantly carbonate formation. To the south, the Rome Formation is overridden by the Blue Ridge Thrust Sheet, which consists of the pre-Rome Formations of Poor Mountain.

During the site investigations carried out by SEA, geologic mapping and borehole drilling provided detailed information about the site geology. The data derived from these studies are discussed in the following three sections to develop the geologic setting of the research area.

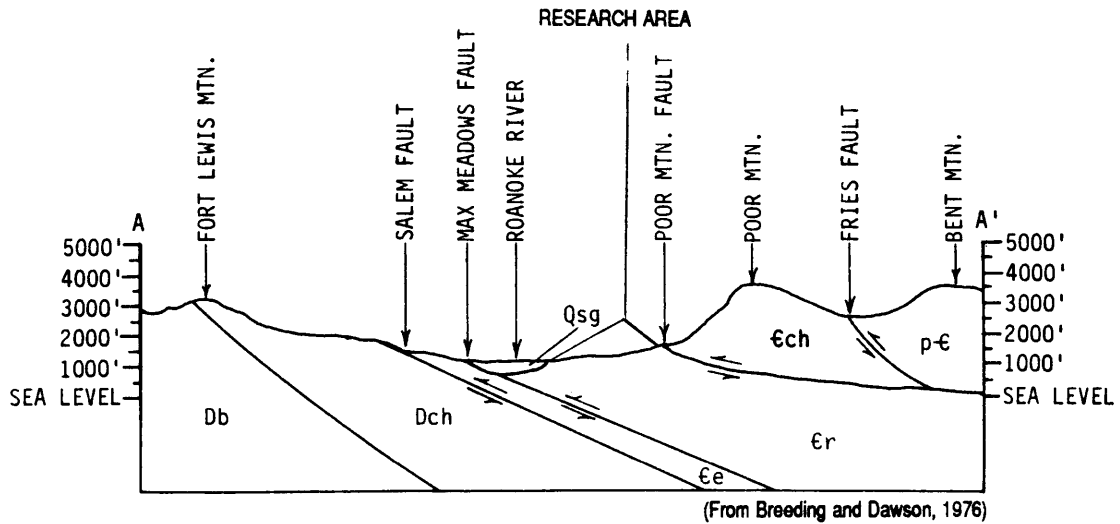


(From Edwards, 1959)

Figure 5

Stratigraphic Column of Roanoke County, Virginia

ARTHUR LAKES LIBRARY  
 COLORADO SCHOOL OF MINES  
 GOLDEN, CO 80401



<b>Q s g</b>	<b>QUATERNARY</b> Unconsolidated sand, gravel silt and clay	<b>ε r</b>	<b>ROME FORMATION</b> Red, green, shale and siltstone with beds of limestone
<b>D c h</b>	<b>CHEMUNG FORMATION</b> Brown sandstone, with olive shale	<b>ε c h</b>	<b>CHILHOWEE GROUP</b> Thin bedded conglomerite, quartzite and shale. Basalt in lower portions
<b>D b</b>	<b>BRALLIER FORMATION</b> Gray shale with interbedded sandstone	<b>p-ε</b>	<b>VIRGINIA BLUE RIDGE COMPLEX</b> Greenish-gray gneiss
<b>ε e</b>	<b>ELBROOK FORMATION</b> Gray dolomite and limestone with some green shale		



See Figure 1 for Location of Cross-Section

Figure 6

Cross-Section of a Portion of the Upper Roanoke River Valley Near the Research Area

#### 6.1.1.1 Lithologies

The geology of the site was mapped in 1985 by SEA as part of a preliminary investigation for the siting of the Spring Hollow reservoir and dam. Figure 7 presents the detailed geologic map produced by SEA in 1989, that was based on additional mapping and borehole data. The lithologies identified include gray, tan and olive shales and calcareous shales, maroon and red siltstones and shales, and dark gray limestones, dolomites and shaley limestones and dolomites. The carbonates are microcrystalline. The strike is nearly east-west, with strata dipping steeply, in places nearly vertical, resulting in a banding of lithologies perpendicular to the axis of the reservoir. The carbonates in Spring and Dry Hollows display features consistent with karst topography. The vertical strata along the east dam abutment are shown in Figure 8. These features include; sinkholes, caves, and springs, many of which are located along an east-west trending "high-solution zone" (Plate 1). Neither Cove Hollow nor Dry Hollow has been mapped in detail for geology. Field reconnaissance indicates that both are similar in geologic character to Spring Hollow, however no similar solution features have been identified in Cove Hollow. Dry Hollow is largely covered by colluvium from erosion of Poor Mountain to the south and could not be mapped beyond the limits shown in Figure 7. Cove Hollow is privately owned and was not accessible for field mapping.



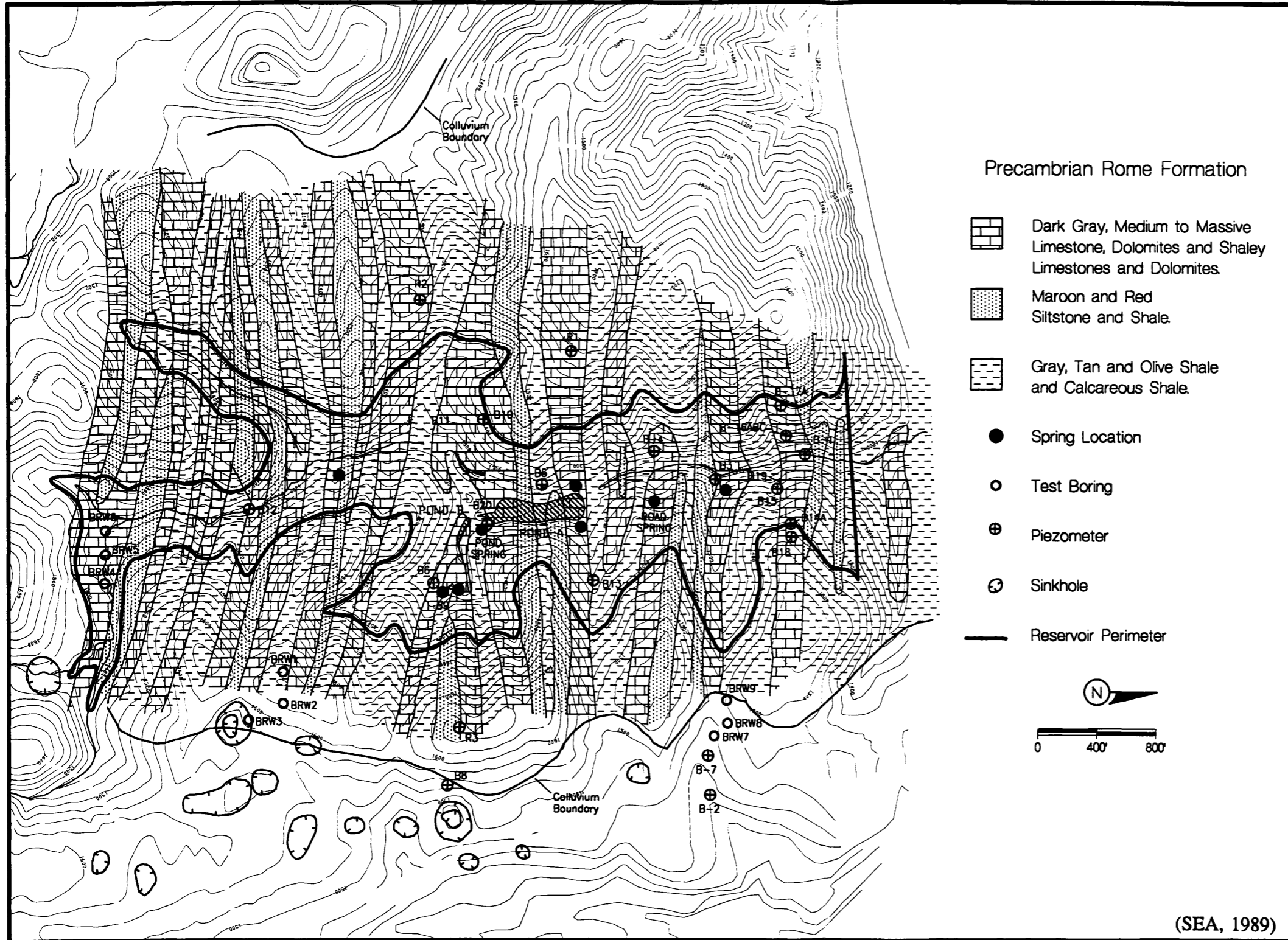


Figure 7  
Detailed Geologic  
Map of the Research Area

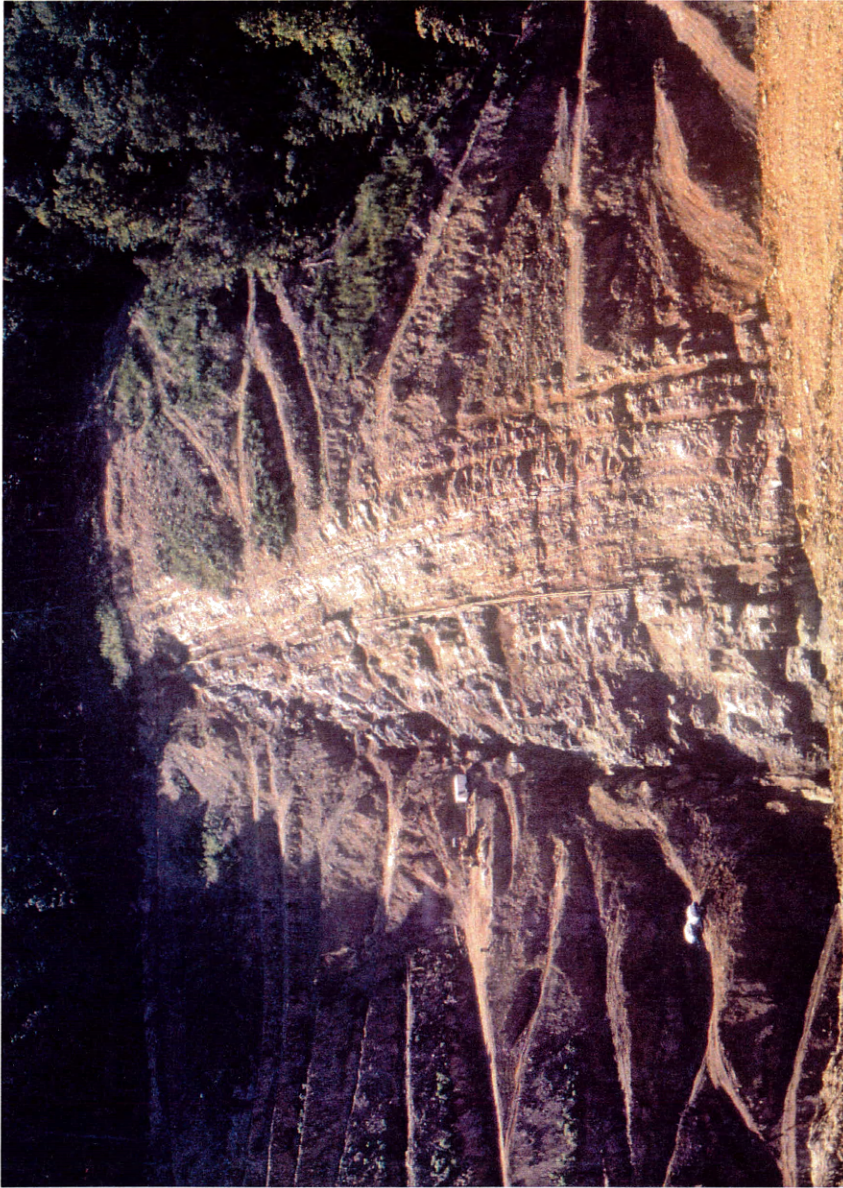


Figure 8

Vertical Strata Striking East-West Along the East Dam Abutment

#### 6.1.1.2 Soils

Soils in the area consist of alluvium, colluvium, and residuum. Colluvium is thick enough in some areas to be mapped as a significant geologic unit (Figure 7). The colluvium is the result primarily of colluvial fans, that are found in drainages along the northwest slope of Poor Mountain (Edwards, 1959) to the south of the site. These colluvial fans are believed to have formed as a result of erosion of Poor Mountain. The author has interpreted the origin of some of the colluvium in the northern reaches of Dry Hollow to be the result of solution weathering and collapse. In Spring Hollow, colluvium is found only in the southernmost reaches of the basin and is as thick as 46 feet in Borehole BRW4 (Table 1, Plate 1). Based on the log of Borehole B7 (Plate 1), where colluvium extends to 130 feet below the surface, colluvium is present in considerable thicknesses in northern Dry Hollow and is a significant geologic unit (Table 1). As shown in Figures 5 and 7, colluvium has also been mapped in southern Cove Hollow, however its thickness is unknown.

Alluvium is found in the stream beds of all three valleys. It is thin and insignificant as a geologic unit.

Residuum is present throughout the study area and has formed along slopes and ridge tops and beneath deep colluvium. In Spring Hollow, it is generally less than 20 feet thick, but has been logged as deep as 60 feet beneath the stream in Well B5 (Table 1, Plate 1). In Dry Hollow, Well B7 ended in residuum at 206 feet, beginning under 130 feet of colluvium. It is considered an important geologic unit in the northern half of the

valley. It is expected that residuum is present in Cove Hollow, but that it is not significant geologically.

#### 6.1.1.3 Structure

The Rome Formation elsewhere in the thrust sheet is known to be highly deformed with a series of imbricate faults that repeat the section, and tight fold structures with drag faulting, smaller reverse faulting and fracture zones (Amato, 1974). Many of these features are also present in the Rome Formation at the site.

Geologic mapping provides detailed data on bedding and fracture orientations and characteristics (SEA, 1987 and 1989) and provides evidence of two major fracture sets (Appendix A). The bedding planes average a strike of N88°W and a dip ranging between 40° to 85° to the north. The two dominant fracture sets are oriented almost normal to stratigraphic strike with a north-south orientation. Fracture set J-1 strikes north-south and dips between 55°West to 80°East. Fracture set J-6 strikes N24°E and dips between 60° to 90° degrees to the southeast. Within Spring Hollow, fold axes, reverse faults and fracture zones trend in an easterly direction parallel to the fault trace. Specifically within the high-solution zone, the beds dip between 65° and 85° to the north, with a dip reversal of 88° to the south near the center of the zone. The author, through field mapping and analysis of borehole data, infers a fault along the high-solution zone (Plate 1). This fault is probably high angle reverse, along the axis of a westward plunging anticline. It may lie on a minor thrust sheet, the trace of which defines the northern edge of the high-

solution zone. Evidence for the presence of a minor thrust fault is presented in Section 6.1.4. Many large and small structures accompany this faulted anticline, further offsetting and complicating the geologic interpretation. All of Spring Hollow shows evidence of faulting and folding, however, the most intense fracturing, the fault breccia, and the highest degree of solutioning distinguish the high-solution zone from the rest of the site.

### 6.1.2 Site Hydrology

Surface water within the three parallel valleys of the study area, Cove, Spring, and Dry Hollows, flows north toward the Roanoke River (Figure 2), draining the uplands to the south. Secondary valleys, perpendicular to the three primary valleys, provide drainage from the ridges between valleys.

The stream-bed elevations of Cove Hollow and Spring Hollow are illustrated in Figure 9. Spring Hollow is cut slightly deeper in the middle and upper reaches than Cove Hollow. Dry Hollow is over one hundred feet higher in elevation along strike than either of the other two valleys throughout their lengths. Within the research area, Spring Hollow and Cove Hollow streams flow year-round. The stream in Dry Hollow, however, disappears at the "sinking point" within the high-solution zone (Figure 9, Plate 1), but appears again downstream.

#### 6.1.2.1 Stream Flow Measurements

Estimates of stream flow in Spring, Cove and Dry Hollows were made during the winter months, December, 1984 to February, 1985 (Table 2) and included some heavy

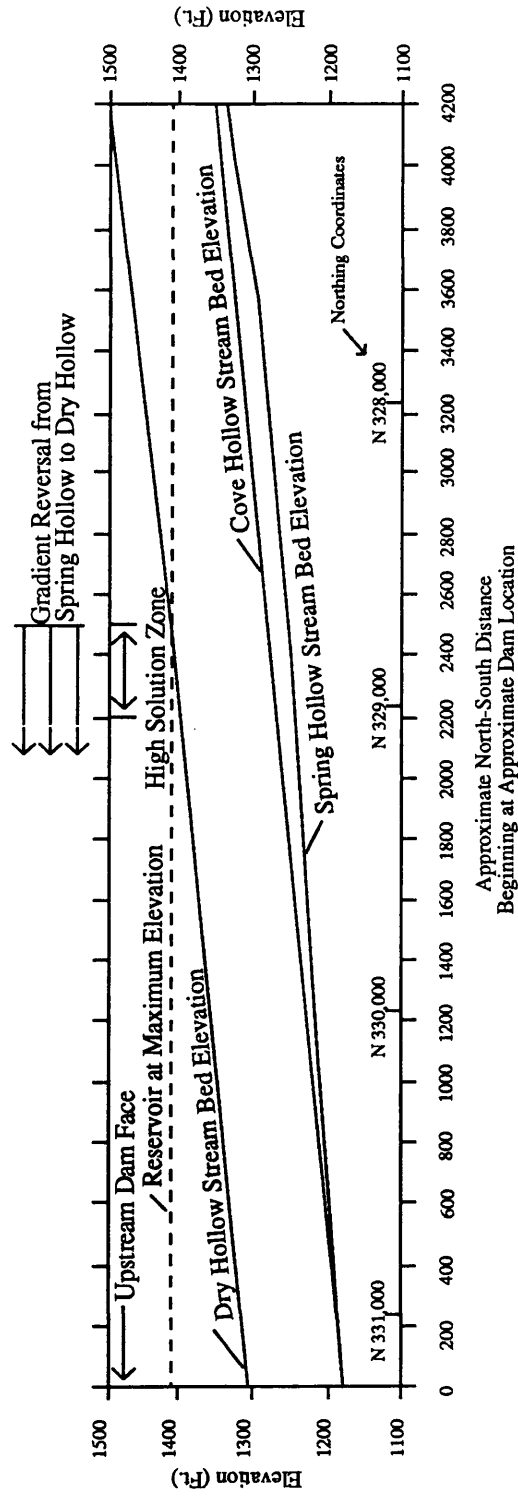


Figure 9  
Stream-Bed Elevations Along Dry, Spring, and Cove Hollows

Table 2  
1985 Stream and Spring Flow Data For the Research Area

	Location <sup>1</sup>	Date	Flow (cfs)	Average (cfs) <sup>4</sup>
Dry Hollow	Above Sinking Point	12/84-2/85	0.9 - 3.5	2.2
Spring Hollow	Stream Flow Station <sup>2</sup>	12/84-2/85	0.1 - 0.2	0.15
	Stream Flow Station 2 <sup>3</sup>	12/84-2/85	0.5 - 1.3	0.09
Cove Hollow	Unknown	12/84-2/85	0.7 - 3.1	1.9

<sup>1</sup> Locations Depicted on Plate 1

<sup>2</sup> Equivalent to Weir A in 1989 Study

<sup>3</sup> Downstream of the Flume, below Pond B

<sup>4</sup> Average of Endpoints

rains (SEA, 1989). No permanent stream flow measuring devices were in place at this time, so the rates are considered estimates. Stream flows in Dry Hollow above the sinking point ranged from 0.9 to 3.5 cubic feet per second (cfs). Dry Hollow is a losing stream in its upper reaches, completely sinking below the stream bed at the projected intersection of the high-solution zone at the stream at about elevation 1405 feet except during heavy rainfall. The sinking point of Dry Hollow in October, 1992 is shown in Figure 10 and Plate 1. Water is found again over 1600 feet downstream at about the 1340-foot stream-bed elevation as puddled water. The stream gradually gains water toward the Roanoke River, but loses again just before its confluence with the river. The Roanoke River is a major discharge zone in Roanoke County (Breeding and Dawson, 1976) and is, therefore, a gaining river along the stretch bordering the research area.

The stream flows in Cove Hollow, measured during the 1984-1985 monitoring period, ranged from 0.7 to 3.1 cfs. Little is known about Cove Hollow, but based on stream-bed elevations and water-level measurements in wells, it appears to be a gaining stream. Spring Hollow was also measured during this field study. It, too, is a gaining stream, readily evident as spring flow. Stream flow measurements of 0.1 to 0.2 cfs were made above Pond A just south of the high-solution zone (Stream Flow Station 3, Plate 1). Below the zone of high-solution the spring flow contribution was 0.4 to 1.2 cfs. (Total flow in Spring Hollow was not measured in the 1984-1985 monitoring period).

A second field study was undertaken in 1987 (Martin and Milner, 1988). Stream and spring flow in Spring Hollow were estimated four times during the months of August,





Figure 10

Sinking Point of Dry Hollow in October, 1992

September and October (Table 3), typically among the wetter months of the year. Spring Hollow flow estimates ranged from 1.31 to 9.55 cfs at Stream Flow Station 1 (Plate 1), 1.14 to 8.59 cfs, at Stream Flow Station 2 (at the north end of Pond A), and 0.54 to 0.72 cfs at Stream Flow Station 3 (located at a point just south of the high-solution zone). In 1989, a longer-term, more detailed field study was undertaken (Table 4) to further characterize the hydrology of the site (SEA, 1989). Two weirs and a Parshall Flume were installed in Spring Hollow to measure stream flow and spring contribution (Plate 1). Flow through the spring box at Spring A, located on the southeast edge of Pond A was measured with a bucket periodically. The period of measurement extended from mid-April through mid-July, 1989. The results of this study are depicted in Figure 11. The precipitation shown on the graph was measured at the Roanoke County Airport, Woodrum Field (Figure 1), which is approximately 13 miles from the site. Some variation in actual rainfall from the airport is expected at Spring Hollow, however, only the magnitude is expected to differ for the larger events. Peak flows were not measured in conjunction with the largest rainfall event of July 7. The flow in the upper part of the hollow, above the high-solution zone, ranged between 0.23 and 2.57 cfs. The flume measured spring flow through the high-solution zone between 0.67 and 3.4 cfs. Spring A flow ranged from 0.1 to 0.45 cfs. The dates of measurement of the lowest flows for the two springs are coincident. The stream flow at Weir B, toward the mouth of the stream ranged from 1.3 to greater than 5.8 cfs.

Table 3  
1987 Stream and Spring Flow Data for the Research Area

Date	Stream Flow Station 1 <sup>1,2</sup> (cfs)	Stream Flow Station 2 <sup>2,3</sup> (cfs)	Stream Flow Station 3 <sup>2,4</sup> (cfs)	Rainfall
8/4/87	0.54	1.14	1.31	Dry
9/15/87	0.71	8.59	9.55	Heavy
9/23/87	0.72	4.09	4.57	Heavy
10/29/87	0.72	1.68	1.94	Light
Average	0.67	3.88	4.34	

(Martin & Milner, 1988)

<sup>1</sup> Equivalent to Weir A in 1989 Study

<sup>2</sup> Location depicted on Plate 1

<sup>3</sup> Downstream of the Flume, below Pond B

<sup>4</sup> Equivalent to Weir B in 1989 Study

Table 4

## Stream and Spring Flow Data for the Research Area

Date	Weir B	Flume	Weir A	Pond Spring	Precipitation
4/20/89					0
4/21/89					0
4/22/89			0.28		0
4/23/89					0
4/24/89					0
4/25/89					TR
4/26/89					0.22
4/27/89			0.44		0.42
4/28/89			0.28		0.54
4/29/89					0.03
4/30/89					0.18
5/1/89					1.92
5/2/89	5.83	3.26	2.57		0.05
5/3/89					0
5/4/89					0.07
5/5/89					1.32
5/6/89					0.88
5/7/89	>5.55	3.6	1.95		TR
5/8/89					0
5/9/89					1.4
5/10/89					0.02
5/11/89					1.01
5/12/89					0
5/13/89	4.37	3.4	0.8		0
5/14/89		3.12			0
5/15/89		2.98			0.16
5/16/89		2.84			0
5/17/89		2.7			0
5/18/89		2.52			0

(continued)

Table 4 (continued)

5/19/89		2.27			0
5/20/89		1.94			0.02
5/21/89	2.77	1.82	0.36		0
5/22/89		1.7			0.58
5/23/89		1.66			0.01
5/24/89		1.55			0
5/25/89		1.37			0
5/26/89		1.26			0.02
5/27/89		1.16			TR
5/28/89		1.1			0
5/29/89		0.97			0
5/30/89	2.31	0.87	0.25		0
5/31/89		0.81			0
6/1/89		0.76			0
6/2/89		0.76			0.03
6/3/89	1.3	0.81	0.23	0.13	0.03
6/4/89		0.73			0
6/5/89		0.87			0.95
6/6/89		1			0.04
6/7/89	2.01	1.48	0.47	0.17	0.86
6/8/89		1.86			0.8
6/9/89		2.57			0.9
6/10/89		2.79			0
6/11/89		2.98			0
6/12/89		3.12			1.87
6/13/89	4.37	3.21	0.47	0.45	TR
6/14/89					0.026
6/15/89					0.02
6/16/89					0.05
6/17/89	3.63	2.84	0.3		0
6/18/89					0

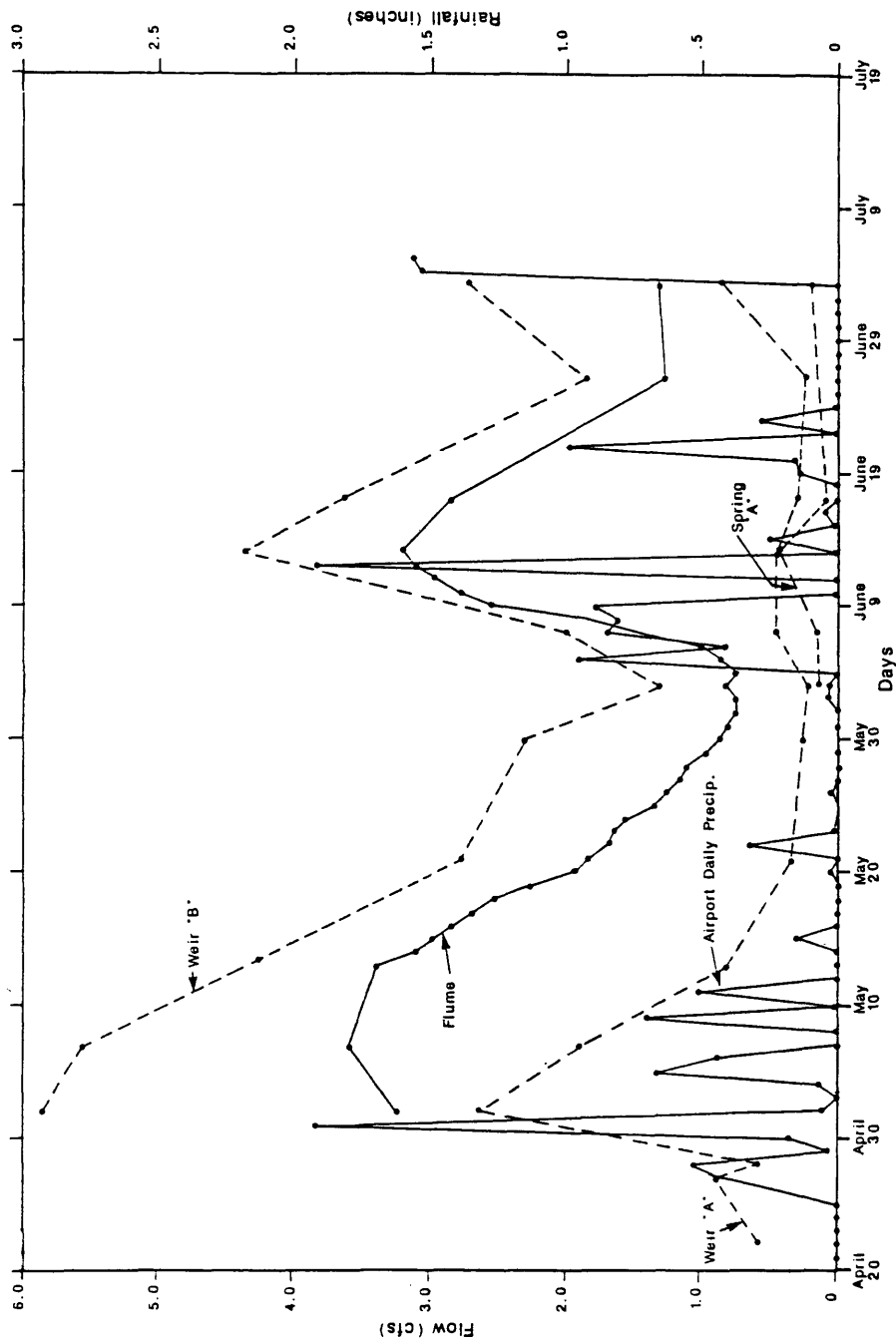
(continued)

Table 4 (continued)

6/19/89					0.15
6/20/89					0.16
6/21/89					0.99
6/22/89					0.01
6/23/89					0.28
6/24/89					TR
6/25/89					0
6/26/89	1.74	1.23	0.25		0
6/27/89					0
6/28/89					0
6/29/89					0
6/30/89					0
7/1/89					TR
7/2/89					TR
7/3/89	1.37	0.67	0.42	0.1	TR
7/4/89					1.54
7/5/89					1.56
7/6/89					2.36
7/7/89					0
7/8/89					0
7/9/89	3.47	2.98	0.26	0.35	0.04
7/10/89					0
7/11/89					0
7/12/89					1.27
7/13/89					0.12
7/14/89					TR
7/15/89					0.41
7/16/89					0.46
7/17/89	2.55	1.34	0.4	0.38	0.38
Average (n = 13)	3.17	2.12	0.535	0.26 <sup>1</sup>	
Standard Dev.	1.51	1.11	0.465	0.15	

<sup>1</sup> n = 6

(SEA, 1989)



(From SEA, 1989)

Figure 11

Summary of Weir, Flume, and Rainfall Data for Spring Hollow

Although all three studies are variable as to flow rates along Spring Hollow, one fact stands out: Spring flow along the high-solution zone contributes the largest component of flow to Spring Hollow, and the magnitude of this flow is related to the magnitude of rainfall. It is reasonable to infer that this flow is related to the high-solution zone and the sinking point in Dry Hollow, since these two features occur along strike within the same carbonate unit. It follows that spring flow in the high-solution zone to a large extent is due to capture of flow in Dry Hollow at the sinking point. Lag time for the effect of capture at the flume has been estimated to be between one and two days (Figure 11). Therefore, the effects of Dry Hollow runoff can be expected to be negligible at the flume after one to two days following a significant rainfall.

Although stream/spring flow data for a full hydrologic year have not been recorded, the 1989 study, conducted in late spring and summer, can be used to estimate average annual conditions. The 1989 stream and spring flow values are intermediate between those of the study in the winter of 1984-1985 and the study in the late summer and early fall of 1987. As shown on Figure 11, a conservative range of the base-flow recessions after the May 1st storm are 2.77 to 1.3 cfs for Weir B, 1.94 to 0.73 cfs for the Flume, and 0.36 to 0.23 cfs for Weir A. The base-flow recessions following the second major storm which culminated June 12th, provides ranges of 1.74 to 1.37 cfs for Weir B, 1.23 to 0.67 cfs for the Flume, and 0.42 to 0.26 cfs for Weir A. The data for Spring A are too sparse to indicate a base-flow recession curve.



#### 6.1.2.2 Water Budget for Spring Hollow

The major components of the water balance equation in Spring Hollow are groundwater flow (seepage and spring flow), precipitation, evapotranspiration and runoff. Spring flow averages measured during three different field studies are variable. An average condition is more appropriately selected from the 1989 study, since the 1987 study appears to be skewed toward wet conditions and the 1984-85 study was done during dry conditions.

For the purpose of calculating the water budget of Spring Hollow, averages of the 1989 flow data will be used. Specifically, averages of the thirteen coincident measurements are 3.17 cfs at Weir B, and 2.12 cfs at the Flume. Spring A flow ranges from 0.45 to 0.1, with an average of 0.28 cfs.

The inflows into the basin are ground water (seepage and spring flow) and precipitation. The combined spring flow contribution at the flume and Spring A is 2.38 cfs, or 1,723 acre-feet per year. Minor springs were not monitored and are, therefore, unaccounted for. The average annual rainfall in Roanoke County is 41.1 inches (State of Virginia, 1995). Using 41.1 inches of rainfall and a total drainage basin area of 480 acres, precipitation contributes 1,645 acre-feet of water into the basin annually. Total inflow is 3,368 acre-feet.

The outflows from the basin include evapotranspiration and stream flow. Evapotranspiration is estimated using the Thornwaite Method (Table 5), which yields a value of potential evapotranspiration of 28.9 inches per year using Roanoke County

Table 5  
 Estimation of Potential Evapotranspiration (PET)  
 Using the Modified Thornwaite Method<sup>1</sup>

Month	Temperature 30-Year Average ° Fahrenheit <sup>2</sup>	Monthly Heat Index i	Precipitation 30-Year Average Inches <sup>2</sup>	Potential Evapotranspiration (inches)		
				Weekly	Daily	Monthly
				Corrected	Corrected	Corrected
January	34.5	0.2	2.62	0.03	0.003	0.089
February	37.3	0.6	3.04	0.06	0.0071	0.2
March	46.8	2.2	3.48	0.23	0.0314	0.974
April	55.6	4.3	3.25	0.43	0.069	2.057
May	64.1	6.9	3.98	0.66	0.11	3.41
June	71.5	9.5	3.19	0.91	0.16	4.8
July	75.6	10.9	3.91	1.07	0.186	5.76
August	74.6	10.5	4.15	1.02	0.166	5.137
September	67.7	8.1	3.5	0.79	0.116	3.47
October	56.5	4.7	3.85	0.45	0.06	1.86
November	47.5	2.4	3.19	0.24	0.03	0.9
December	38.3	0.7	2.97	0.07	0.007	0.221
TOTAL		61	41.13			28.878

<sup>1</sup> Palmer and Havens, 1956

<sup>2</sup> State of Virginia, 1995

Airport 30-year average monthly precipitation and temperature (State of Virginia, 1995). Considering that the site is densely vegetated and that vegetation remains green throughout the growing season, it is assumed that potential evapotranspiration is close to true evapotranspiration. The potential evapotranspiration of 28.9 inches per year removes 1,156 acre-feet of water from the basin annually. Average stream flow is 3.17 cfs, or 2,295 acre-feet annually bringing total outflow to 3,451 acre-feet.

Inflows = Outflows +/- Change in Storage

(Spring Flow + Precipitation) - (Evapotranspiration + Stream Flow) =  
Change in Storage

(1723 + 1645) - (1156 + 2295) = -83 acre-feet

Assuming no change in storage, this 83 acre-feet is a discrepancy of about 2%, which represents 0.18 cfs. This amount of flow may be due to a number of small, unmonitored springs, as well as measurement errors.

### 6.1.3 Geomorphologic Interpretation

A geomorphologic analysis of the site was completed in order to understand the interrelationship of the hydrology and geology and the processes working to shape the land. Although the reservoir area and adjacent ridges have been mapped, the research area extends beyond the ridges into the adjacent valleys, Cove and Dry Hollows. The geomorphologic interpretation was used to extend the geology into the unmapped areas. Aerial photography (State of Virginia, 1972), a topographic map (USGS, 1972) and geologic maps (SEA, 1985, 1989) were used in this analysis.

### 6.1.3.1 Processes and Climate

There are a number of processes that are influencing and have influenced the site in the past, including compressive tectonism, erosion and stream development, and karstification.

The site is located within the Valley and Ridge physiographic province of the Appalachians, and is dominated by the compressive tectonics characteristic of this region. Compressive tectonics produce structural features such as thrust faults, folds, high-angle thrust faults, and fracture zones as discussed in Section 6.1.1.3.

Erosion and stream development occur as water is carried from Poor Mountain and the higher elevations of the site into the three parallel streams that are tributary to the Roanoke River bordering the site on the north. Karstification is also taking place as is evidenced by the presence of a sinking stream, caves, springs and sinkholes.

The first process, tectonics, has a large influence on the latter two processes, both in the landforms developed and the trends of those landforms. The climate is humid, with a mean annual temperature of 56.1 degrees Fahrenheit (SEA, 1989).

### 6.1.3.2 Landforms

The landforms present include karst features, such as springs, caves, sinkholes (Figure 12), and a sinking stream (Plate 1). The karst features have developed in the carbonate beds that strike from valley to valley, allowing mapping of carbonates where these features appear.



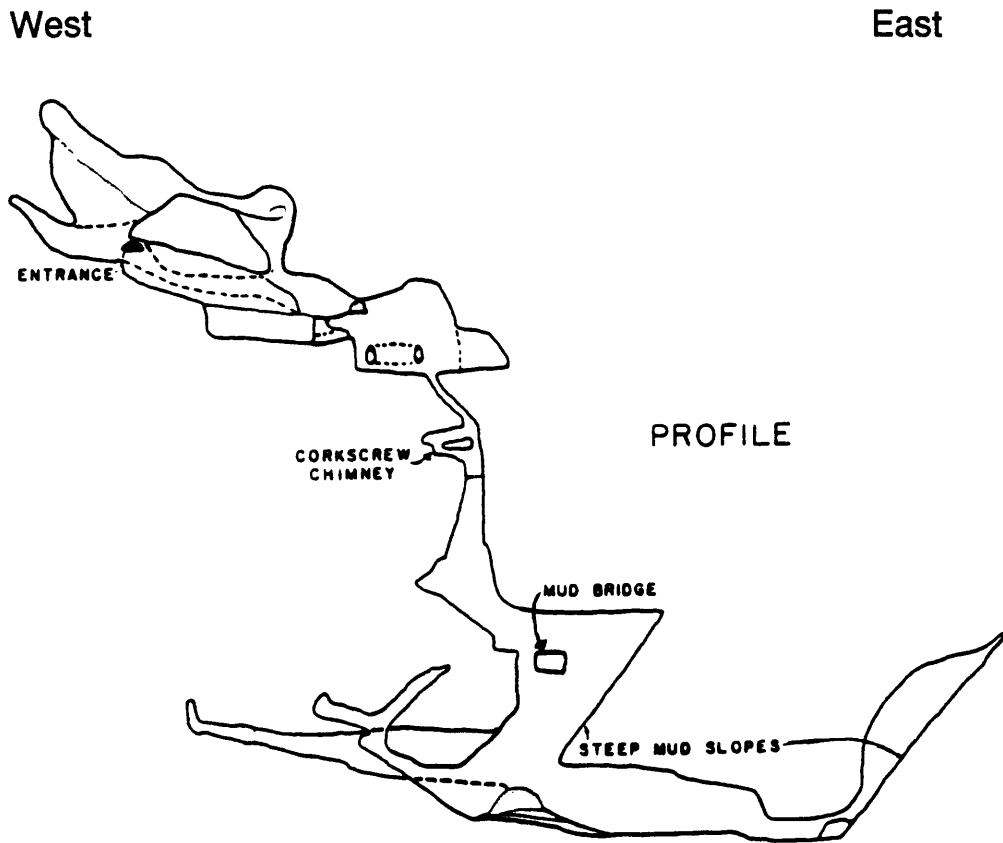
Figure 12

Large Sinkhole Along East Rim of Reservoir

Spring Hollow, named for the springs found in the valley, also contains a small cave located south of Pond A, within the high-solution zone. The distinctive topographic relief of the high-solution zone has been named the "bird foot structure" (SEA, 1989). This feature has also been observed east of Cove Hollow and on the west slope of Dry Hollow (Plate 1).

Dry Hollow, so named because of its sinking stream, contains a number of large sinkholes, all above the present-day stream level. It also contains a large cave, the Blankenship Cave, that is at least 128 feet deep (Holsinger, 1975). Figure 13 is an illustration of the physical dimensions of the cave. The Dry Hollow stream sinks below ground surface in the upper reaches of the stream along strike with the high-solution zone of Spring Hollow just upgradient of the Blankenship Cave. About 1600 feet downstream the water reappears in the stream bed. Limited field reconnaissance of Cove Hollow revealed no evidence of caves and sinkholes or springs, although the name implies otherwise.

Other landforms present include parallel, north-south trending valleys and ridges consistent with the Valley and Ridge Province (Figure 2). Ridge-formers tend to be siltstones and shales, and valley-formers are carbonates. The shales, with a low compressive strength, deform when folded and compressed. The more competent carbonates are more likely to fracture, with the fractures then allowing dissolution of the rock and the development of drainages. The topographic map reveals a broad and rounded Dry Hollow valley (Plate 1). This broadening trends north-south, parallel to the



(From State of Virginia, 1975)



Figure 13

Schematic of Blankenship Cave in Dry Hollow

valley and is pocked by sinkholes, that seem to parallel this trend. It is possible that a wide shear zone exists along the valley and that fracturing and faulting have promoted weathering and solutioning that have had the effect of broadening the valley.

Spring Hollow is a V-shaped valley for all but a section along the high-solution zone (Plate 1). At this point the valley flattens and widens, probably due to imbricate faulting running east-west. Cove Hollow is a V-shaped valley in its lower reaches, but exhibits a broader valley in its upper reaches.

The study area is well-dissected, and somewhat chaotic. Although the hollows and secondary drainages follow major fracture trends that are transverse to each other, the complicating structures of folding and imbricate thrust faults disrupt this pattern. Along Spring Hollow and Dry Hollow there has been deep dissection, and the drainages correlate across the ridge, indicating the presence of a continuous carbonate strata. Correlation from one side of Spring Hollow to the other is not as clear as the Spring Hollow - Dry Hollow correlation. However, the bird foot features correlate across all three valleys. It may be possible that there is some offset of the geology along the tear fault forming Spring Hollow below the high-solution zone.

#### 6.1.3.3 Drainage Analysis

A drainage analysis of the study area, Figure 14, suggests that the three hollows run along parallel north-south trends, transverse to stratigraphic strike and in line with the north-south fracture trend discussed in Section 6.1.1.3. They appear to have developed



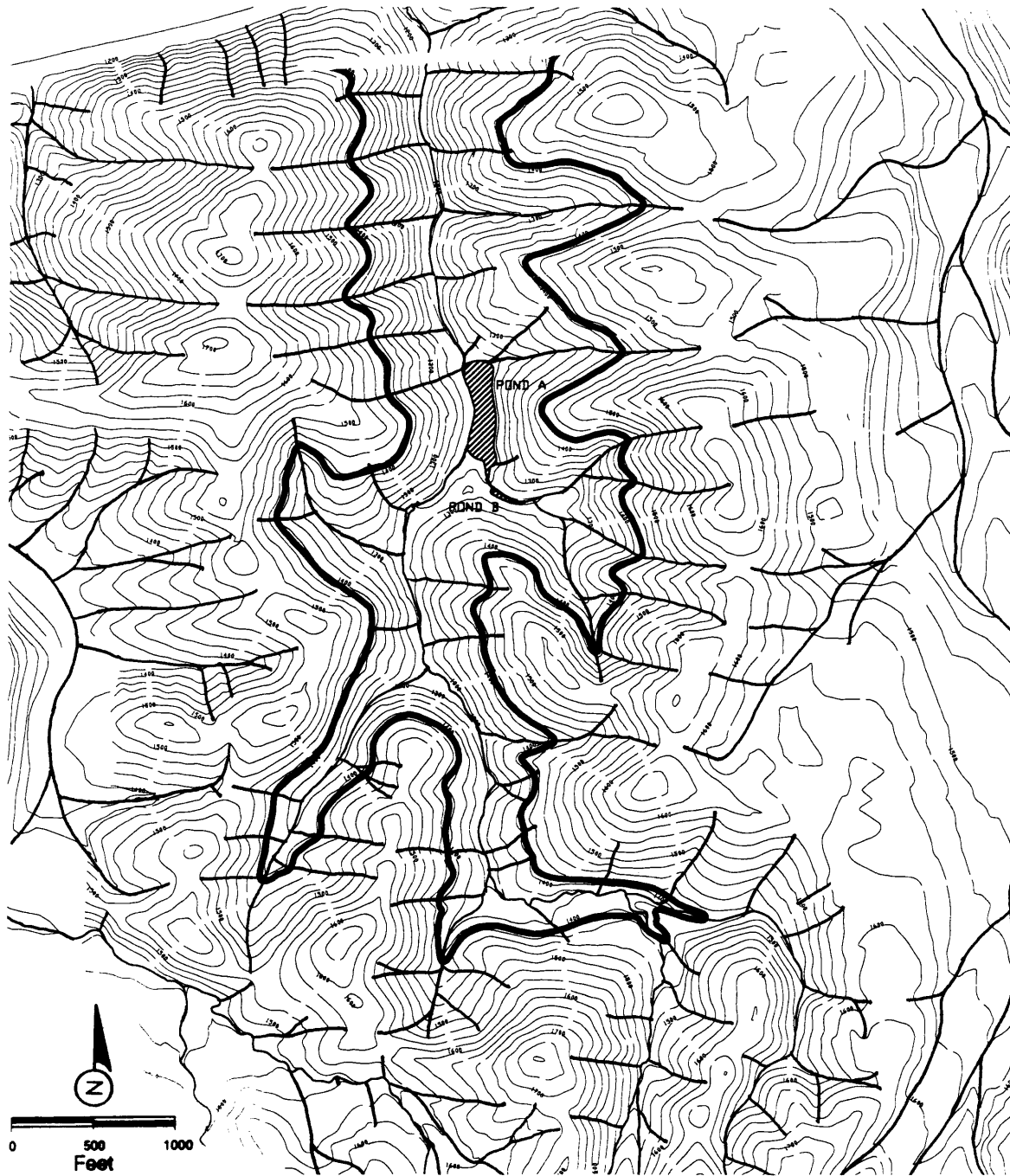


Figure 14

Drainage Analysis of the Research Area

along tear faults transverse to the thrust fault trace, and parallel to the direction of compressive force. Most of the secondary drainages have developed at right angles to the three hollows forming a distinctive drainage pattern. These secondary drainages run parallel to the fracture trend and transverse to the compressive force. There exists a difference in the density of the drainages with right-angle fracture control. The areas with the highest density of streams indicates the presence of interbedded carbonates and shales. The areas with less dense drainages signal the presence of colluvial material or massive carbonates. An absence of drainages indicates shale and siltstone.

A change in lithology and structure is evident in the change in drainage pattern at the south end of the site. The drainage pattern is dendritic, with secondary drainages developing at less than right angles with the main stream. The change in patterns indicates the change from the carbonates of the Max Meadows Thrust sheet to the PreCambrian rocks of the Blue Ridge Thrust sheet.

#### 6.1.3.4 Vegetation

An analysis of air photography taken in January, 1972 (State of Virginia, 1972), allowed the delineation of four vegetation types, including coniferous, deciduous, mixed coniferous/deciduous, and cleared/agricultural land as depicted in Figure 15. In Spring and Cove Hollows and on the ridges between Spring Hollow and the adjacent hollows, the vegetation assumes a pattern of east-west trending, alternating bands of coniferous and deciduous vegetation types, that are perpendicular to the strike of the hollows. This

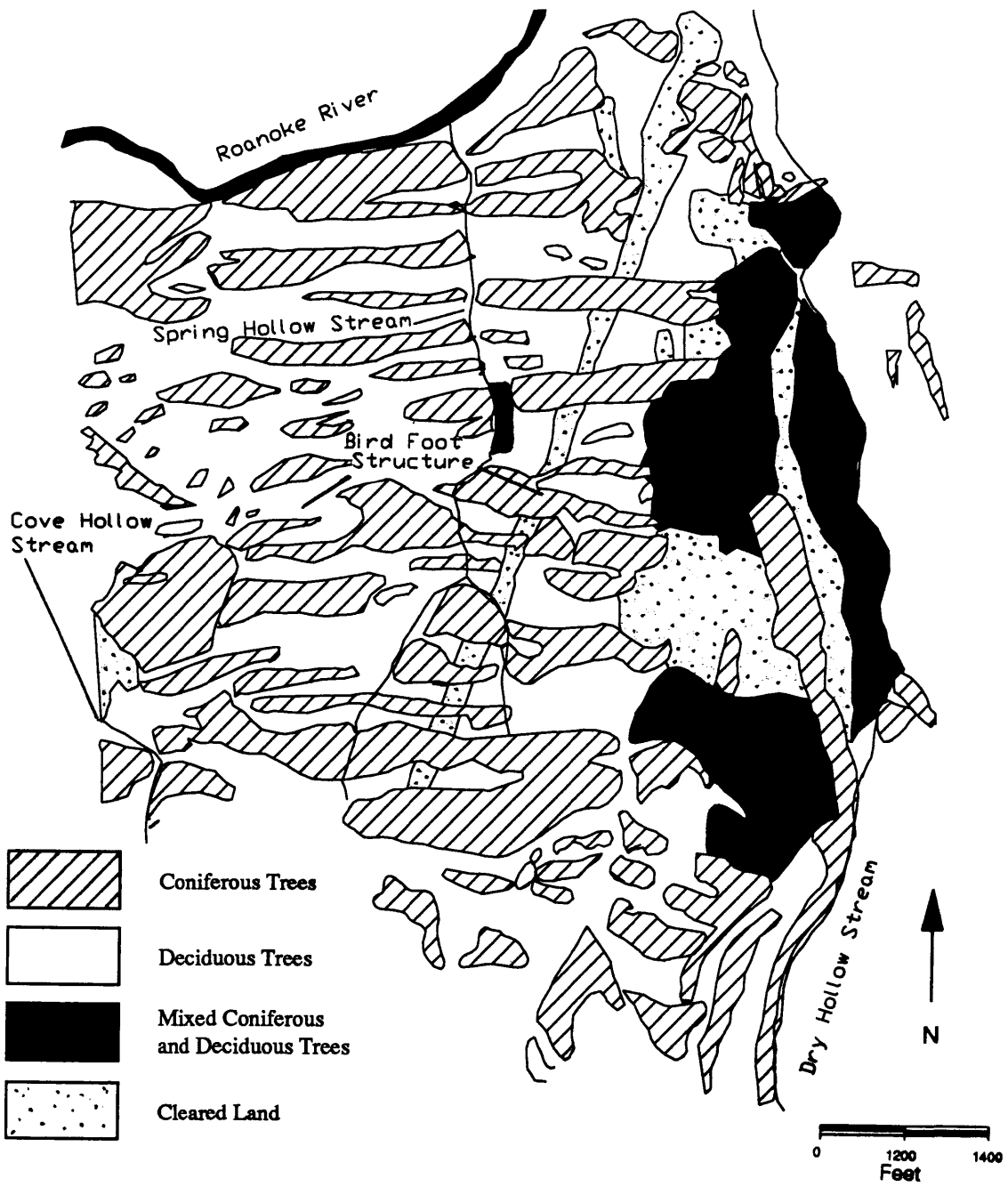


Figure 15

Vegetation Analysis of Research Area

banding is similar to the banding of lithologies present on the geologic map (Figure 7). Coniferous vegetation appears concentrated along the secondary drainages, while deciduous vegetation is found along ridges between the secondary drainages. A strip of cleared land cuts across Spring Hollow, along a utility power line.

The vegetation pattern and the vegetation types in Dry Hollow are strikingly different from that of Spring and Cove Hollows. The pattern of vegetation types runs north-south, paralleling the stream bed of Dry Hollow. The majority of the vegetation is mixed coniferous/deciduous and coniferous, but there is also an abundance of cleared/agricultural land.

#### 6.1.3.5 Anthropogenic Activities

Scattered residential buildings are present in both Dry Hollow and Cove Hollow. Numerous domestic wells tap the water-table aquifer. Spring Hollow has been the site of little anthropogenic activities, except for the construction of two small dams to create two ponds, both for recreational use. A small wooden building once stood near the larger pond, Pond A. Utility power lines also cross the site (Plate 1).

#### 6.1.3.6 Extension of Geologic Units

An extension of the bedrock geology from Spring Hollow to Dry Hollow and Cove Hollow is presented in Figure 16. The extension of geologic units was based on the integration of the results of the geomorphologic analysis and the 1989 geologic map

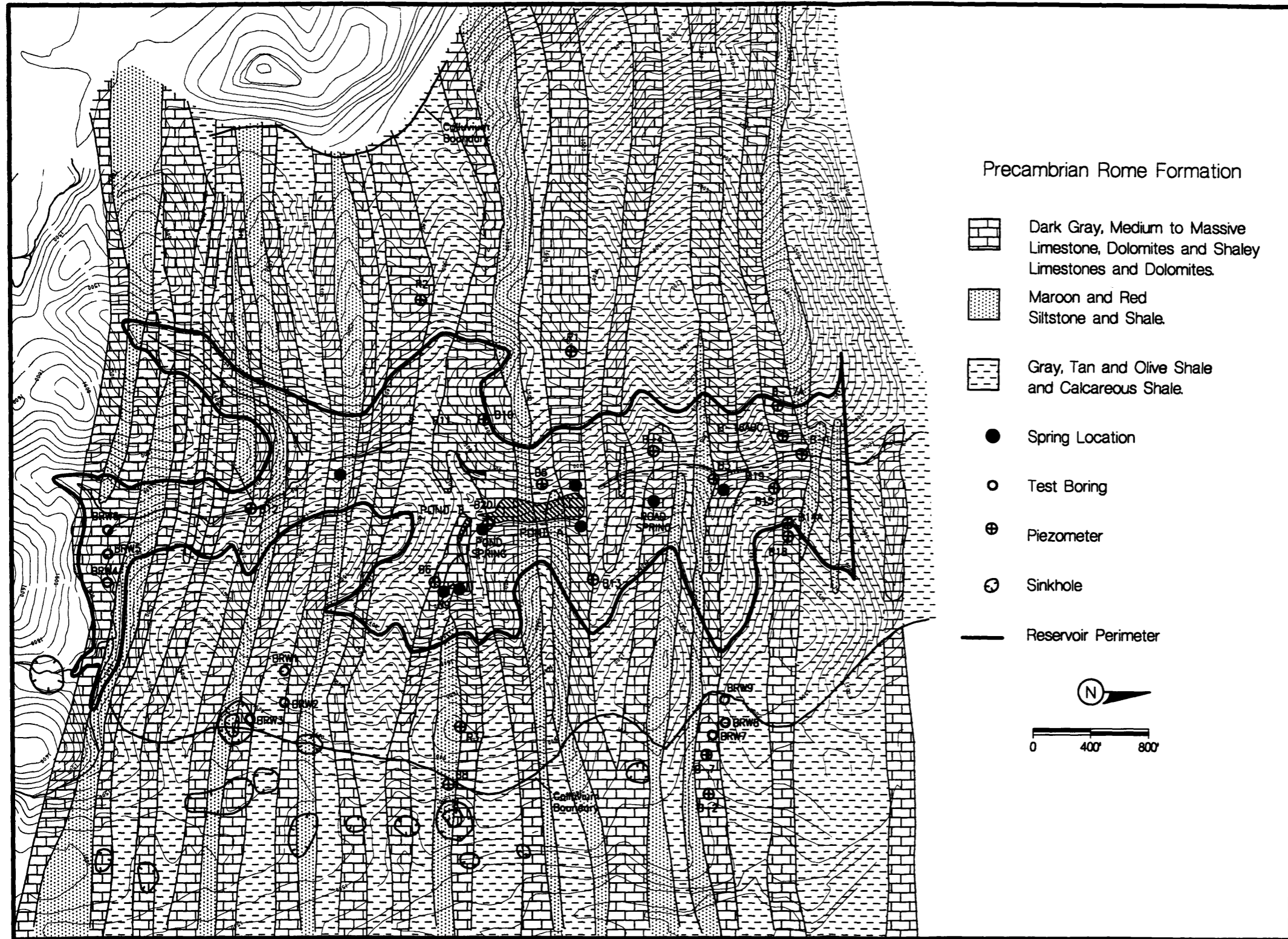


Figure 16  
Bedrock Map of the Research Area  
Based on Geomorphologic Analysis

(Figure 7). The extension of carbonates from the geology mapped in Spring Hollow followed drainages, karst features, and coniferous vegetation. The major carbonate units mapped in Spring Hollow fit this criteria well, and extension into Cove Hollow was straightforward. Shales (and siltstones) were extended from mapped areas in Spring Hollow along areas where drainages are not present, and along areas of deciduous vegetation.

In much of Dry Hollow, the secondary (east-west) drainage pattern is difficult to follow. There is an abundance of karst features, and the vegetation pattern is quite different from that of the rest of the research area. This is due to the mantel of colluvial material that produces a different vegetation pattern and type, sparse drainage development and a broad topographic relief. There appears to be some disruption of the vegetation pattern in Cove Hollow (Figure 15), and this may be the result of colluvial cover, that is consistent with 1989 mapping.

Not all carbonates mapped in 1989 (Figure 7) can be correlated to these three factors. Some carbonates appear on the geologic map in areas that are not drainages, do not have karst features, and are not within areas of coniferous vegetation. The carbonate lithology is verified in boring logs, however, and these carbonates have very high recoveries and rock quality descriptors and evidently have undergone less fracturing and little solutioning. Not all carbonates are prone to solution, and for the purposes of grouting and modeling, it is not important whether they are mapped as carbonates or shales. Rather, it is the hydraulic characteristic of the rock that is important.

#### 6.1.4 Site Hydrogeology

The hydrogeology of the site is complex due to the complicated structure and the karst terrain. Regional ground-water flow is to the north toward the Roanoke River (Breeding and Dawson, 1976). Locally, although it has a component of flow consistent with the regional flow pattern, the ground-water flow is dominantly east-west. The vertical beds in the research area, consisting of solutioned carbonates encased in low permeability shales and siltstones, act as a series of horizontal conduits channeling ground water and some surface water from valley to valley and ridge to valley in a direction transverse to local surface-water flow and regional ground-water flow (Breeding and Dawson, 1976).

##### 6.1.4.1 Aquifer Description

A review of the wells at the site revealed diverse and complex conditions, as is often the case in fractured and faulted rock (Table 1). In general, the average water levels in the wells indicate that the ground-water condition is that of an unconfined aquifer. Shallow perched aquifers, as well as locally confined aquifers are reflected in the water levels in other wells. Shallow perched aquifers are common in karst terrain, forming as a result of solution depressions above the water table (Fetter, 1980). The water levels in Wells B7, B14, and B18 exhibit this condition. Flowing ground-water wells, such as Wells B1 and B12, may be the result of locally confined conditions within anticlines, or the steep hillside topography.

Water-table wells may have strikingly different water levels even though they are located near each other. This is due to the great range in hydraulic conductivities between vertical beds of lower hydraulic conductivity shales, siltstones and carbonates next to carbonates with high secondary porosity.

The ground-water regime at the site is complicated, with localized variations in conditions of total head. A useful hydrogeological model of the site should reflect general conditions to be of predictive value.

#### 6.1.4.2 Pre-Grout Ground-Water/Surface-Water Interaction

As part of the 1989 site investigation, a water-table map (Figure 17) was developed using the average of water levels measured in monitoring wells in 1989 (ASI, 1989) (Table 1), and on stream elevations. Based on this map, there exists a slight ground-water divide between Spring Hollow and Cove Hollow, and a gradient from Dry Hollow to Spring Hollow.

The absence of a ground-water divide between Spring and Dry Hollows is a result of the development of large solution features in the carbonates between the two hollows. As mentioned previously, the most highly developed solution features occur in the high-solution zone between Dry and Spring Hollows. This abrupt increase in solution porosity creates a head drop of over 120 feet across this zone from south to north. This head drop extends from Dry Hollow to Spring Hollow and is evident in the water levels of a number of wells. The water in Dry Hollow, just upstream of the high-solution zone, sinks below



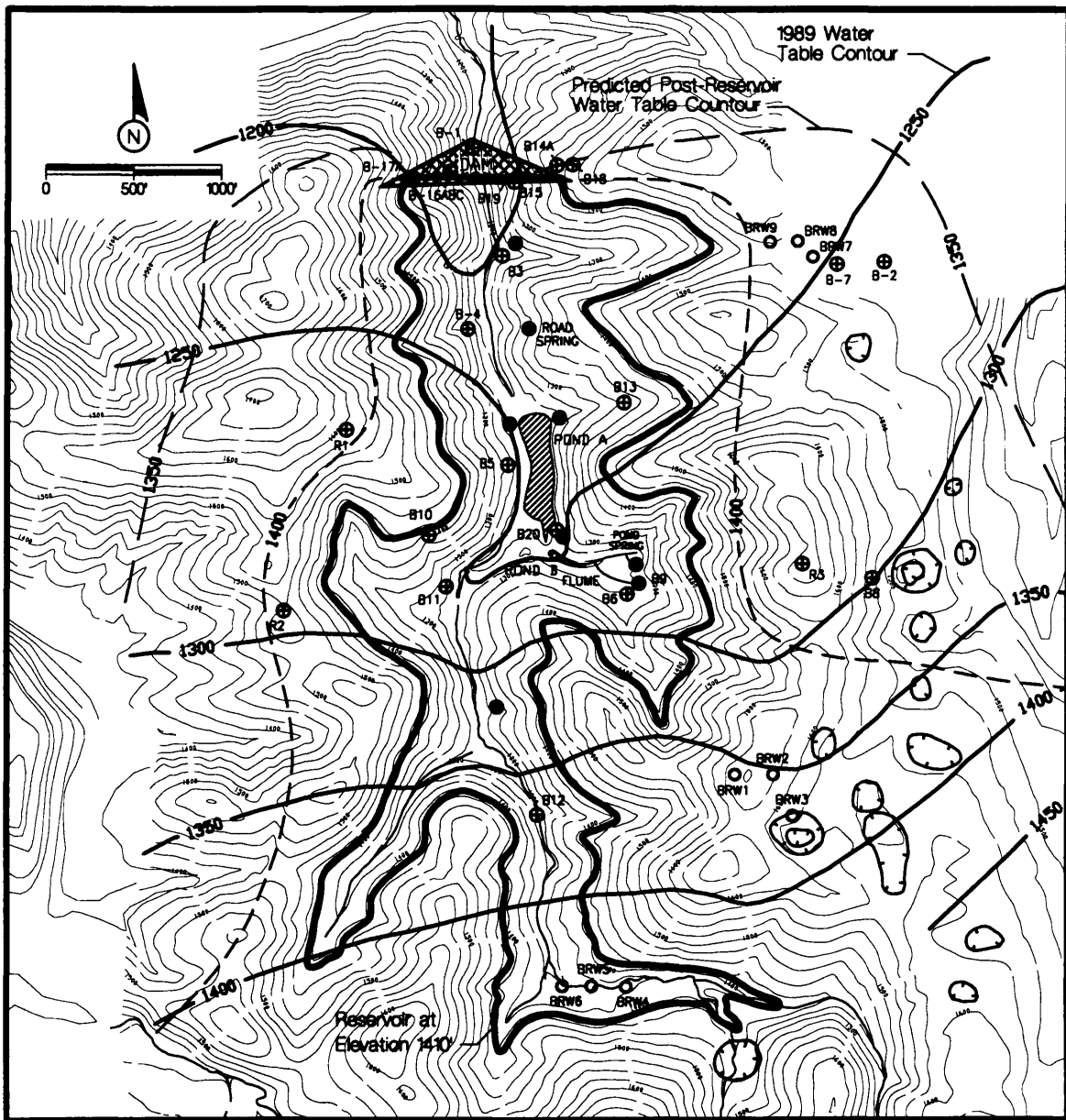


Figure 17

Water Table of the Research Area Reflecting  
Pre-Reservoir (1989) and Post-Reservoir Conditions

the stream bed at elevation 1405 feet. The average water level in Well R3, located within the high-solution zone between Dry and Spring Hollows, is about elevation 1270 feet. The Doyle Well, located downstream of the sinking point and within the high-solution zone, (Plate 1), has an average water-level elevation of 1268 feet. The Blankenship Cave, which is on strike with the high-solution zone on the east side of Dry Hollow and near the Doyle Well, is dry, with the bottom of the cave at approximately elevation 1330 feet.

Based on the ground-water contours, the water balance of the Spring Hollow drainage basin, and the loss of water in Dry Hollow, the water that flows from the large-volume springs in Spring Hollow was diverted from Dry Hollow to Spring Hollow through the high-solution zone. The high-solution zone is bounded on the north by an imbricate fault running east-west along the high-solution zone (Plate 1). The large head drop across the high-solution zone is a result of the well-developed solution porosity that has formed along the brecciation of the fault zone. The brecciation has created "pipes" that carry water flow from Dry Hollow into Spring Hollow. The shales that abut the thrust fault have a low conductivity in comparison with the high conductivity of the solution pipe(s) and act as barriers to down-valley flow.

The diversion of ground water along the high-solution zone resulted in a reduced flow in the northern half of Dry Hollow promoting diffuse solutioning and the absence of large solution features such as caves and sinkholes. Percolating rainfall and the rise and fall of ground water have caused deep weathering, over 200 feet deep, in the northern half of the site.

#### 6.1.4.3 Conceptual Model

The site hydrogeology is profoundly affected by rock type and structure, and solution features. Lithologies change abruptly in a north-south direction due to the almost vertical dip of the rocks. The interbedded and sometimes massive limestones, dolomites and shales are nearly vertical, and with the solution features present in many of the carbonates, act as a laterally heterogeneous aquifer, with higher heads in the less permeable shales and lower heads in the solutioned carbonates.

The orientations of the two major fracture sets have a significant effect on the ground-water flow system. Ground-water flows predominantly in an east-west path along stratigraphic strike parallel to the bedding plane fractures, with Spring Hollow as a discharge site. As discussed above, the carbonates, with low primary porosity, are subject to solutioning along fracture and fault trends. There is a northerly component of ground-water flow, particularly in the shales and siltstones. This is due to the second major fracture set, oriented north-south and dipping almost vertically. This fracture set allows an interconnectedness to the aquifer as a whole and on a large scale can be viewed as a matrix porosity, although it is overshadowed by the dominant hydraulic characteristics of the solution features.

This lithologic and structural control has allowed development of a local ground-water system with a strong component of east-west flow that is in contrast with the regional gradient to the north toward the Roanoke River. A conceptualization of the

localized hydrologic system is presented in Figure 18. Spring Hollow and Cove Hollow are sites of ground-water discharge, and Dry Hollow is a recharge area. Ground-water flow, within this localized system, has an upward gradient within the aquifer below the Spring Hollow stream, which acts as a fully penetrating stream, with flow lines converging upward from depth.

Water-table contours (Figure 17) indicate that ground water flows predominantly from Dry Hollow toward Spring Hollow, particularly along the losing (dry), middle section of Dry Hollow (Plate 1).

The evidence for a ground-water gradient from Dry Hollow to Spring Hollow is found in the preponderance of springs in Spring Hollow and a lack thereof in Dry Hollow, tracer tests results (SEA, 1987), water levels in wells, and loss of water in the corresponding on-strike Dry Hollow stream bed.

The evidence for a ground-water divide between Spring Hollow and Cove Hollow is found in both water levels in wells and the relative stream-bed elevations, as shown in Figure 9. Even though the stream-bed elevation of Cove Hollow is slightly higher than that of Spring Hollow, both streams are gaining streams. Water levels in Wells R1 and R2 are higher than the on-strike stream-bed elevations of Spring and Cove Hollows, indicating the formation of a ground-water divide.

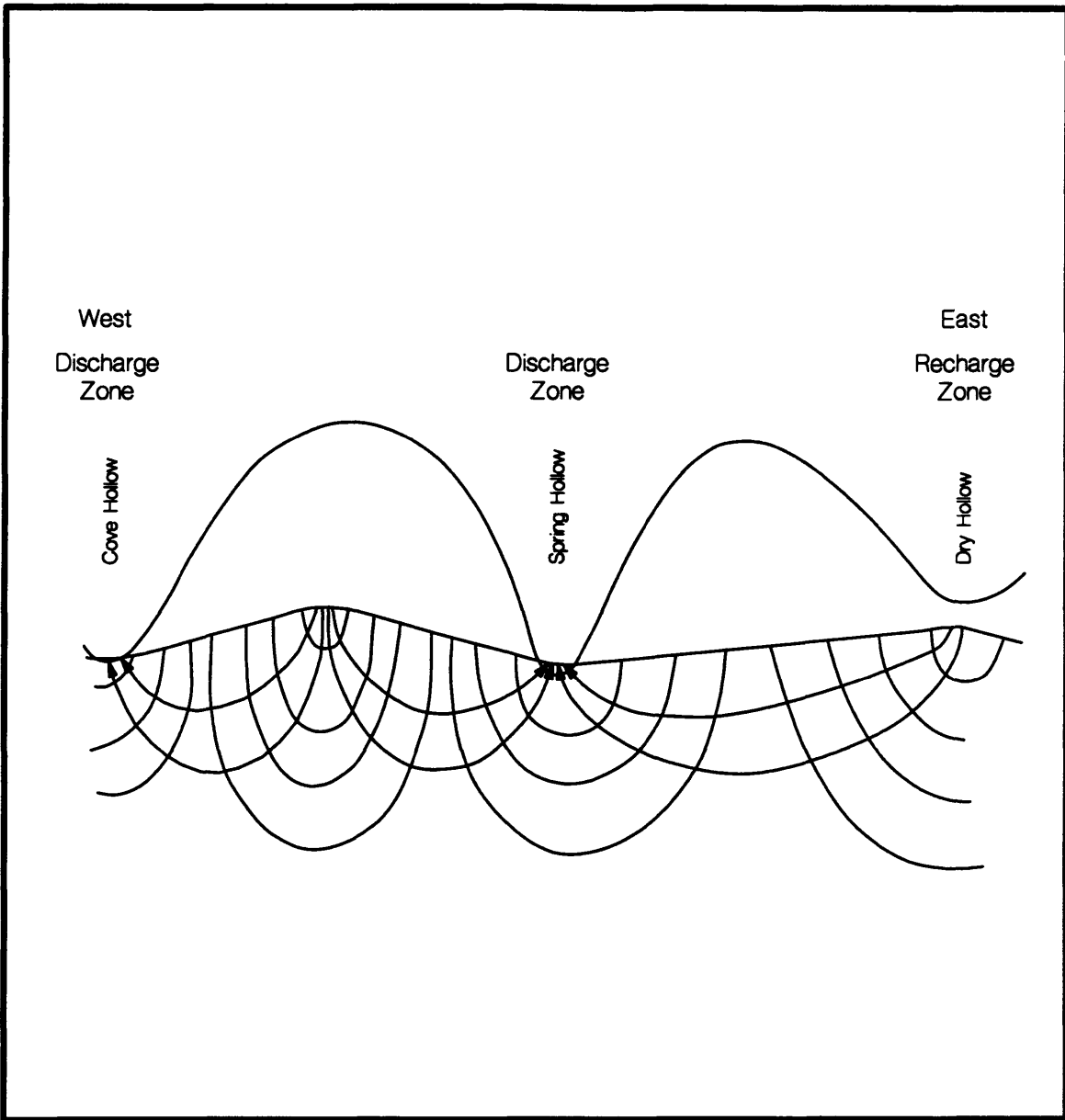


Figure 18

Hydrologic System of the Research Area

## 6.2 Delineation of Zones with Seepage Potential

Optimization of the grouting program implies minimizing the amount of time in the field drilling holes and placing grout. To accomplish this, only selected zones, those with a potential for high seepage rates, should be grouted. This results in a minimum of field time and grout volumes while reducing predicted seepage rates to an acceptable level. The results of the site characterization indicate that the solutioned and fractured carbonates will be the conduits through which unacceptably high seepage rates will occur. Identifying the carbonates that are highly fractured and solutioned is essential to a successful selective grouting program.

Three factors, each directed toward locating solutioned carbonates, were used to evaluate the seepage potential along the reservoir perimeter, including, reversal of gradient, presence of karst features, and degree of dissection of drainages. A scoring system was devised for each factor, and the reservoir was zoned according to the score for each factor, resulting in the creation of three maps. The maps were overlain, and the reservoir was again zoned to reflect the sum of the scores. The result was the seepage potential map, with a high score indicating a high seepage potential.

The dam and reservoir level were designed to be at a maximum elevation of 1410 feet (SEA, 1989). The results of the geologic, hydrologic, and geohydrologic investigations have indicated that under pre-reservoir conditions, the ground-water gradient is from Dry Hollow to Spring Hollow, and there is a ground-water divide between Spring Hollow and Cove Hollow. When the reservoir is full, the ground-water

flow system will be altered. Cove Hollow and Dry Hollow, below the stream-bed elevation of 1410 feet will be downgradient from Spring Hollow Reservoir at full capacity. Seepage out of the perimeter of the reservoir will occur on-strike with stream-bed elevations less than 1410 feet in Cove and Dry Hollows. Two zones are presented in Figure 19. The first zone includes portions of the reservoir that will be subject to seepage as a result of gradient reversal and was given a score of one. The second zone included areas of the reservoir that are not be subject to seepage as a result of gradient reversal and was given a score of zero.

Karst features, such as springs, caves, and sinkholes are indications of the presence of fractured and solutioned carbonates with high secondary porosity and potentially high seepage. The area surrounding the seepage perimeter depicted in Figure 19 was examined for evidence of karst features both within the reservoir valley, and outside the reservoir along strike. Additionally, the logs of the three wells on the ridges surrounding the reservoir valley were reviewed for evidence of subsurface solution features. The reservoir perimeter was divided into two zones. Zone 1 includes all areas with karst features and was given a score of 1, as illustrated in Figure 20. Those areas not correlated with karst features were included in Zone 2 and were given a score of zero.

The presence of a drainage in the research area is associated with a fracture zone within a carbonate, as discussed in Section 6.1.1.3. Fracture zones in carbonates promote solution porosity and represent a high seepage potential. Drainages were rated according to the degree of dissection, with the highest degree of dissection related to the highest





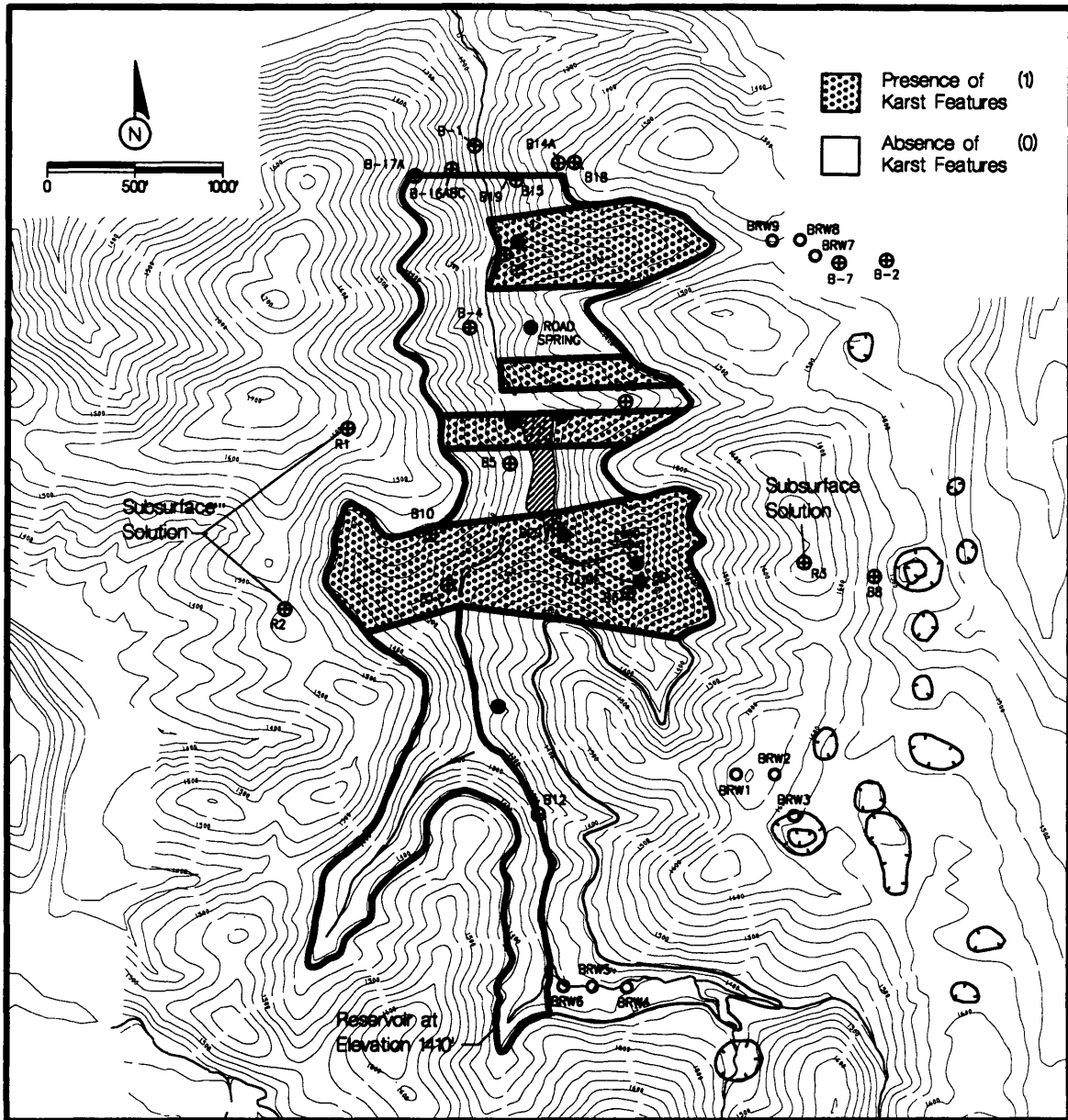


Figure 20

Zonation the Reservoir Based on the Presence of Karst Features

potential for seepage. This process resulted in four seepage potential zones, as illustrated in Figure 21. The degree of dissection was rated from one to four, with four being the most dissected.

The highest degree of drainage dissection is four times the score for the presence of karst. This discrepancy in value is not intended to suggest that a high degree of drainage dissection is a better indicator of seepage potential than the presence of solution features. Rather it reflects the uncertainty of the orientation of the fracture set with which the solution features are related. Many of the karst features in Dry Hollow follow a north-south trend which may indicate development along a fracture set related to valley development as opposed to the fracture set affecting reservoir seepage which is oriented along strike.

The three factor maps were overlain to generate the seepage potential map of Figure 22. The final zonation rating was achieved by summing the scores for each zone. New zones were generated where there was overlap. The sum of scores resulted in totals ranging from one to six, with six receiving the rating of the potential for the highest seepage rates.

Three areas with very high seepage potential occur on the east side of the reservoir, the high-solution zone, and two areas on the east perimeter of the reservoir. An area with high seepage potential occurs also on the Dry Hollow side of the reservoir.

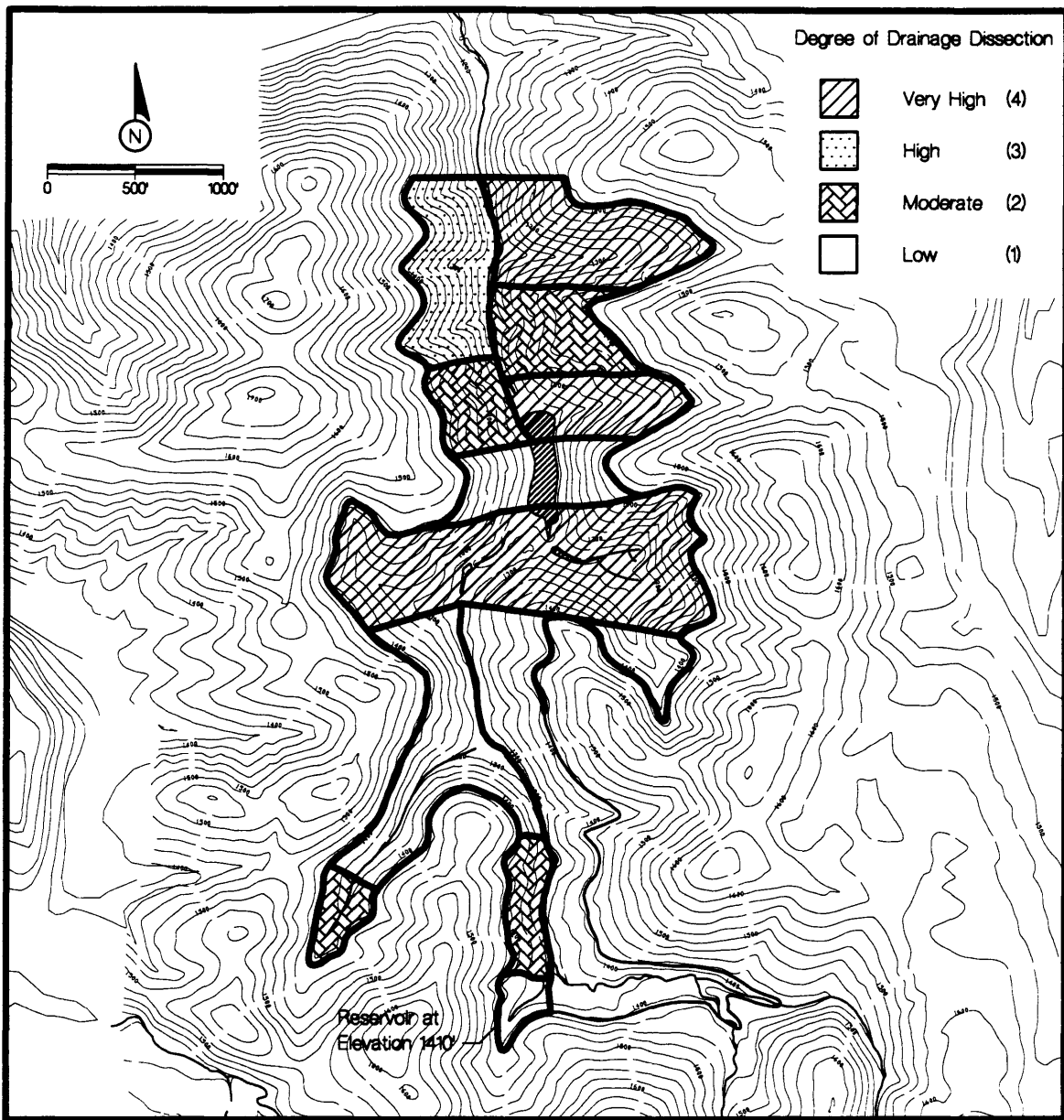


Figure 21

Zonation of Reservoir Based on the Degree of Drainage Dissection

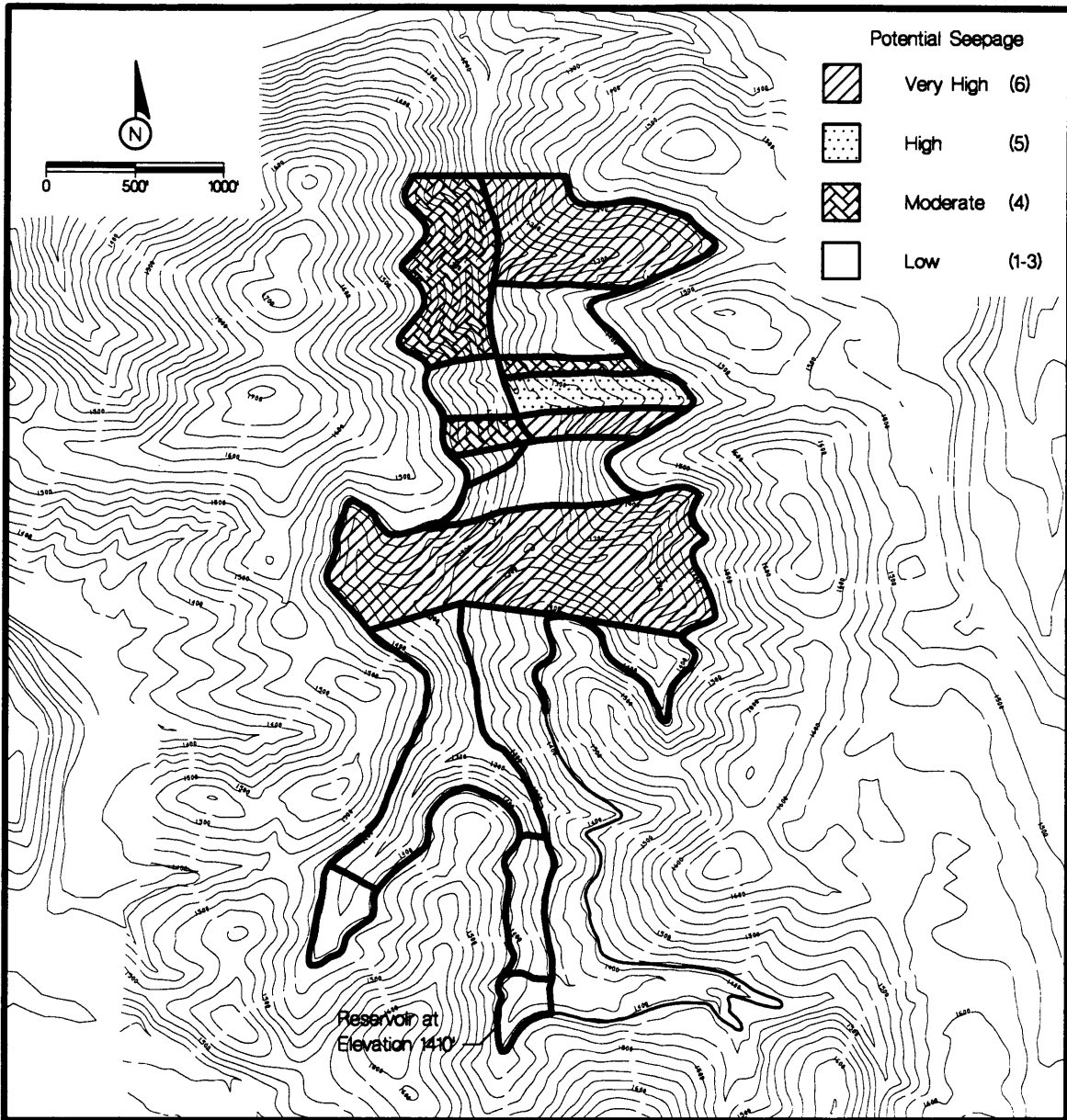


Figure 22

Seepage Potential Map of the Reservoir

### 6.3 Estimate of High-Solution Zone Seepage

In order to determine whether the area of highest seepage potential, the high-solution zone, will require grouting as a mitigation measure, the quantity of ground-water flow that an ungrouted reservoir would induce through this zone was evaluated. The results of a simplified analytical solution indicated that seepage would be excessive. An expanded numerical simulation of the high-solution zone confirmed the necessity of grouting.

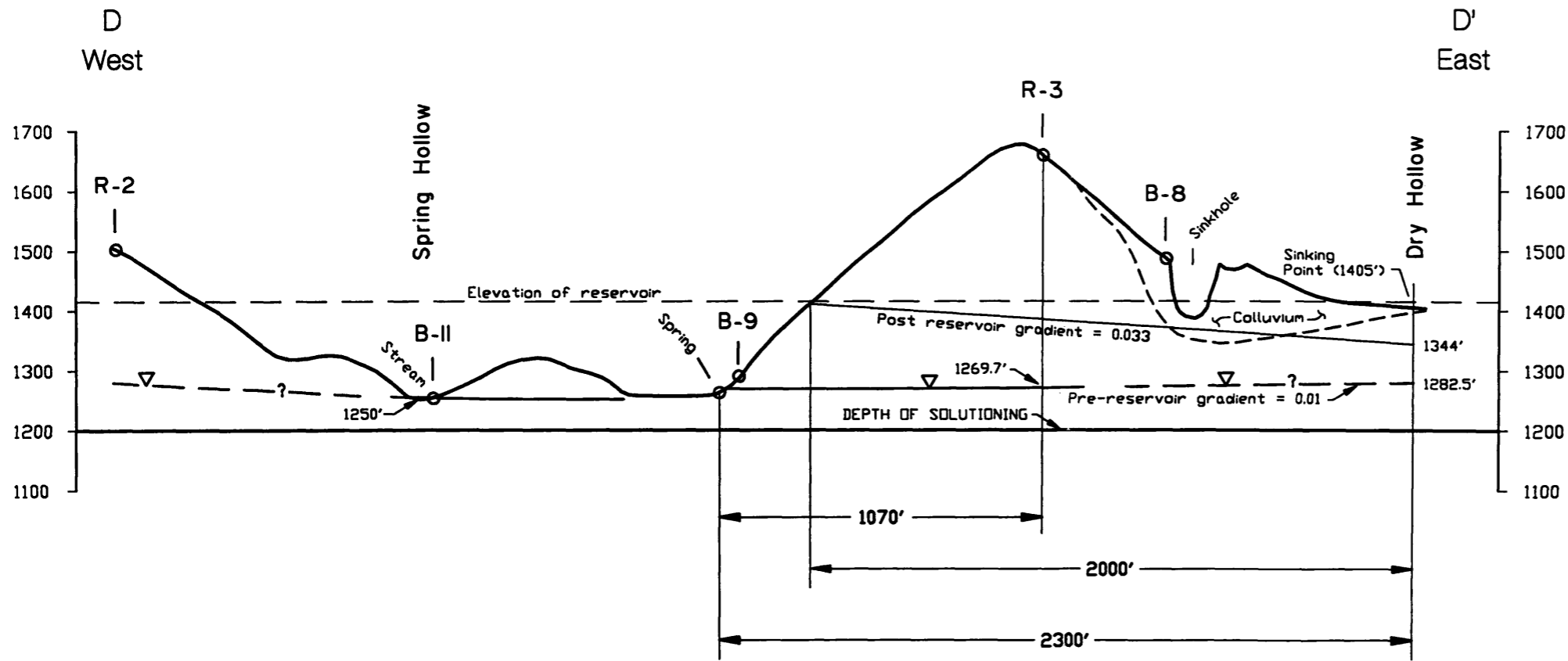
#### 6.3.1 Analytical Estimate of Seepage

A simplified analytical estimate of the amount of seepage through the zone rated as having the potential for the highest seepage rates out of the reservoir was performed using Darcy's Law as follows:

$$Q=kia$$

where:        **k** = hydraulic conductivity  
                  **i** = hydraulic gradient =  $\Delta h/\Delta l$   
                  **a** = area

Figure 23 represents a cross-section of the high-solution zone from Spring Hollow to the sinking point in Dry Hollow, and presents the physical information used for the solution of Darcy's Law. The rainfall/spring-flow records of 1989 (Figure 11) were used to calculate the average linear ground-water flow velocity ( $v^*$ ), and thereby, an estimate of hydraulic conductivity.



See Plate 1 for location of section

Figure 23

Cross-Section Through the High-Solution Zone From Spring Hollow to Dry Hollow

$$v^* = ki/n_e$$

where:  $n_e$  = effective porosity

The lag time for Dry Hollow runoff-induced spring flow was estimated to be one to two days, as discussed in Section 6.1.2.1. The distance along strike from the sinking point in Dry Hollow to the spring is 2300 feet (Figure 23). This distance and a time of 1.5 days were used to calculate an average linear ground-water velocity of 1533 feet per day (fpd). Since the water-table elevation beneath the dry stream bed is unknown, the hydraulic gradient between Well R3 and Spring B (Figure 23) was used. The distance between the well and the spring is 1070 feet. A water-level elevation of 1269.7 feet for Well R3, and Spring B elevation of 1259.5 feet were used to calculate a hydraulic gradient of 0.01. An extrapolation of this gradient and the distance between the spring and Dry Hollow yields a water-level elevation of 1282.5 feet below the stream bed.

Freeze and Cherry (1979) provide a range of 0.05 to 0.50 for the porosity of karst limestone. Both values were used as effective porosity to provide a range of hydraulic conductivity. The calculation was completed as follows:

$$k = v^* n_e / i$$

where:  $v^* = 1533$  fpd  
 $n_e = 0.5$   
 $i = 0.01$   
 $k = 76,650$  fpd

This value exceeds the range of hydraulic conductivity for a karst limestone given by Freeze and Cherry (1979) as  $2.8 \times 10^{-1}$  fpd to 2800 fpd. Use of 0.05 for the effective porosity only lowers the hydraulic conductivity by a factor of ten, to 7,665 fpd.

The spring and the sinking point are on strike with the Blankenship Cave (Plate 1), located to the east of Dry Hollow. The cave is described as being over 120 feet deep, with a base elevation of 1322 feet. It contains numerous interconnected passages, some as high as 7 feet and as long as 60 feet. In addition, an intermittent stream flows to a deep siphon within the cave (Holsinger, 1975). Review of the Well R3 well log, also within the high-solution zone, shows a ten-foot cavern between elevations 1278 to 1288 feet. When viewed in the context of these caverns, the magnitude of the hydraulic conductivity estimates seem reasonable.

In order to estimate the quantity of seepage that a reservoir at full capacity might induce through this zone, the area of flow was approximated. Based on field observations, most of the spring flow appeared to be issuing from two carbonate units as depicted in Figure 24. The combined effective width of the carbonate units was estimated to be 200 feet. The solution features within the carbonates occur along distinct pathways within unsolutioned competent rock. The percentage of the rock with secondary porosity is less than 50%, and probably around 10%, producing an effective thickness of between 20 and 100 feet and an average effective thickness of 60 feet. The saturated thickness is based on the average of the extrapolated water-table elevation beneath Dry Hollow and the reservoir elevation of 1410 feet, plus an estimated solution depth of fifty feet below



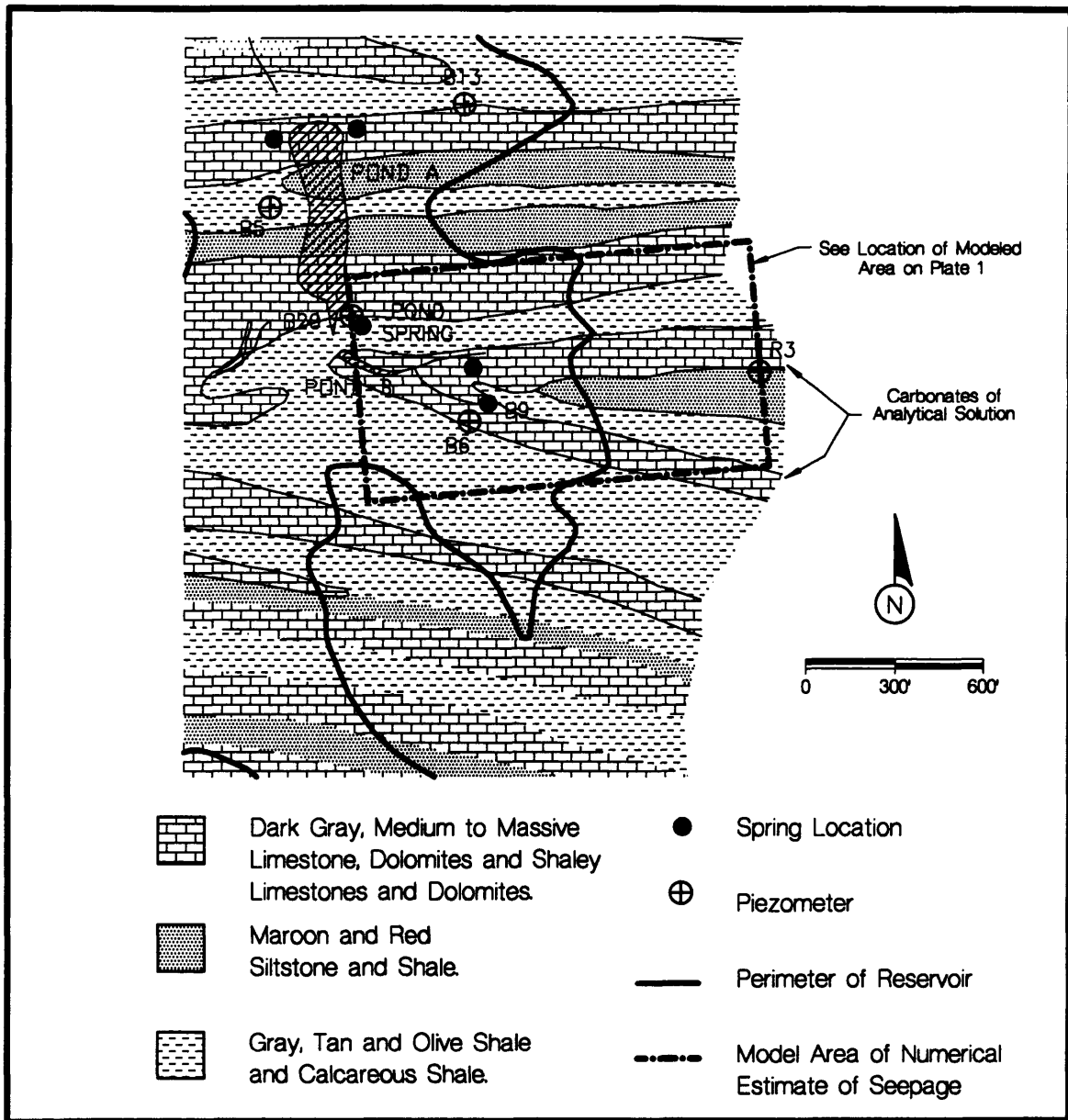


Figure 24

Geology of the High-Solution Zone Modeled for an Estimate of Seepage

the base of the on-strike elevation of the stream in Spring Hollow (1250 feet), as depicted in Figure 23. This results in a saturated thickness of 146 feet, and an area of 8,760 square feet (ft<sup>2</sup>). A post-reservoir gradient was calculated using the average of the Dry Hollow stream bed elevation of 1405 feet and the pre-reservoir Dry Hollow water-table elevation of 1282.5 feet. This average, 1344 feet, together with a distance of 2000 feet, yielded a post-reservoir gradient of 0.033.

Applying Darcy's Law, and using the calculated hydraulic conductivities, a flow of 22 million cubic feet per day (mcf/d), or 166 mgd is calculated for a hydraulic conductivity of 76,650 fpd, and a flow of 2 mcf/d, or 17 mgd for a hydraulic conductivity of 7,665 fpd. Both of these values represent seepage rates that are unacceptably high. The results suggest that mitigation of the seepage through grouting will be necessary and that a more detailed estimate of seepage is warranted.

To check for the validity of Darcy's Law, the Reynold's Number was calculated for both cases as follows:

$$R = \frac{\rho v d}{\mu}$$

where:       $\rho$  = density of water at 15° C  
                   $v$  = velocity of water  
                   $d$  = diameter of pore space  
                   $\mu$  = viscosity of water at 15° C

The velocity of the ground water was obtained by dividing the post-reservoir flows by the area. The first flow, 22 mcf/d, yielded a velocity of 0.029 fps, while the second flow of

2 mcf/d, yielded a velocity of 0.0029 fps. Using 1.940 slugs per cubic foot for the density of water,  $2.36 \times 10^{-5}$  pound force-second per square foot for the viscosity of water, and a diameter of 0.013 feet which is the equivalent of the diameter of fine gravel (Fetter, 1980), the Reynold's Numbers were calculated with the two velocities. The higher velocity resulted in a Reynold's Number of 31, while the lower resulted in 3.1. A Reynold's Number of 10 is considered by Fetter (1980) to be the upper limit of laminar ground-water flow. It is possible that conditions of turbulent flow exist in the high-solution zone.

### 6.3.2 Numerical Estimate of Seepage Rates

A simplified, steady-state, numerical simulation of the high-solution zone was performed using MODFLOW (McDonald and Harbaugh, 1991). The model was a three-dimensional approach in which the solution zone was calibrated to pre-reservoir conditions using spring flow as the calibration target. The model was executed again to simulate post-reservoir conditions for the purpose of obtaining a potential seepage rate through the high-solution zone under reservoir conditions. The modeled area includes a third carbonate in addition to the two carbonates used in the analytical solution (Figure 24).

#### 6.3.2.1 Model Setup and Input Parameters

The area of the model, the grid, and the boundary conditions are illustrated in Figure 25. The grid consisted of 27 rows and 31 columns. Boundary conditions used in

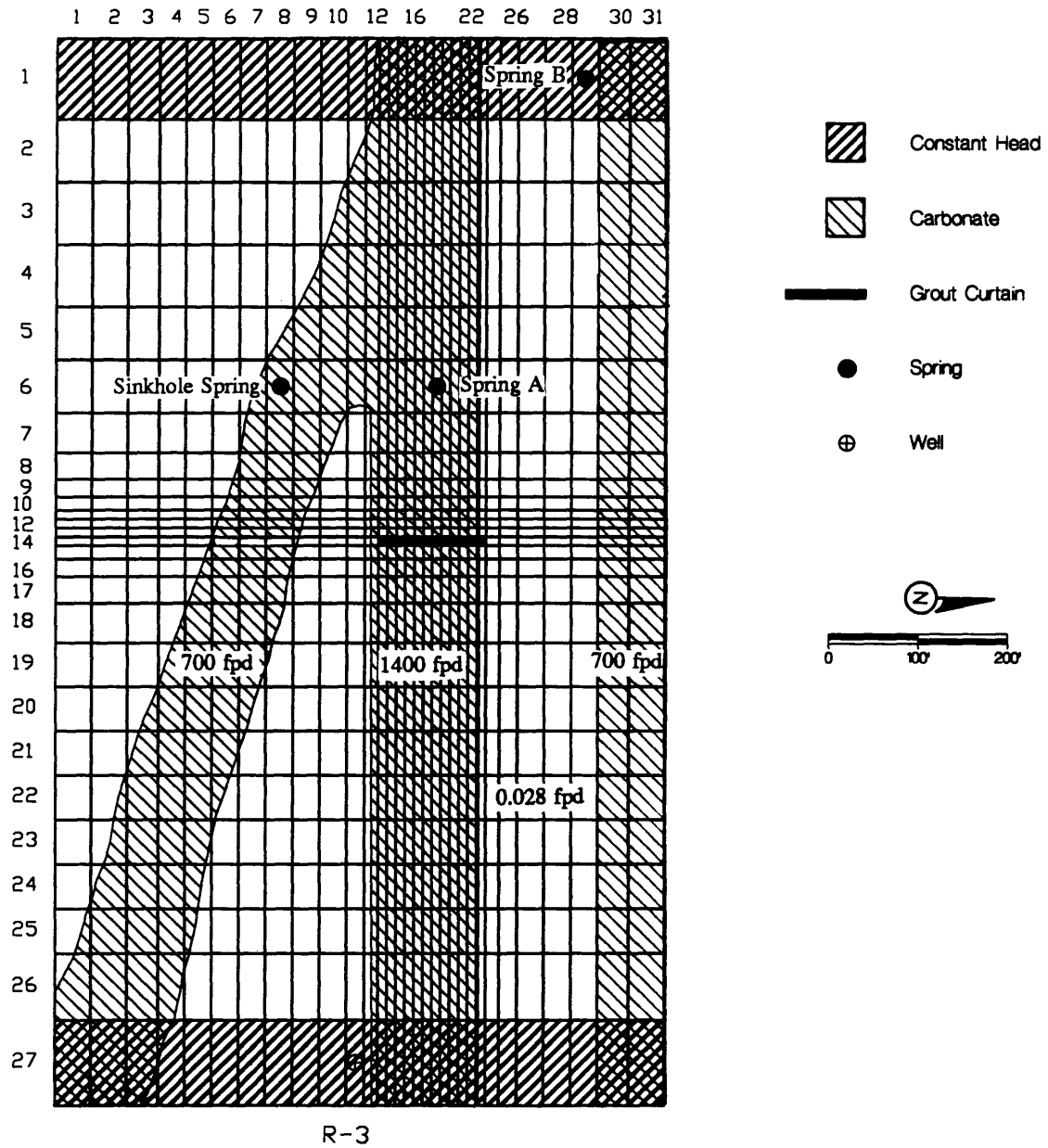


Figure 25

Model Grid Used For a Numerical Estimate of the Seepage Rate Through the High-Solution Zone

the model included constant heads on the upgradient and downgradient boundaries as indicated on Figure 25. The average of the water-level data available for Well R3 at the time of modeling, 1268.5 feet, was used as the value for constant heads on the upgradient boundary. The Pond B water elevation of 1256.5 feet provided a value for the downgradient boundary constant heads. Lateral no-flow zones were simulated implicitly at the model grid boundaries.

The thickness of the solutioned zone was assumed to extend about 50 feet below the average on-strike Spring Hollow stream-bed elevation of 1250 feet. This assumption was based on the fact that all solution features were encountered within a 50-foot interval below Pond B in boreholes drilled during the 1984 through 1988 field studies. The base of layer one was set uniformly at 1200 feet to reflect the depth of solutioning. A second layer was used to simulate the unsolutioned carbonates at depth. A thickness of 100 feet was used for layer two.

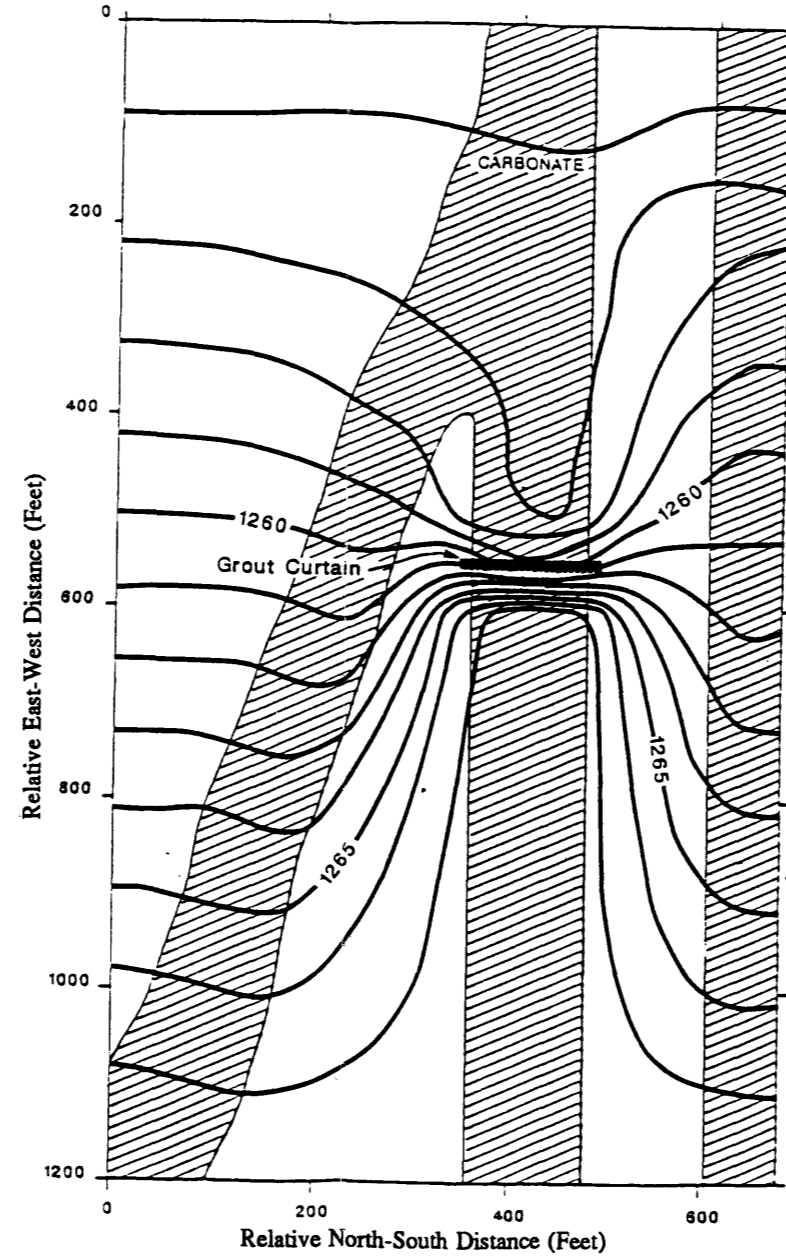
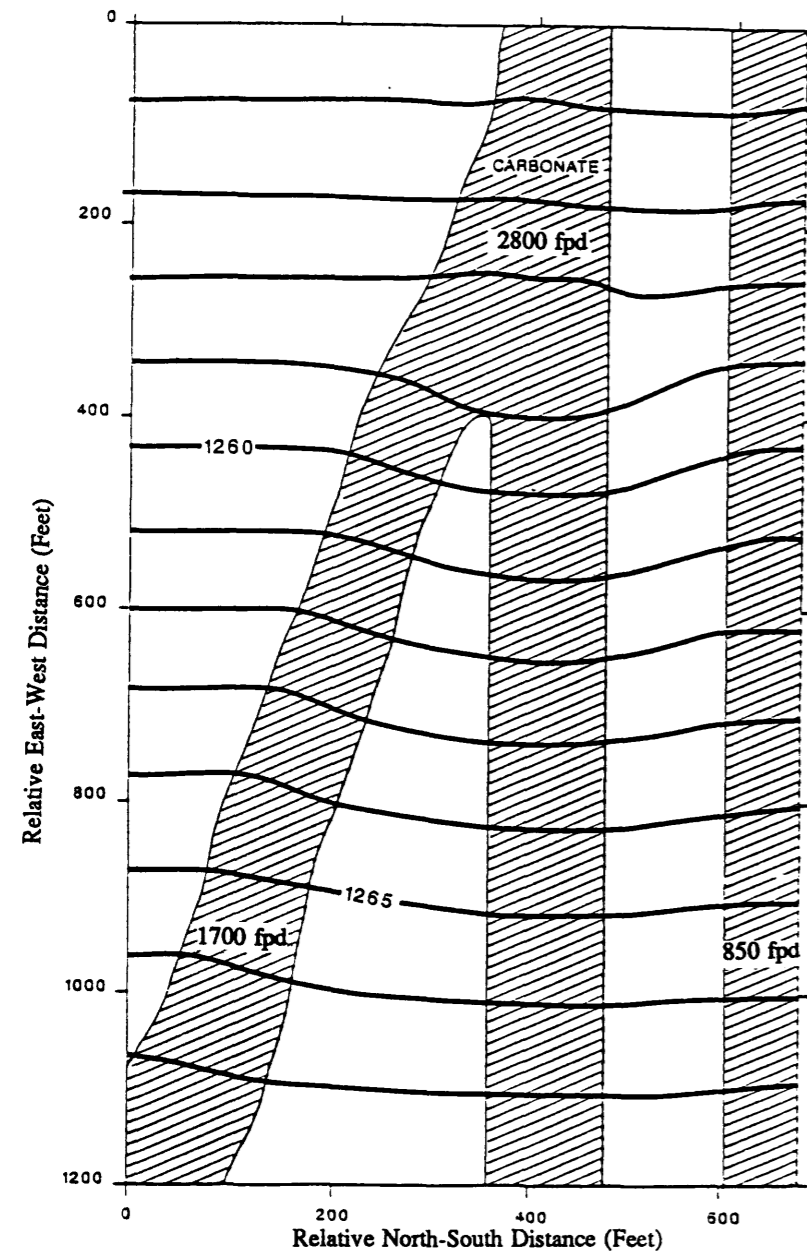
The geology of the site was simplified to represent the three major carbonate beds mapped in the high-solution zone. Initial estimates of hydraulic conductivity were derived from packer-permeability tests conducted during the 1989 field activities. These data are presented in Appendix B. Most of the hydraulic conductivities fell within the  $1 \times 10^{-4}$  to  $1 \times 10^{-6}$  cm/sec range (0.28 to 0.0028 fpd) or were listed as "impermeable." One test failed to meet pressure, suggesting the presence of significant secondary porosity due to solutioning. The bipolar results indicated that the matrix porosity of the lithologies were fairly low, whereas secondary porosity was very high. The initial hydraulic conductivities

used were 1400 fpd ( $5 \times 10^{-1}$  cm/sec) and 700 fpd ( $3 \times 10^{-1}$  cm/sec) for the carbonate beds and 0.028 fpd ( $1 \times 10^{-5}$  cm/sec) for the shale and siltstones in the top layer (Figure 25). The carbonates of layer two were assumed to be unsolutioned and, therefore, 0.028 fpd ( $1 \times 10^{-5}$  cm/sec) was used as the hydraulic conductivity for all lithologies in the second layer.

#### 6.3.2.2 Calibration and Results

The calibration was a simplified process due to the generalized conditions of the system. Calibration consisted of changing hydraulic conductivities until simulated spring flow was similar to measured spring flow. Three springs were present in the modeled area, the sinkhole spring, Spring B, and Spring A (Figure 25, Plate 1). The modeling was based on data collected during the 1989 field activities. The flume data shown on Table 4 reflect a combination of the flow from the sinkhole spring and Spring B. Spring A was measured separately. A calibrated combined spring flow of 3.02 cfs represented a conservative scenario. This value of spring flow is within the higher end of the values presented in Table 4, and was considered a satisfactory calibration.

The calibration process produced hydraulic conductivities for the lithologies enabling simulation of post-reservoir conditions. The calibrated pre-reservoir heads and the hydraulic conductivities of the three carbonates (2800 fpd, 1700 fpd, and 850 fpd) are presented in Figure 26.



(SEA, 1989)

Figure 26  
Simulated Pre-Grout and Post-Grout  
Heads of the High-Solution Zone

For the simulation of post-reservoir conditions, constant heads were set at the approximate 1410-foot elevation, Row 13 on Figure 25, to reflect the reservoir perimeter at maximum capacity. The cells downgradient of the constant heads were removed from the model. In order to approximate the change in head at Well R3 which would accompany the change in the hydrogeologic regime precipitated by a full reservoir, the upgradient boundary constant heads were set at 1375.5 feet. This value was estimated from the post-reservoir water-level contours presented in Figure 17.

Results of the simulation indicated that the total seepage out of the reservoir through the high-solution zone would be in excess of 4 mcf/d, or 30 mgd. This seepage rate compared favorably to the 17 mgd calculated with the analytical solution for the lower value of hydraulic conductivity.

Both the numerical and analytical methods for estimating seepage relied on significant simplification of the site geology and resulted in high flow quantities. Although not reliable as absolute values, they provide an indication of the magnitude of potential reservoir seepage through the high-solution zone on the east reservoir rim. A grouting program is clearly indicated.

#### 6.3.2.3 Grout-Effectiveness Piezometers

In order to optimally site piezometers so that the effectiveness of a grout curtain through the high-solution zone could be evaluated during a grouting program, post-grout/pre-reservoir conditions were simulated using the pre-grout calibration grid. The



grout curtain was simulated as ten feet thick, with an effective hydraulic conductivity of 0.028 fpd, the same as the surrounding shale and siltstone. Results of the simulation are illustrated in Figure 26. A piezometer located 50 feet upgradient of the grout curtain is predicted to register a water level rise of approximately six feet to over 1268 feet.

## Chapter 7

### EVALUATION OF GROUTING ALTERNATIVES

The results of the seepage potential analysis indicated that grouting would be necessary to mitigate seepage. In order to assess whether a grouting program would be effective in minimizing reservoir seepage to an acceptable rate, and to develop a selective grouting program, a procedure for the evaluation of grouting alternatives was developed.

The evaluation was based on the results of the Test-Grout Program (SEA, 1991a) and consisted of two parts, both aimed at assessing the impacts that a grouting program would have on seepage. The first was the demonstration that grouting could impact the flow in the high seepage zone. This was achieved through analysis of ground-water and surface-water data collected during the Test-Grout Program. Secondly, this data was utilized as input into a numerical model for the purpose of calibrating the effective hydraulic conductivity of the grout curtain and, thereby, evaluating various grouting alternatives. Essentially, an evaluation of the various grouting alternatives was directed towards optimizing a grouting plan (minimizing grouting) through selective grouting, while reducing seepage to an acceptable level.

## 7.1 Test-Grout Program

A test-grout program (SEA, 1989) was implemented in July and August, 1991 (SEA, 1991a), the site of which is shown on Figure 27. This program was developed to assess the impact of the grout on seepage through the high-solution zone on the east rim of the reservoir. Measurement of how well the grout reduced seepage was achieved by monitoring spring flow with a Parshall Flume located downgradient of the springs, and by monitoring water levels in strategically-located, up-gradient monitoring wells as indicated on Figure 28. The wells provided a method of verifying the impact of the grout while reducing the need for "check" boreholes traditionally drilled to examine core for the presence of grout. During grouting, the 1415-foot contour was stripped with a bulldozer to make an access road for drilling equipment. The geology along this road was mapped in detail.

### 7.1.1 Grouting Results

By the end of the program in August, 1991, 6065 cubic feet of grout had been placed (SEA, 1991a) along the perimeter of the 1415-foot topographic contour in an area believed to include the highly solutioned carbonates in line with the springs (Figure 27).

Numerous solution features were encountered during drilling, including large voids and intervals described by the drillers as "honeycombed." These features were consistent with the seepage potential rating of very high. Rock core descriptions and surface mapping along the grout curtain access road substantiated the karst character of the rock and

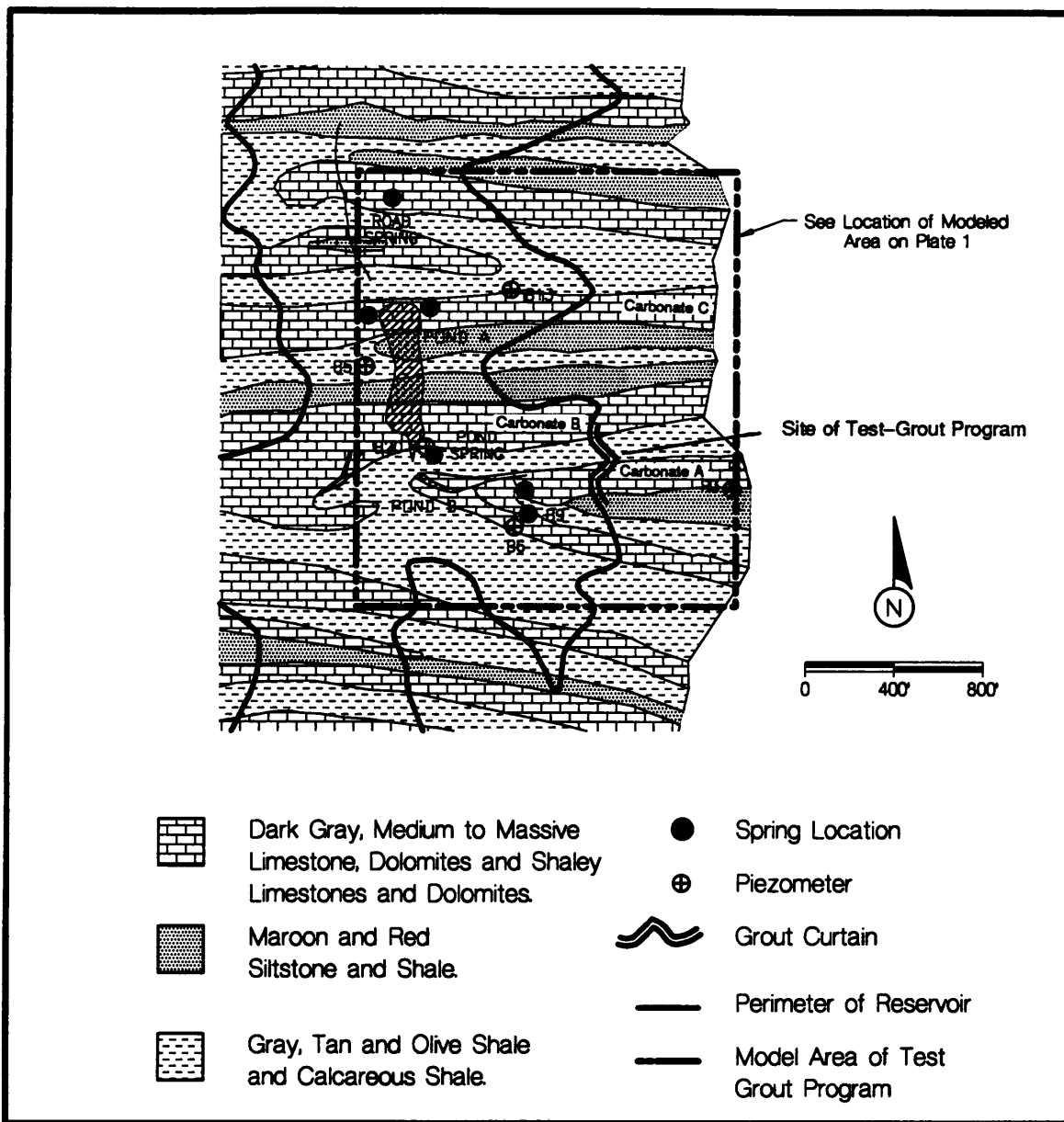


Figure 27  
 Area of the Test-GROUT Program

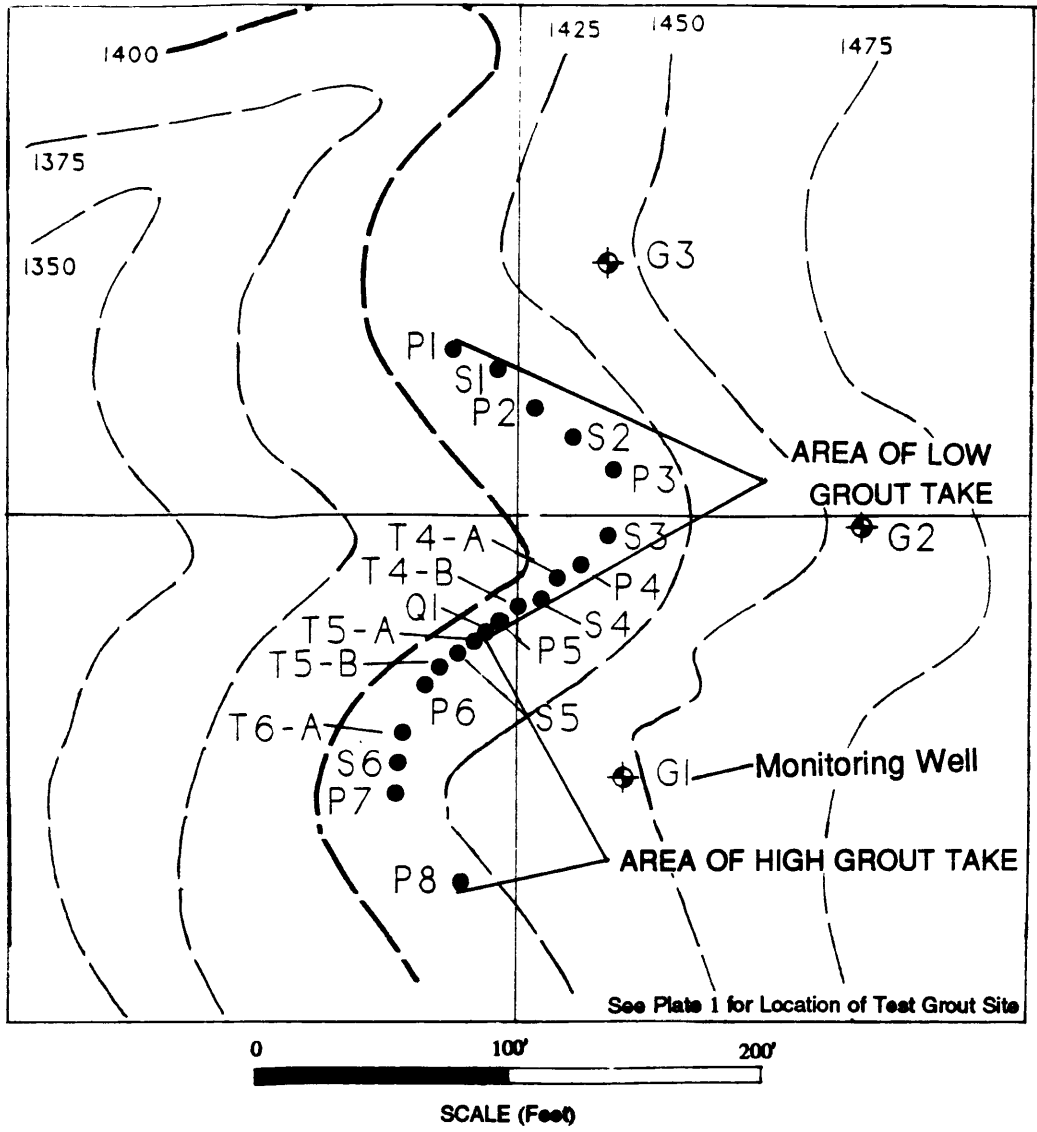


Figure 28

Locations of Grout Holes at the Test-Grout Site

validated the designation of this zone as "high solution." The limestones exhibit more solutioning than the dolomites. Where either the limestones or dolomites are associated with the calcareous maroon shale, the solution porosity is the greatest. Additionally, both surface and subsurface geology indicate that this is a fracture zone, evidenced by the presence of breccia, intense fracturing and offset bedding. Based on surface mapping, strata in this area dip between 65 and 85 degrees to the north. The detailed geology along the length of the grout curtain is shown in cross-section in Figure 29.

In zones of very high secondary porosity, a large amount of grout was placed. In some holes, the grout failed to meet pressure and much of the grout moved into other holes, and muddied water flowing from the springs. This indicated not only that solution porosity was large, but also that the springs were directly connected to the solution features in the holes.

Only in a qualitative sense can the amount of grout be related to hydraulic conductivity. High grout takes indicate high solution porosity, and, therefore, high hydraulic conductivity. The areas of the greatest grout takes are indicated on Figure 28. Grout volumes per grout holes are listed in Table 6. The highest grout takes were coincident with the limestone/maroon shale association.

#### 7.1.2 Ground-Water and Surface-Water Monitoring

As part of the program, three wells were installed upgradient of the grout curtain to monitor rises in water levels concurrent with emplacement of grout (Figures 28 and

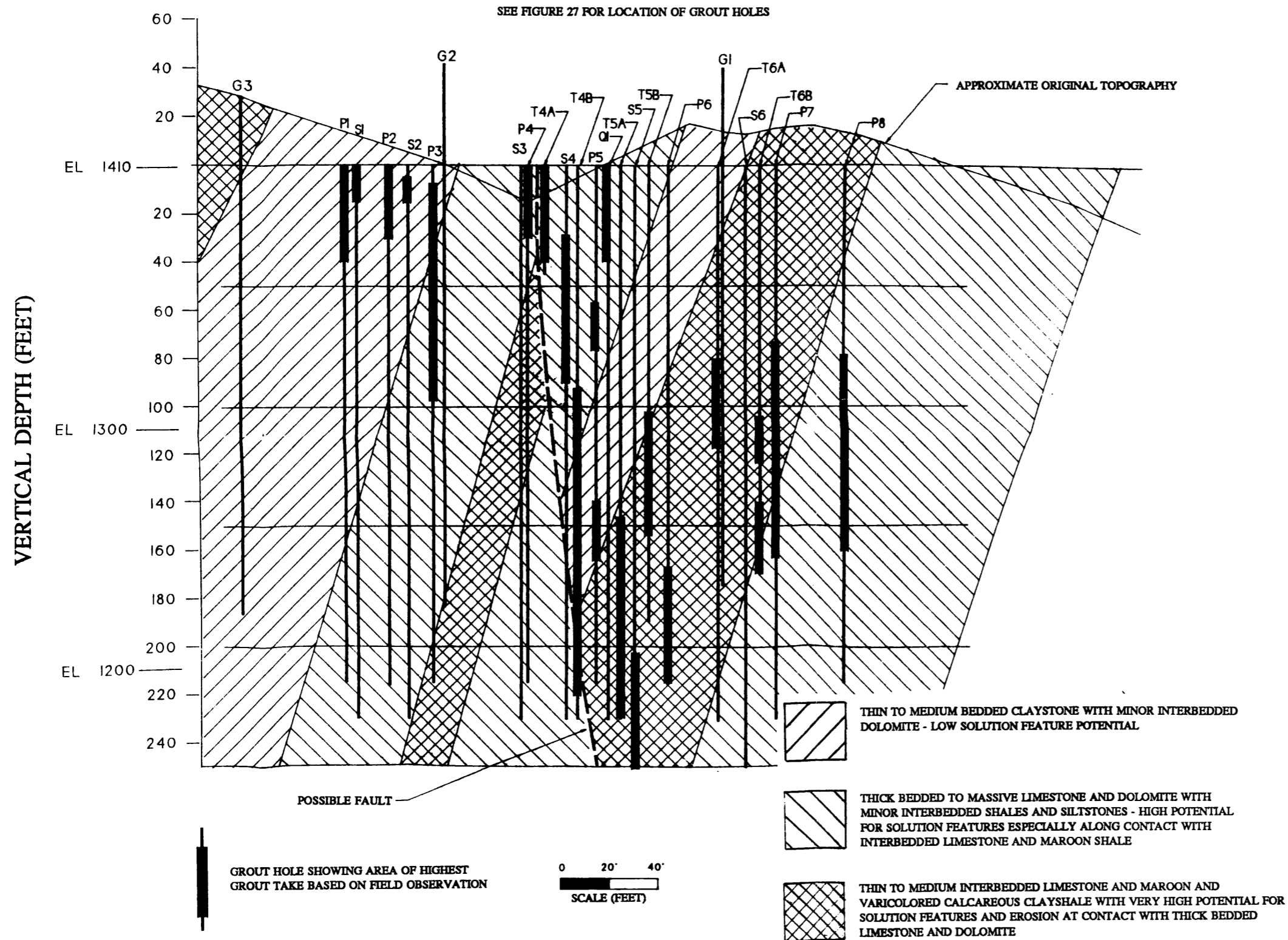


Figure 29  
Geologic Cross-Section  
of the Test-Grout Site

Table 6

## Grout Volume per Grout Borehole

Grout Hole	Cubic Feet of Grout
P-1	12
P-1	18
P-3	39
P-4	38.5
P-5	40
P-6	640.3
P-7	271.9
P-8	721.2
S-1	13
S-2	27
S-3	6
S-4	28
S-5	21.4
S-6	644.9
T-4A	40
T-4B	NA
T-5A	182.45
T-5B	129
T-6A	78.5
T-6B	1904.9
<b>TOTAL</b>	<b>1904.9</b>

NA Not Available



29). Of these three wells, only Well G1 proved suitable for use. Well G2 corresponds to the shallower water table discussed in Section 6.1.4.1. Well G3 displayed little to no variation in water elevation over time, and it may well have been sealed by migrating grout during the program. Well R3 was also monitored throughout the test program. The Parshall flume measuring the spring flow from the high-solution zone was monitored on a daily basis.

### 7.2 Evaluation of Grout Impact on Seepage

Grouting practices often employ a shotgun approach in a grout program, thereby insuring through sheer magnitude of the volume of grout and continuity of the curtain that a reduction in seepage is achieved. However, a selective grouting program, when designed with a sound knowledge of the site geology and hydrology can achieve the same result with a reduced level of effort.

The success of a grouting program is evaluated in the field through two common methods, grout take and permeability testing (Bowen, 1981). Using the grout-take method of evaluation, the grout is considered adequate when there is refusal, that is, when the hole will take no more grout under the grout pressure being applied or when the hole takes grout at less than a prescribed minimum rate (Sherard, et al., 1963). The adequacy of grouting can be evaluated through the use of "check" holes (up to 10% of the holes) which are cored for the purpose of observing the presence of grout and which are generally not grouted. The effectiveness of the grout can also be measured by pressure

testing a secondary set of grout holes prior to grouting (Kipko, et al., 1993). The grout is effective if the test provides a result close to the permeability standard set prior to the grouting program.

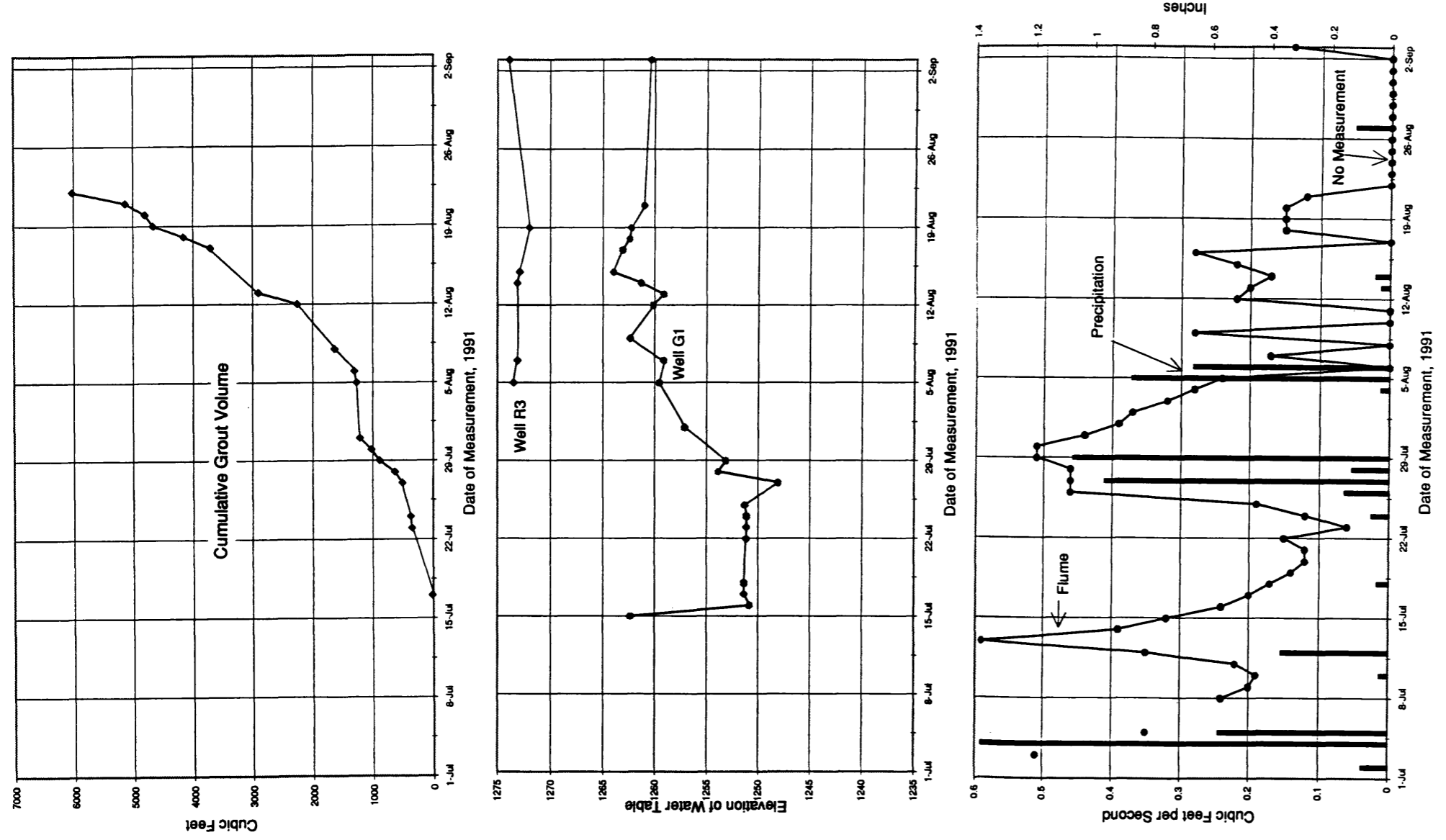
Performance evaluations, that is, assessments of how well the grout curtain actually reduces seepage after the grouting program is completed, are rare. This is primarily due to the expense involved (Bowen, 1981). Performance assessments are generally post-grout in nature and involve laboratory testing. This may be more relevant for compaction grouting where strength is the objective of the grouting program. Where reduction in seepage is the objective of grouting, meaningful post-grout performance assessments must be field-oriented and directed toward the performance of the grout curtain as a whole.

In order to evaluate the performance of the grout curtain at the Spring Hollow Reservoir site, two approaches were employed to evaluate the impact of the grout curtain on seepage. First, an analysis of surface-water and ground-water data collected during the Test-Grout Program provided a means of quantifying the success of the program while in the field. The analysis allowed a means of day-to-day feedback on the effectiveness of the grout. Second, a numerical model of the site of the Test-Grout Program was used to quantify and predict seepage by using the data provided by the grouting and monitoring activities. This numerical model was used to develop a site-wide grouting strategy by evaluating grouting alternatives and optimizing a method while minimizing seepage to an acceptable level, based on the predictive abilities of the model.

### 7.2.1 Ground-Water and Surface-Water Monitoring

Both Wells G1 and R3 exhibited a positive response to grouting (Figure 30). As the volume of grout increased over time, the water levels in both wells rose. The average water level in Well R3, prior to grouting, was 1268 feet. During the grouting program, from mid-July through the late August, 1991, the water levels rose five feet to 1273 feet in R3 and nine feet to 1259 in G1. This is consistent with the results of the steady-state numerical modeling of this zone discussed in Section 6.3.2.3, where a conservative estimate of a six-foot rise in the water level 50 feet behind the grout curtain was predicted. Well G1 is located 88 feet upgradient of the grout curtain.

The variation in spring flow during the grouting program can be related to the affects of grouting. Prior to grouting, the combined spring flow of Spring A and the sinkhole spring was measured at the flume as just under 0.2 cfs. This is much lower than the 1989 low flow (SEA, 1989) of 0.67 cfs measured in early July (Table 4). Grouting appeared to be reducing spring flow to less than 0.1 cfs on July 23, but over two inches of rainfall occurred on July 25th, and the spring flow increased to 0.6 cfs. Based on 1989 data, a rainfall of this magnitude would have been expected to increase spring flow by a much greater quantity. For example, a 1989 rainfall of 5.5 inches over three days, produced a spring flow of 2.98 cfs. Another rainfall of 4.5 inches over five days in July, 1991 (again during the grouting program), resulted in only a 0.6 cfs spring flow indicating that the grouting program had a significant impact on seepage through the high-solution zone. At the completion of the test-grout program, the base spring flow had been reduced



(From SEA, 1991)

Figure 30  
Hydrologic and Grout Data,  
Recorded During the Test-Grout Program

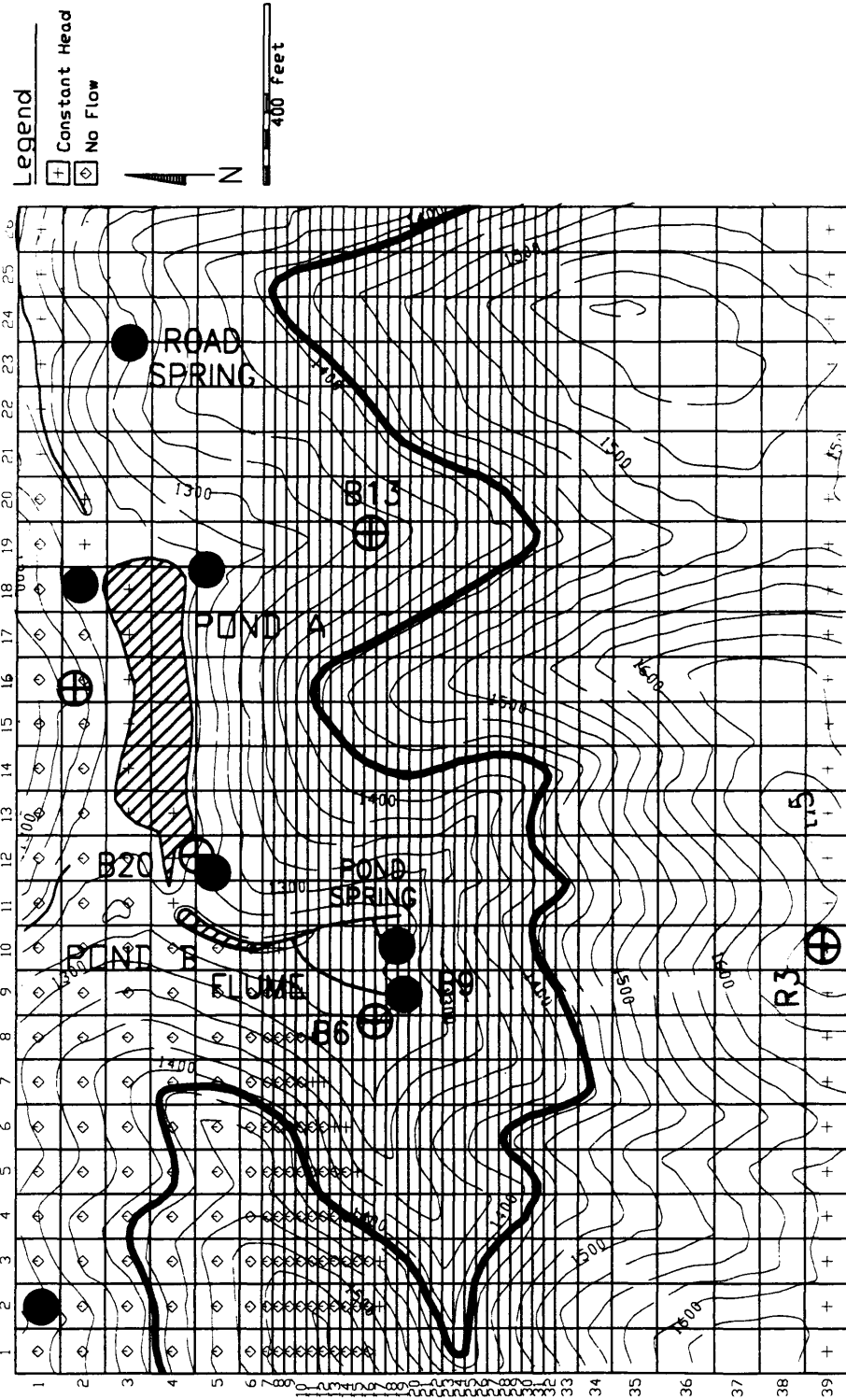
from about 0.2 cfs at the beginning of the program to 0.05 cfs at the end of the program. It is noted that the grout curtain was not completed at the end of the test program, due to depletion of funds. Total shutdown of the spring flow at the flume, therefore, was not achieved.

### 7.2.2 Numerical Simulation and Prediction

In order to quantify the success of the Test-Grout Program and to develop and evaluate a grouting program, the pre-grout conditions of a portion of the site were simulated in a simplified, steady-state, two-dimensional numerical model using MODFLOW. Spring-flow, water-level, and physical-properties data used for setting up and calibrating the model were obtained during the Test-Grout Program. Included in the simulation were Carbonate A and B (Figure 27) of the high-solution zone including the carbonate on strike with the Pond Spring (just to the north of the high-solution zone), as well as Carbonate C farther to the north.

#### 7.2.2.1 Model Setup and Input Parameters

The modeled area is shown in Figure 27. The grid and the boundary conditions are illustrated in Figure 31. The grid consisted of 39 rows 26 columns and one layer. Boundary conditions included constant heads on the upgradient boundary near Well R3, along the ridge separating Spring Hollow and Dry Hollow, and downgradient along the stream valley. These constant heads provided a controlled source of ground-water flow



See Plate 1 for Location of Test Grout Model

Figure 31  
Test-Grout Program  
Numerical Model Grid and Boundary Conditions

into and out of the model boundaries. Initial heads and values for constant heads were based on the water-table contours illustrated in Figure 17. No-flow zones were implicitly modeled along the south and north boundaries.

The geologic mapping along the high-solution zone during field activities provided information on the number of carbonate beds and their relative solution state. The range of hydraulic conductivities (Appendix B) was wide. Generally at depths below the influence of surface conditions, the shales, siltstones, and unsolutioned carbonates were fairly tight, with an average hydraulic conductivity of  $2.8 \times 10^{-2}$  fpd ( $1 \times 10^{-5}$  cm/sec). The presence of solutioned carbonates was recognized in core and by failure of the packer to pressurize during water pressure testing and grouting. Results of field mapping and core logging during the Test-Grout Program suggested a correlation between the occurrence of a carbonate adjacent to a maroon shale and the development of large solution features. These carbonates can have a hydraulic conductivity of 2800 fpd (1 cm/sec) or higher. During the grouting program, both Spring B and the sinkhole spring muddied as the upgradient carbonate (the north carbonate on Figure 24 and Carbonate A on Figure 27) was grouted, indicating interconnection. Carbonate A is in contact with a maroon shale. Two other carbonates within the modeled area were identified as occurring adjacent to maroon shales, and are labeled as Carbonates B and C on Figure 27. For the purposes of modeling, initial hydraulic properties of the lithologies present can fall into one of these two categories, either low hydraulic conductivity, on average  $2.8 \times 10^{-2}$  fpd, or high hydraulic conductivity, 2800 fpd.

Based on the depth of grout holes at the test-grout site, the depth of the aquifer was estimated to be 80 feet below the water table shown in Figure 17. This thickness was based on data obtained during grout-hole drilling, where significant solution features were found at elevation 1159 feet, 251 feet below the ground surface of 1410 feet. This is approximately 80 feet below the on-strike stream-bed elevation of 1240 feet.

#### 7.2.2.2 Calibration and Results

The calibration of the model was achieved through adjusting hydraulic conductivities so that simulated heads were similar to field head trends, while matching the total flow into the constant heads at the stream to the spring flows through Carbonates A and B. Only two wells fell within the modeled area, Wells R3 and G1. Well R3 was within a constant head cell and, therefore, could not be considered a target well. No seasonal data were available for Well G1 since it was installed immediately prior to grouting. However, the initial water-level elevation of 1250 feet was used loosely as a pre-grout target. To represent a worst-case scenario, the target for the combined flow of Spring B and the sinkhole spring through Carbonate A was the high end of the flows measured at the flume during the 1989 field study (Table 4, Figure 11), approximately 3 cfs. A Pond Spring flow of 0.26 cfs (based on estimates made during the Test-Grout program) was used to calibrate Carbonate B.

Calibration resulted in hydraulic conductivities of 2340 fpd for Carbonate A and 320 fpd for Carbonate B, with spring flows at 2.9cfs and 0.26 cfs. The simulated water



level for Well G1, which occurs within Carbonate A was 1255 feet. The northernmost carbonate, Carbonate C was assumed to have the same hydraulic conductivity as Carbonate B. The unsolutioned carbonates and the claystones retained their initial hydraulic conductivity of  $2.8 \times 10^{-2}$  fpd. Data input files for the calibrated model are listed in Appendix C.

### 7.3 Development of Grouting Alternatives

In order to develop a grouting program, grouting alternatives were explored. The grouting alternatives represented the level of effort and expense associated with a grouting program in terms of effectiveness of the grout curtain. Additionally, the evaluation of alternatives presented a level of expectation of seepage reduction associated with effectiveness of the grout curtain.

Using the calibrated pre-grout model, post-grout conditions were simulated to establish the hydraulic conductivity of the grout curtain (Figures 27 and 28) in the high-solution zone. The hydraulic conductivity of the grout curtain was calibrated against the change in head of Well G1 from pre-grout through post-grout conditions. The head in Well G1 at the end of grouting was 1259 feet, which represents a nine-foot change in head. This produced a grout curtain hydraulic conductivity of 50 fpd ( $1.8 \times 10^{-2}$  cm/sec) and a simulated head of 1264 feet in Well G1. This head represents a 9-foot rise from the pre-grout simulated head of 1254 feet.

In order to provide a baseline against which to gauge the effectiveness of the grout curtain under reservoir conditions, an estimate of seepage of the reservoir without a grout curtain was simulated. Execution of the model for post-reservoir, pre-grout conditions within this zone was performed by setting heads constant at the 1410-foot elevation contour to simulate the reservoir at maximum capacity. This resulted in maximum seepage rates of almost 53 million gpd, with 41 million gpd through the high-solution zone Carbonate A alone (Table 7).

This was followed by a series of simulations assessing seepage reduction at various grout curtain hydraulic conductivities. The grout curtain was simulated in the cells of the three carbonates at the 1410-foot elevation representing the reservoir at maximum capacity. The first simulation was with a grout curtain hydraulic conductivity equal to that achieved during the Test-Grout Program, 50 cfd. This grout curtain resulted in a 50% seepage reduction from that of the reservoir without a grout curtain (Table 7). The results of simulations using other grout curtain hydraulic conductivities are presented in Table 7. Based on the results of these analyses, a grout curtain effective hydraulic conductivity of 2.8 fpd ( $1 \times 10^{-3}$  cm/sec) is sufficient to reduce reservoir seepage by 91% to almost 5 million gpd, which is within tolerable limits. An examination of Table 7 also indicates that a grout curtain effective hydraulic conductivity of 0.28 fpd ( $1 \times 10^{-4}$  cm/sec) would reduce the reservoir losses to about 708,000 gpd, well within the desirable seepage range of 1 to 2 mgd (SEA, 1989).

Table 7  
 Seepage Through Carbonates A, B, and C at Various Grout Curtain  
 Hydraulic Conductivities with Reservoir at 1410-Foot Elevation

Location	No Grout Curtain	Hydraulic Conductivity of Grout Curtain				
		1.8x10 <sup>-2</sup> cm/sec <sup>1</sup> (50 fpd)	1x10 <sup>-3</sup> cm/sec (2.8 fpd)	1x10 <sup>-4</sup> cm/sec (2.8x10 <sup>-1</sup> fpd)	1x10 <sup>-5</sup> cm/sec (2.8x10 <sup>-2</sup> fpd)	
Carbonate A (cfs) (Flume)	63	23	2	0.2	0.02	
Carbonate B (cfs) Pond Spring	9.8	8.1	1.8	0.2	0.02	
Carbonate (cfs)	9.1	8.6	3.8	0.6	0.07	
Total (gpd)	52,785,000	25,878,000	4,936,000	708,000	115,000	
Percent Reduction	NA	50	91	99	99.8	

<sup>1</sup> Effective Hydraulic Conductivity of Grout  
 Curtain at Test-Grout Program Site

The results of the Test-Grout Program and the numerical simulations based on the results of the Program indicate that grouting can achieve significant reduction in seepage at the site. Additionally, selective grouting of carbonates to achieve a grout curtain hydraulic conductivity as high as 2.8 fpd can reduce seepage to a tolerable level. A grouting program to reduce grout curtain hydraulic conductivity to 0.28 or 0.028 fpd is an alternative which may not be cost effective, since a gain in seepage reduction of only eight or nine percent represents a much greater effort.

## Chapter 8

### EVALUATION OF GROUT EFFECTIVENESS

The subsurface conditions exposed during drilling in the high-solution zone during the Test-Grout Program validated the method of delineating potentially high seepage areas. The results of the subsurface investigation also verified the designation of a zone with a high potential for the presence of a high solution porosity in the form of voids and caverns. This field verification lends credibility to the reliability of the seepage potential map and allowed the development of a selective grouting program.

Based on the seepage potential map (Figure 22), four areas of very high potential seepage and two areas of high potential seepage were considered for selective grouting. The grout zone plan recommended by SEA in 1991 included four grout zones, Zones 1 through 4, and is shown in Figure 32, overlain on the seepage potential map. The selected grout zones included all of the areas designated as having very high and high seepage potential (Figure 22), except for the area just south of the dam on the east rim of the reservoir. It was omitted as a grout zone because the spring is very low-flow, and there are no visible karst features. Additionally, an area designated as having a low seepage potential was included in Zone 1. This low seepage potential area was included

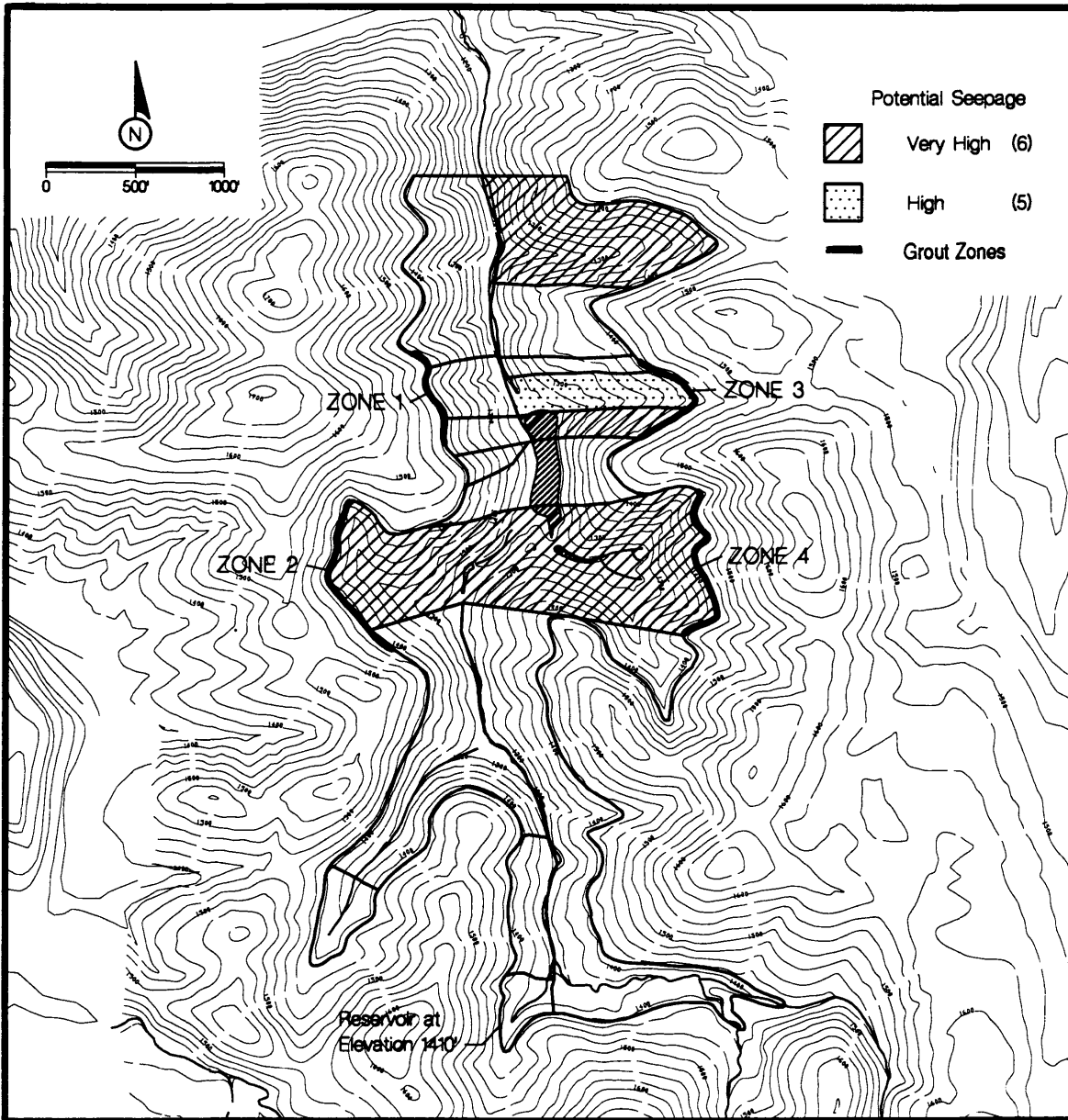


Figure 32

Selected Grout Zones for the Reservoir-Wide Grout Program

because it is on-strike with the very high seepage potential area across the stream in Zone 3.

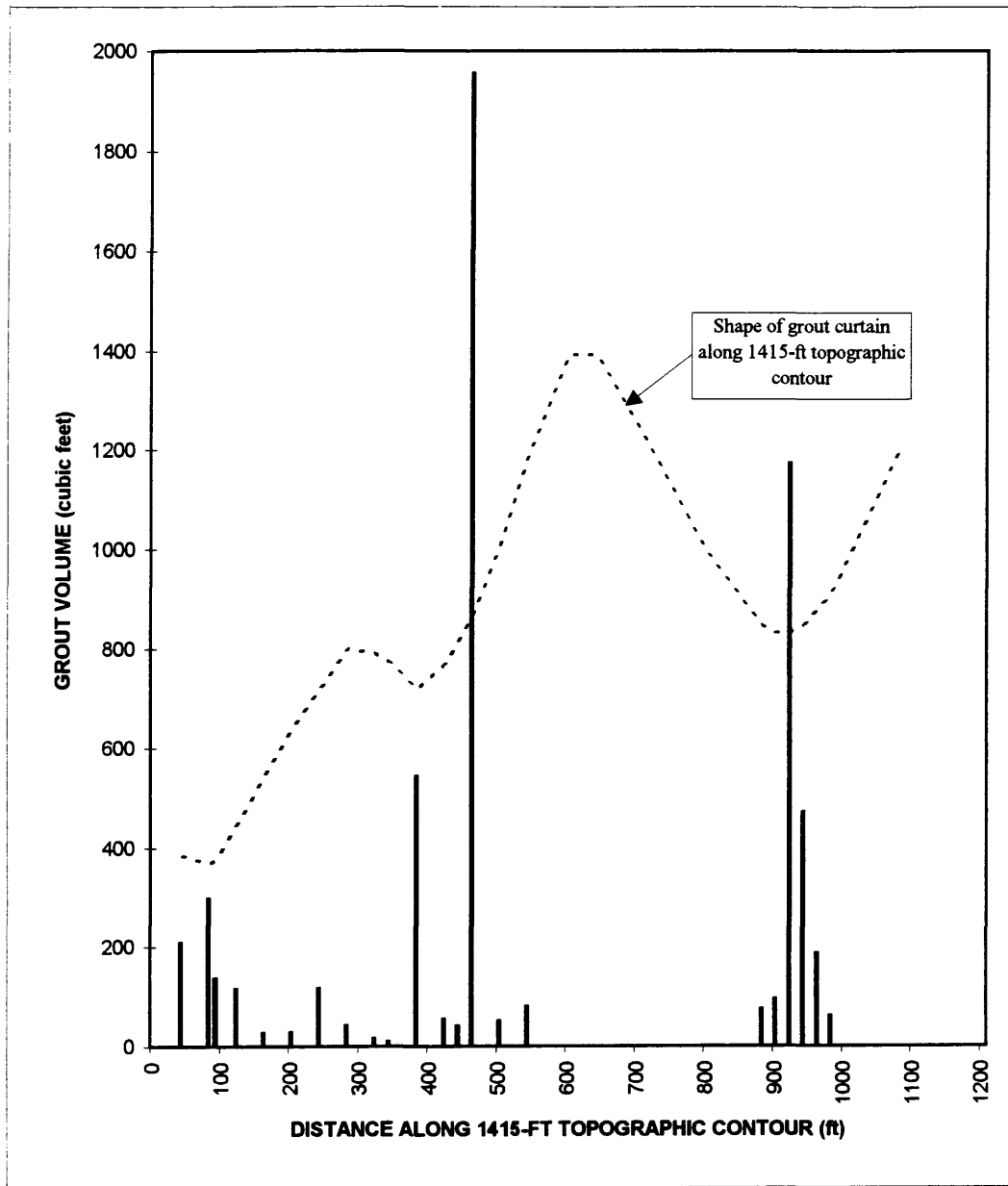
The reservoir-wide grouting of the four zones (Figure 32, Plate 1) took place in 1992. Additional grouting along the 1315-foot elevation above the Pond Spring (Plate 1) was completed in late 1993. In order to assess the success of the grouting program and to predict post-reservoir seepage rates, an evaluation of the grout effectiveness was conducted.

### 8.1 Reservoir-Wide Grouting Program

The grouting program began in January, 1992 with the construction of a road along the perimeter of the reservoir at the 1415-foot elevation. Geologic mapping of the reservoir perimeter along this road was initiated in January. Piezometers were installed and exploratory holes were drilled in each zone during February, 1992. By March of 1992, grouting had begun in earnest.

#### 8.1.1 Grout and Concrete Volumes

Grouting began in Zone 1 in June, 1992. By August 13, 1992, 4,556 feet of 3-inch hole and 1185 feet of 6-inch hole were drilled with 2,646 cubic yards (cy) of grout (dry volume of cement and water mix) and 122.3 cy of concrete (dry volume of sand, cement, water and bentonite mix) placed. Figure 33 is a representation in bar graph form of the volume of grout placed per grout hole along the 1415-foot topographic contour.



Grout curtain location is shown on Plate 1.

Figure 33

Grout Volumes in Grout Zone 1



No substantially porous intervals were encountered, however one hole took 1958 cubic feet (cf) of grout and concrete.

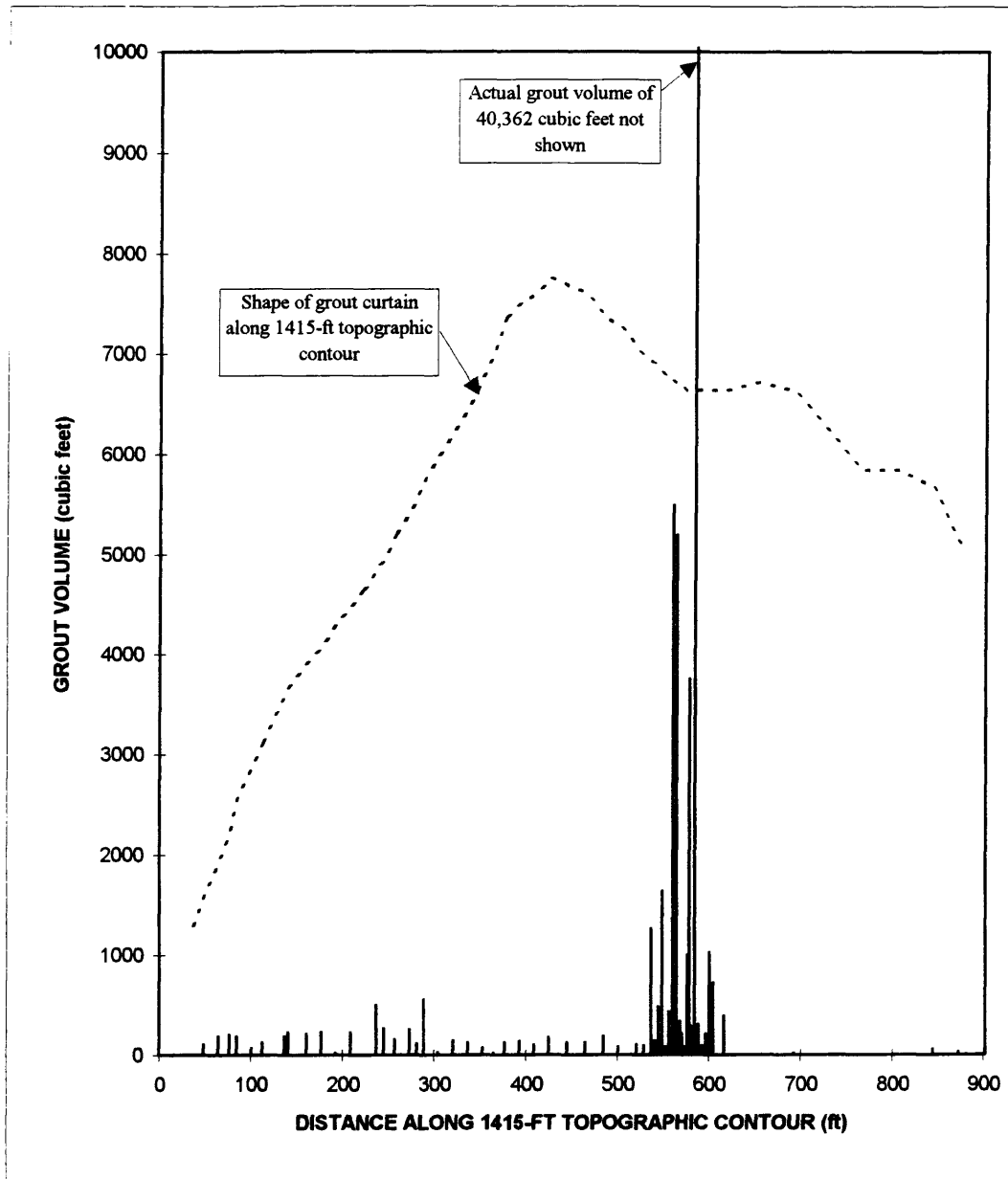
Zone 2 grouting commenced on April 30, 1992. By September 21, 1992, 9156 feet of 3-inch hole and 5919 feet of 6-inch hole had been drilled with 17,295 cf of grout and 1,946 cy of concrete placed (Figure 34). Consistent with the seepage potential map, a significant amount of solution features were encountered in this zone. Over 40,368 cf of grout and concrete were placed in a single hole.

Grouting in Zone 3 was completed during March and April, 1992. Over 6442 feet of 3-inch hole were drilled and grouted with 8764 cf of grout (Figure 35). One hole took almost 3000 cf of grout, but no significant solution features were encountered.

Grouting resumed in Zone 4, the high-solution zone, in March, 1992. An additional 79,472 cf of grout and 3,320 cy of concrete were placed in 18,376 feet of 3-inch drill hole and 23,268 feet of 6-inch drill hole (Figure 36). In one ten-foot interval, 36,011 cf of grout and cement were placed.

Additional grouting in Zone 4 near the Pond Spring was conducted in November, 1993 and ended in January, 1994. A volume of 15,138 cf of grout and 137 cy of concrete was placed in 4,455 feet of drill hole (Figure 37). The largest take in a single hole was 2,425 cf.

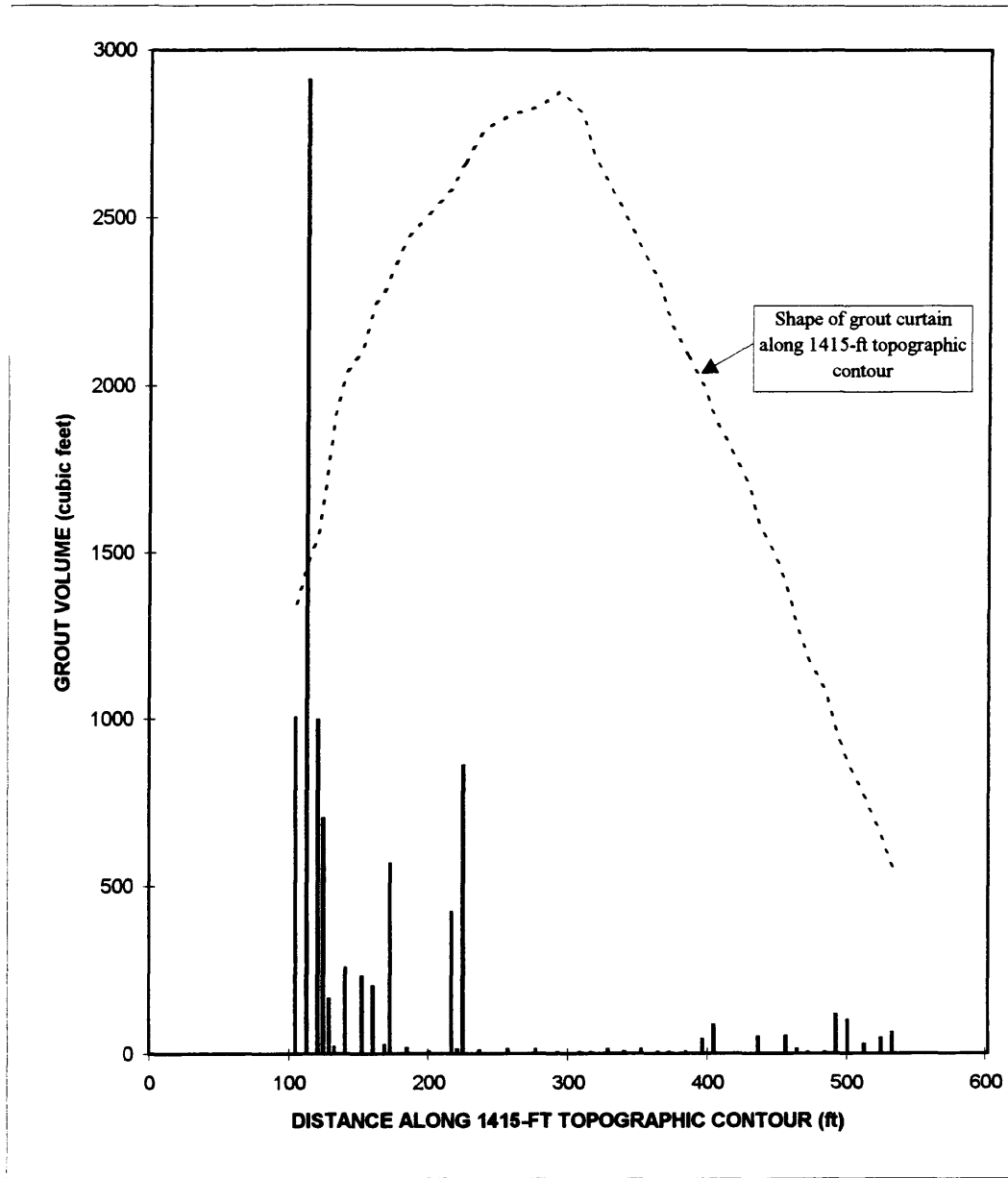
It is apparent that Zone 4, the high-solution zone on the east side of the reservoir, had the highest grout take, representing the greatest seepage potential. However, it is



Grout curtain location is shown on Plate 1.

Figure 34

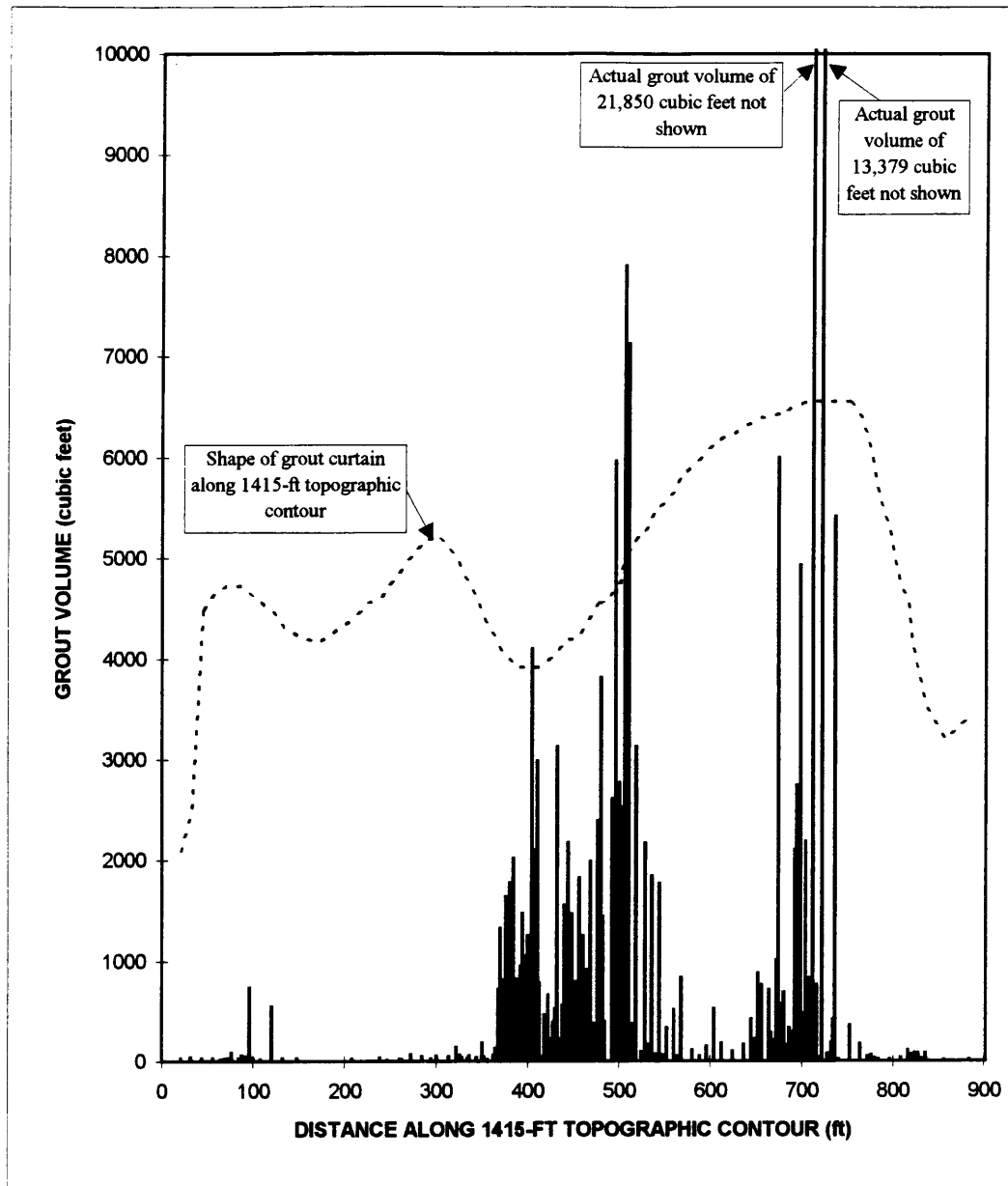
Grout Volumes in Grout Zone 2



Grout curtain location is shown on Plate 1.

Figure 35

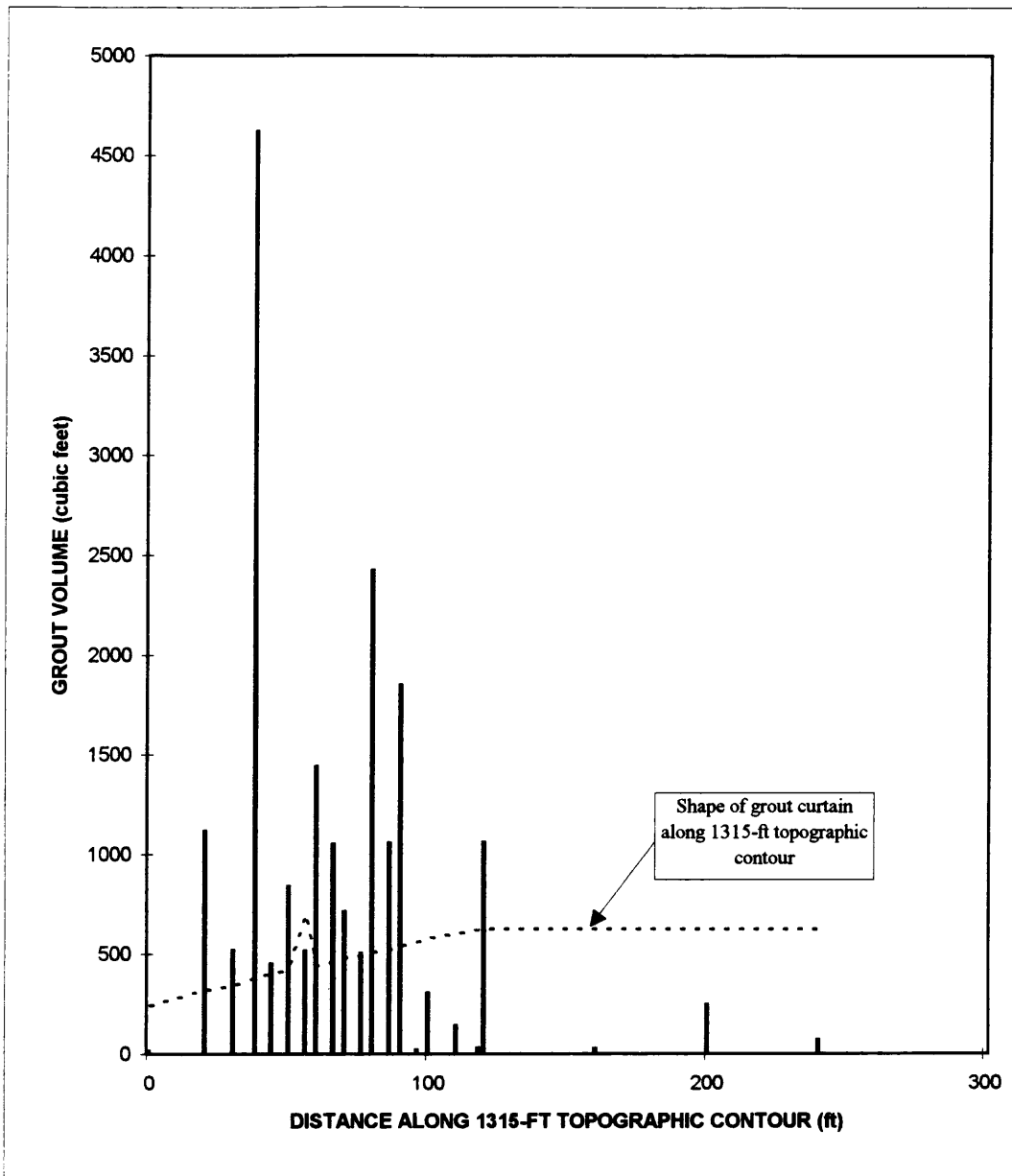
Grout Volumes In Grout Zone 3



Grout curtain location is shown on Plate 1.

Figure 36

Grout Volumes in Grout Zone 4



Grout curtain location is shown on Plate 1.

Figure 37

Grout Volumes in the Pond Spring Grout Zone

noted that the largest take for a single hole occurred in Zone 3, between Spring and Cove Hollows, between which a ground-water divide has been assumed.

### 8.1.2 Ground-Water Monitoring

Five monitoring wells, through G8 (Table 1, Plate 1), were installed in January and February, 1992, immediately preceding reservoir-wide grouting. All of these wells, except Well G8, functioned properly as monitoring wells. Wells G4 through G7, as well as the twelve pre-existing wells were monitored throughout grouting activities and into mid-1994, although of these 12, Wells G2 and G3 were not usable. Six more wells, P1 through P6, were installed in May and June, 1993 after the 1992 grouting program had been completed, and before the additional grouting along the Pond Spring in late 1993 (Table 1, Plate 1). All were monitored into mid-1994. The water level in Well P1 does not reflect the general condition of the ground-water system, and may relate to a locally confined system. Well P6 was completed above the water table.

The new ground-water wells provided data that allowed the development of a detailed pre-grout water-table map, Figure 38. All wells were reviewed with respect to lithology, completion details and water levels and classified according to type of aquifer (Table 1). Only those classified as a water-table aquifer were used in generation of the water-table map. The average of all water-level measurements of record for each well was used to develop the water-table map. The average water levels in Wells G4 through G8 and P1 through P6, installed during the site-wide grout program, were used in a

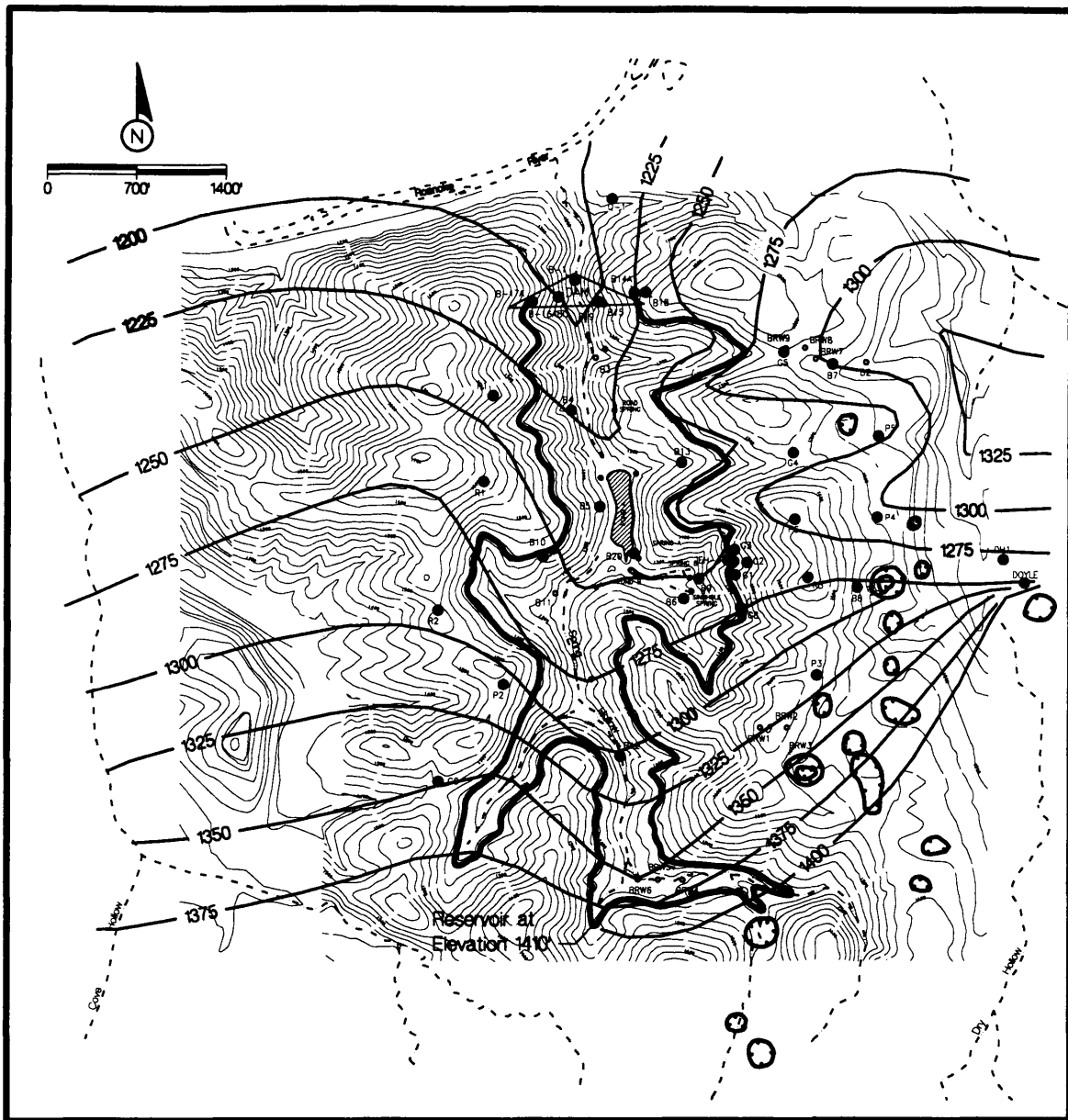


Figure 38

Pre-Grout Water Table of the Research Area

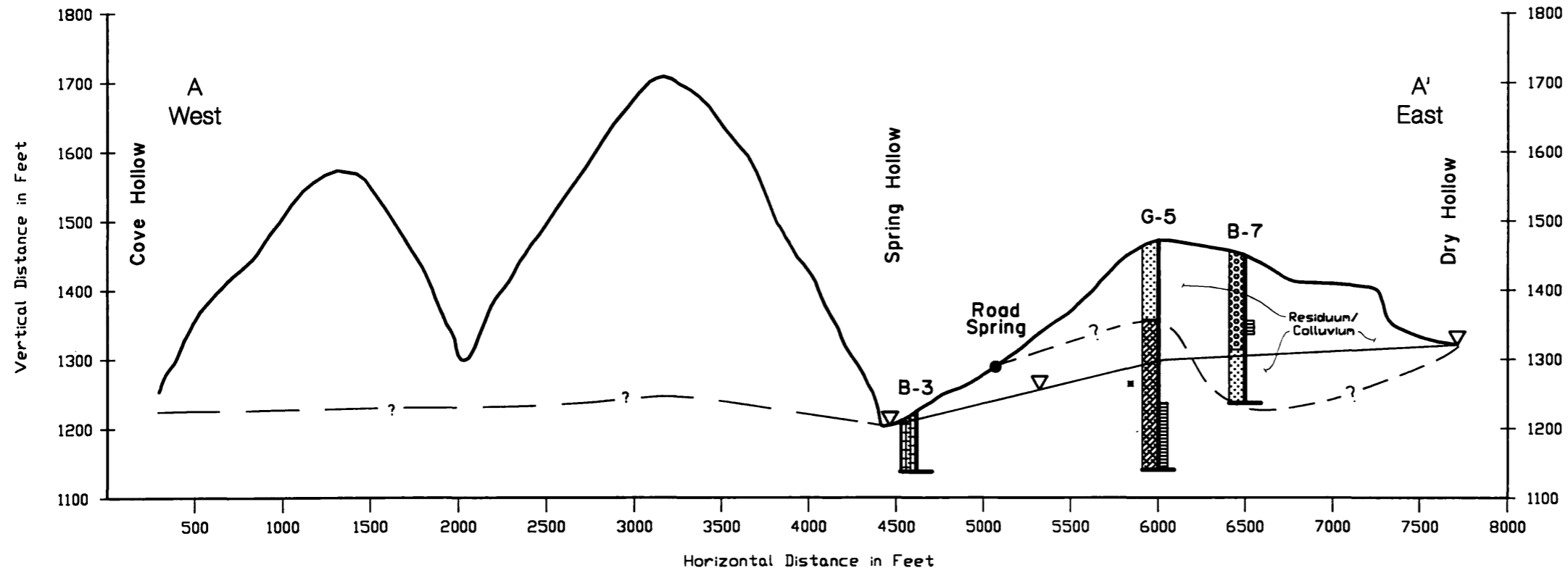
qualitative manner in the generation of a water-level map. The average heads were used to ensure that the water-level elevation contours were not higher than the average water-level elevations at the wells.

The control that the solutioned carbonates have on the flow field is apparent in the pattern of the water-table contours between Dry and Spring Hollows. This control along lithologic strike is not present in the water-table contours between Cove and Spring Hollows. The new data supports the conceptual model of Section 6.1.4.3, particularly the gradient from Dry Hollow to Spring Hollow. This is illustrated in the cross-sections from Dry Hollow to Cove Hollow shown on Figures 39, 40, and 41. Water-level data from Wells G4, G5, and P5 substantiate this gradient.

### 8.1.3 Geologic Mapping

Geologic mapping of the perimeter of the reservoir by SEA resulted in a more detailed map of the Spring Hollow geology, presented in Figure 42. This map provided a clearer understanding of the interrelationships of lithology and structure, enabling a classification of solution potential by lithology (SEA, 1992f). The area was mapped with four geologic units. Unit 1, varicolored shales and siltstones, ridge-formers with a low solution potential, are fractured and generally display no solution features. A second unit, fault breccia and associated deformed varicolored shales, not previously recognized on the basis of genesis, was mapped only in the high-solution zone. This unit is highly deformed, fractured, and brecciated and contains pods of brecciated dolomite and shaley



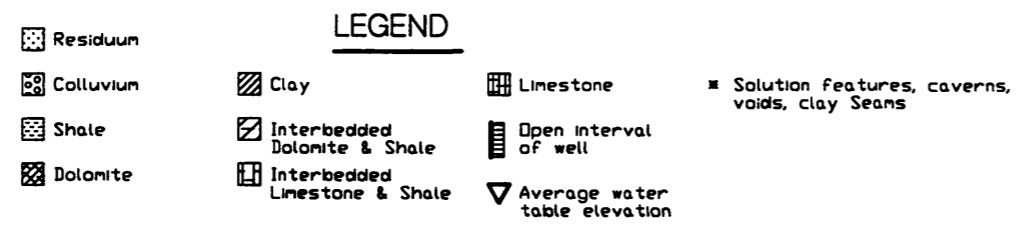
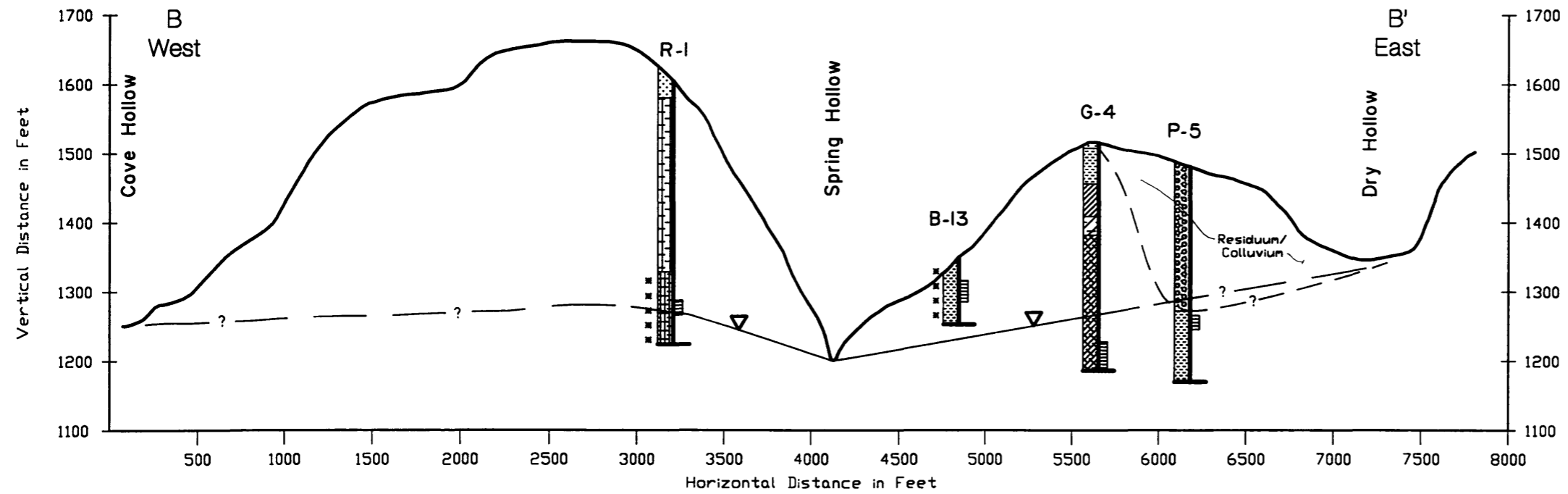


**LEGEND**

- Residuum
- Colluvium
- Dolomite
- Limestone
- Open interval of well
- Average water table elevation
- Solution features, caverns, voids, clay seams

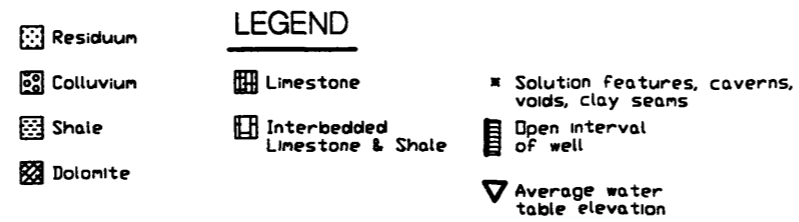
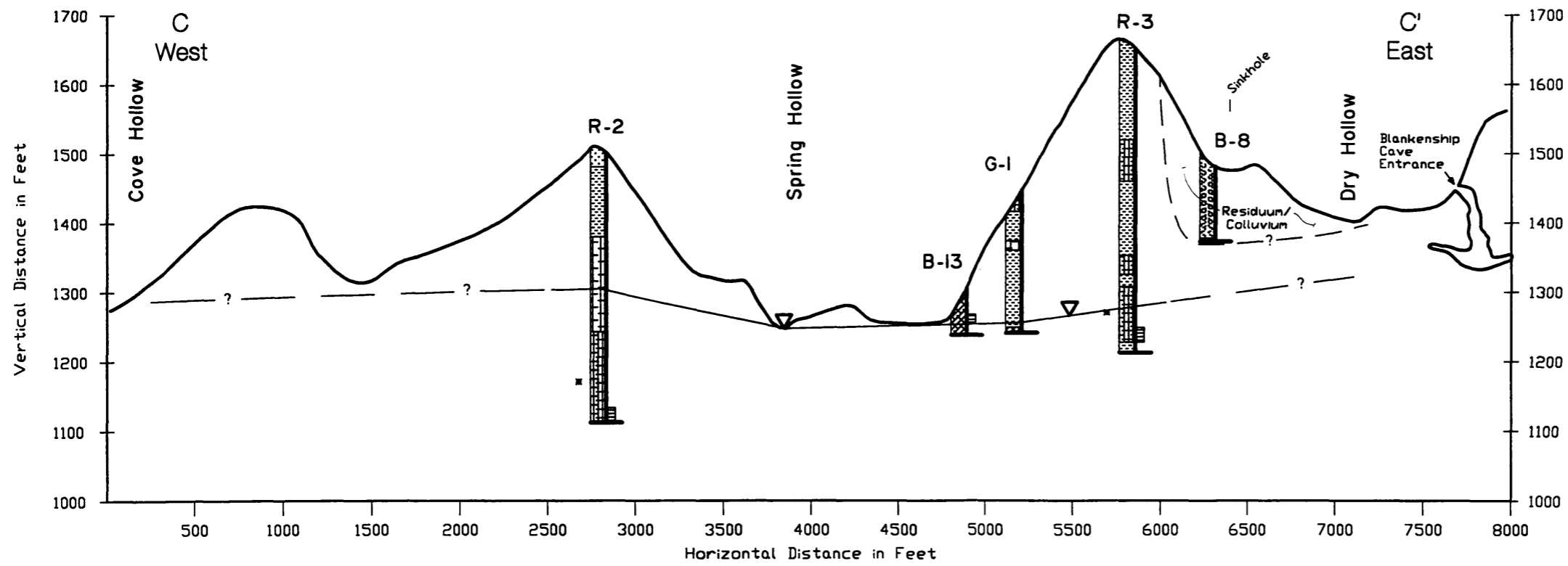
Section A  
See Plate 1 for  
location of section

Figure 39  
Geologic Cross-Section A



Section B  
See Plate 1 for  
location of section

Figure 40  
Geologic Cross-Section B



Section C  
See Plate 1 for  
location of section

Figure 41  
Geologic Cross-Section C

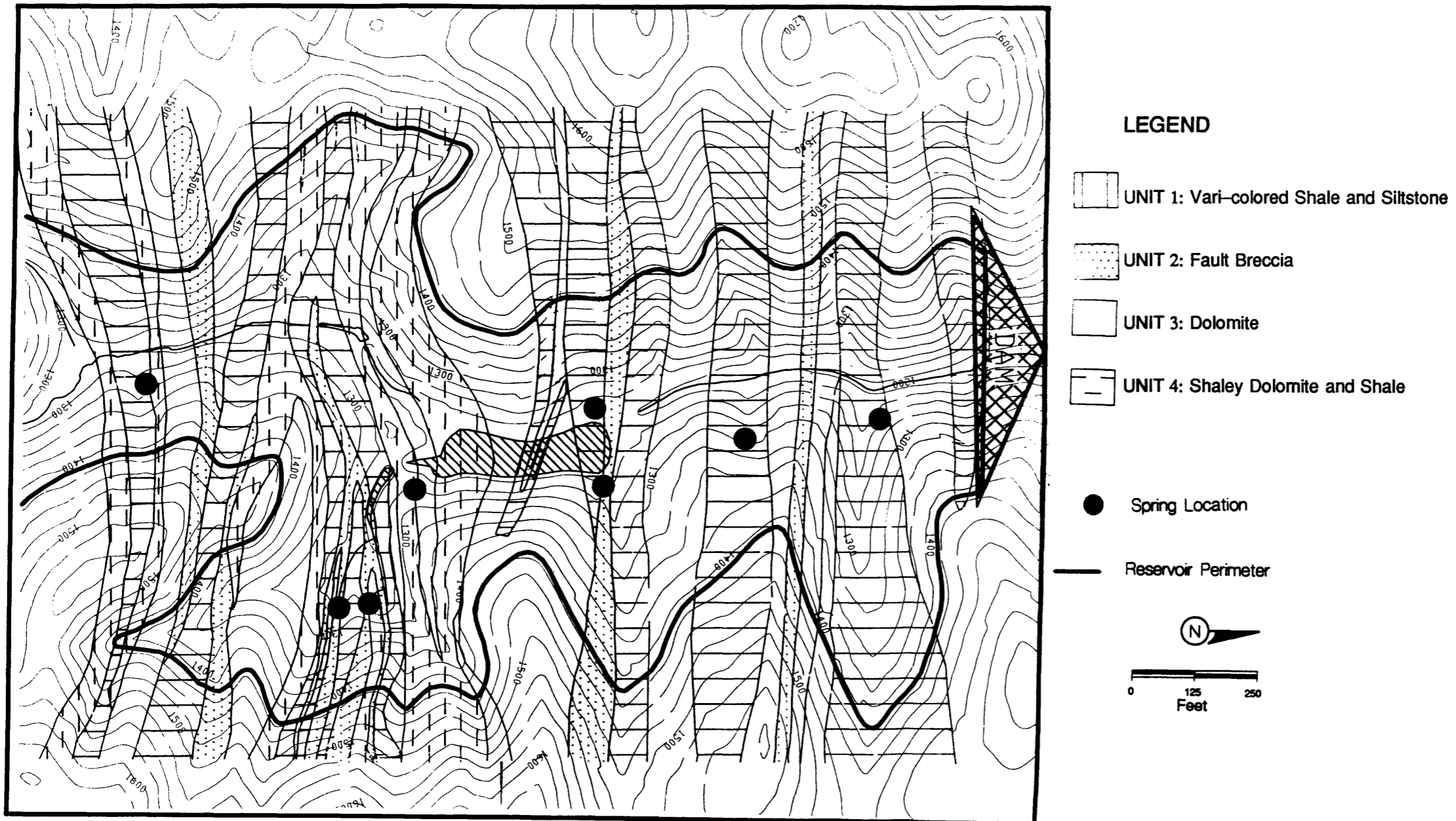


Figure 42

Geology Map Produced During  
the Reservoir-Wide Grout Program

dolomite. Although the fault breccia is a ridge-former, it has a high solution potential at its contact with carbonates (Unit 3, dolomites) and shaley dolomites and shales (Unit 4), in the form of voids, caverns, and mud-filled seams. In the high-solution zone, this unit was previously mapped as maroon shale and siltstone (Figure 7). The presence of fault breccia, also a maroon or red color, is present only in and just south of the high-solution zone. Elsewhere, the maroon shales and siltstones of Figure 7 correlate with Unit 1, varicolored shales and siltstones. Unit 3 dolomites are valley-formers, are highly to moderately fractured and contain solution features, such as voids and cavities. They have a high solution potential where they contact Units 2 and 4. The Unit 4 shaley dolomites and shales also display solution features, are most often found in contact with Unit 3 dolomites, and display a high solution potential when in contact with both Units 2 and 3. Shallow depth solution features are frequently found in the shaley dolomites and shales.

The severely deformed and brecciated shales of the high-solution zone substantiate the presence of a fault or faults in this zone. Further, the faulting and accompanying brecciation have produced bedrock that is more susceptible to solutioning than less fractured rock present in the rest of the valley. It is probable that this zone represents the greatest seepage potential and that a successful grouting program in this area is essential.

With few exceptions, bedding measured along the reservoir perimeter dips to the north. Since there is no indication of stratigraphic up, the preponderance of northward dips may signify overturned, faulted folds, consistent with a thrust belt.

Figure 43 is a photograph of a fracture in the vertical bedrock exposed along the east dam abutment. It is similar in orientation to one of the major fracture sets, J-6, discussed in Section 6.1.1.3. It strikes approximately north-south and dips to the southeast. Its orientation promotes solutioning along its length and an interconnectedness to the aquifer, allowing movement of water across lithologies.

The logs of Wells G4 through G8, and P1 through P6 provide additional insight into the subsurface geology of the areas adjacent to the reservoir valley (Figures 39 and 40). The colluvial/residual thicknesses logged in Wells G5, P4 and P5 confirmed the presence of an extensive mantle of unconsolidated material in Dry Hollow as illustrated in Figure 44. The colluvial/residual thicknesses are 105 feet in G5, 271 feet in P4 and 240 feet in P5. The base of this unit extends below the water level in Wells P4 and P5, and implies an influence by this material on the ground-water flow pattern. The other well logs do not contain references to colluvium or residuum, but do indicate the presence of mud seams and voids, consistent with the hydrogeological model set forth in Section 6.1.4.

## 8.2 Effectiveness of Grout

In order to assess the effectiveness of the grout in reducing seepage, the impact of the grout on the flow system was evaluated. This evaluation was based on ground-water and surface-water data, grout-take data and geologic data collected during the grouting program. The effectiveness of the grout was assessed qualitatively by analyzing

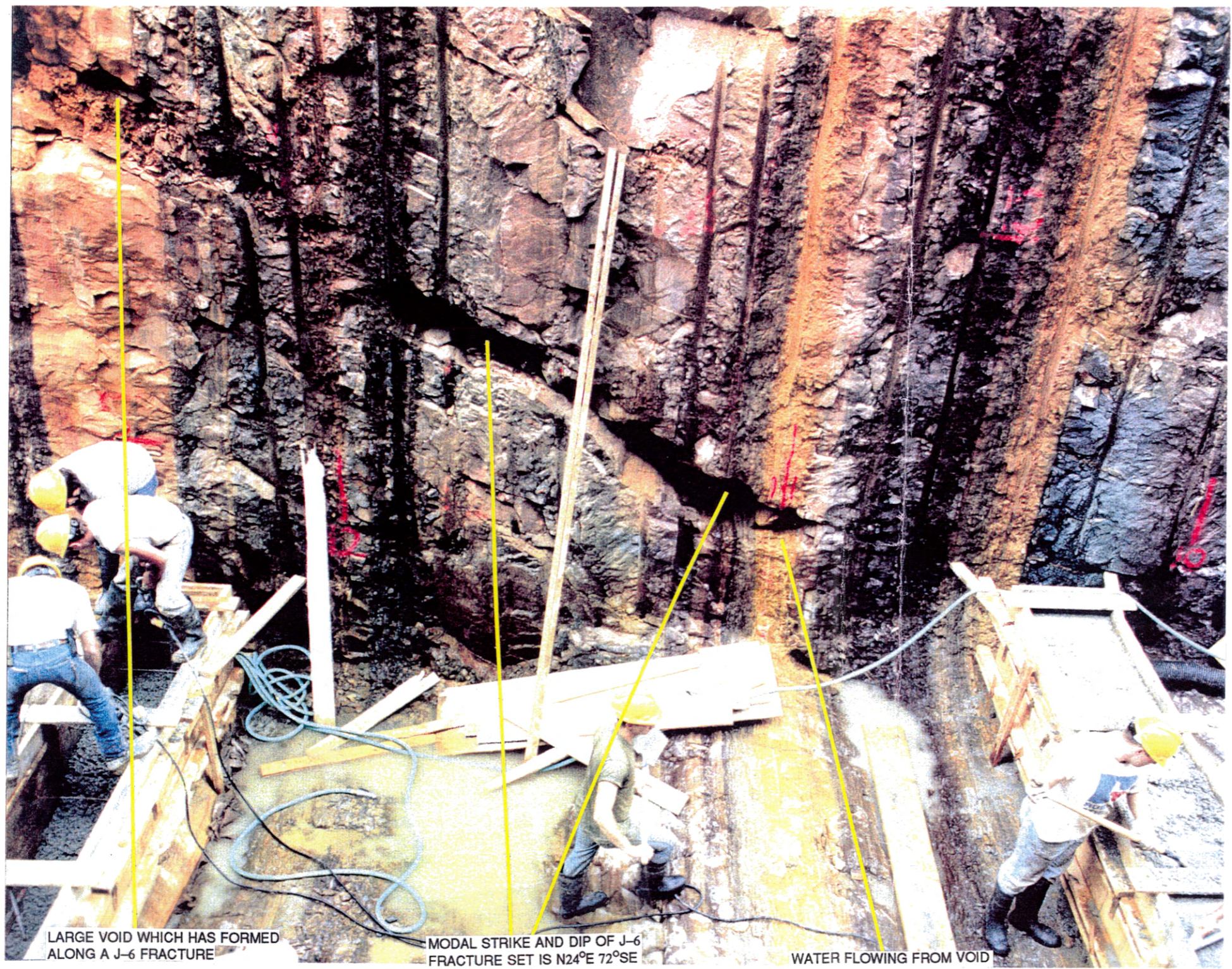


Figure 43

Photograph Along the East  
Dam Abutment Displaying  
Fracture Set J-6

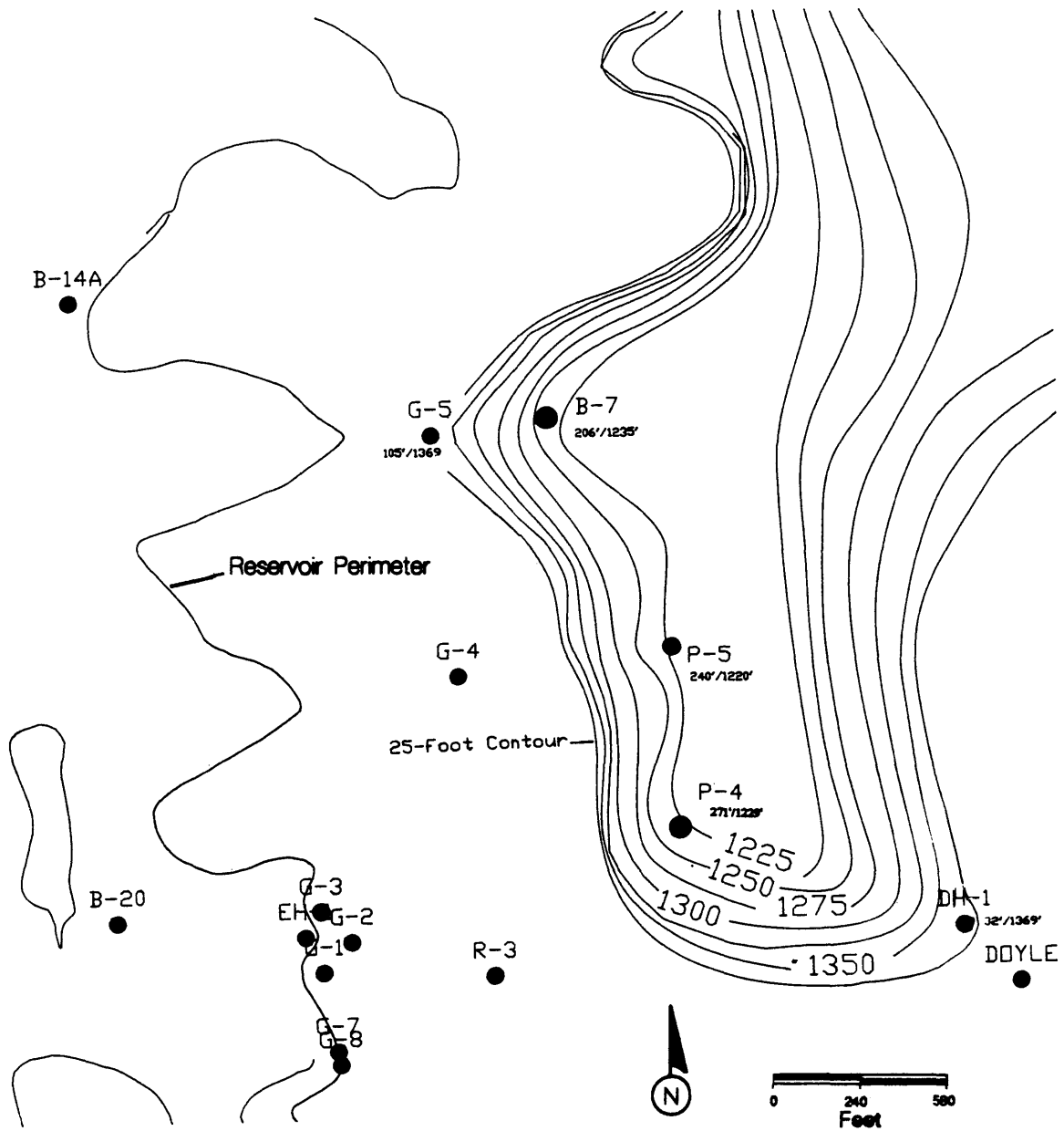


Figure 44

Base of Colluvial/Residual Material in Dry Hollow



ground-water and surface-water data for impacts of grouting. Additionally, the effectiveness of the grouting program was evaluated quantitatively through a numerical simulation of the site, based on the data collected throughout the characterization and grouting programs. Seepage rates were predicted at staged rises in reservoir elevations to quantify the effects of increasing head on seepage rates.

### 8.2.1 Qualitative Approach

The effectiveness of the grout was evaluated qualitatively, in the same way that it was for the Test-Grout Program described in Section 7.1. Ground-water data were analyzed for evidence of rises in head that correlated with the emplacement of grout. Monitoring-well water levels were expected to rise not only in the zones where grouting had occurred, but along the outside of the reservoir perimeter, so that not only the effectiveness of the grout itself was evaluated, but the selective grouting method as well.

#### 8.2.1.1 Ground-Water Monitoring

The water levels of twenty-one wells were monitored during the various phases of development of the Spring Hollow Dam and Reservoir. Of this number, twelve wells were existing and were monitored during pre-grout conditions. The remaining nine wells were installed during or after grouting. All twenty-one were monitored for water levels throughout grouting activities and into mid-1994.

#### 8.2.1.1.1 Pre-Grout Monitoring Wells

Review of the twelve pre-grout well hydrographs reveals that Wells R3, G1, R1, and R2, responded to the 1992 grouting activities, as expected. The annotated hydrographs of these four wells are presented in Figures 45 and 46. The hydrographs of the remaining eight wells are presented in Appendix D. Wells R3 and G1 underwent dramatic water level rises, indicating a highly effective grout curtain. DH1, a dry well located along the dry stretch of Dry Hollow, remained dry (Appendix D, Plate 1). The water level of the Doyle well (Figure 47), located east of Dry Hollow, did not respond. The lack of response in these two wells supports the fault-as-barrier scenario discussed in Section 6.4.1.3, that would allow water levels to rise south of the barrier, leaving downstream conditions essentially unchanged. Additionally, since the Pond Spring flow remained unchanged, the relationship between the Doyle Well and the Pond Spring was strengthened, indicating that they are hydraulically connected along the same carbonate unit. This is consistent with the results of the geomorphologic extension of geology (Figure 16).

Grouting along the west rim of the reservoir in Grout Zones 1 and 2 had some impact on the ground-water system. This impact is apparent in the hydrographs of Wells R1 and R2 (Figure 47).

As illustrated by their hydrographs (Figure 47), additional grouting in late 1993 along the 1315-foot elevation adjacent to Well B20 (Plate 1) resulted in an immediate response in B20 and a gradual rise in the water level of the Doyle Well. The

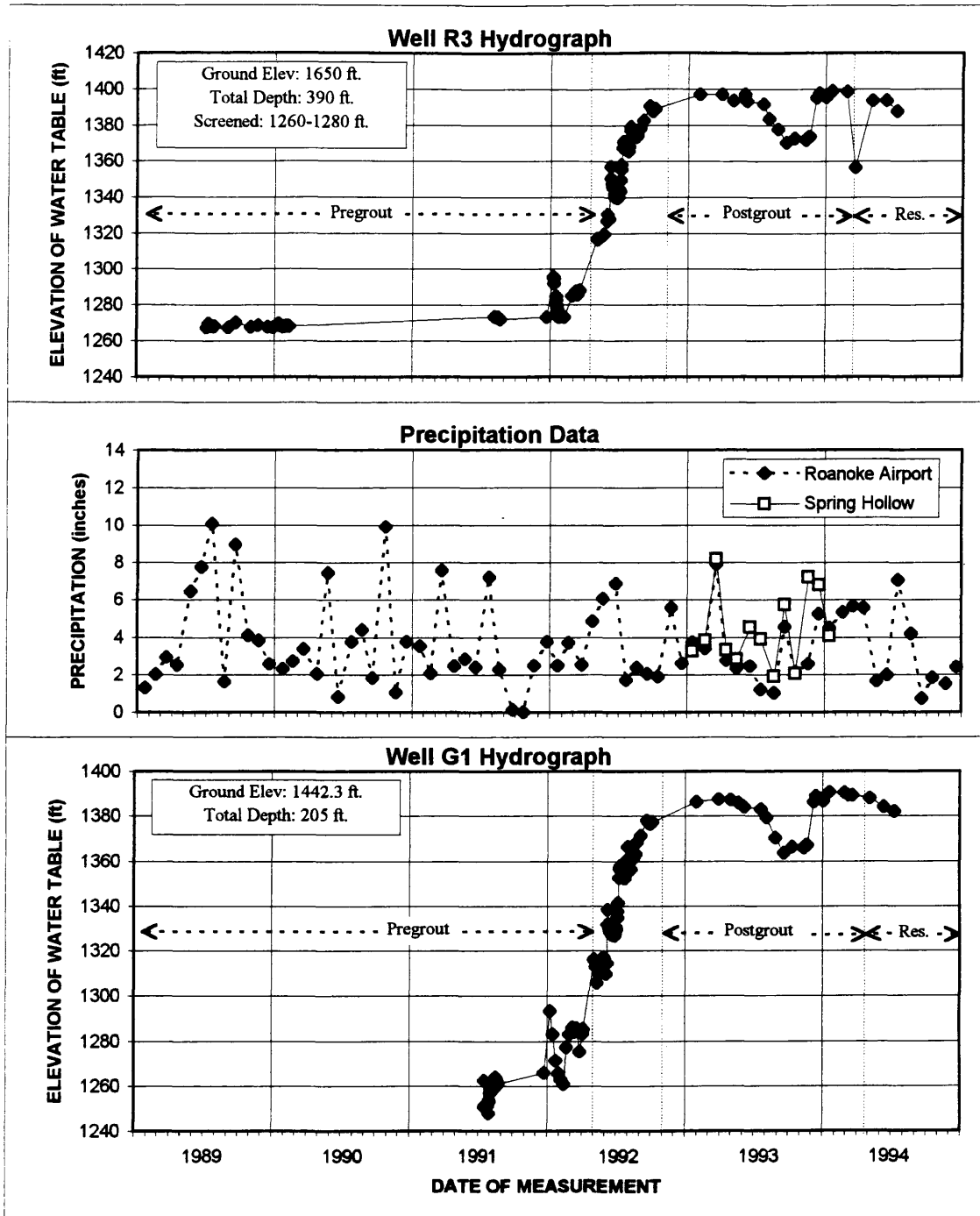


Figure 45

Hydrographs of Wells R3 and G1

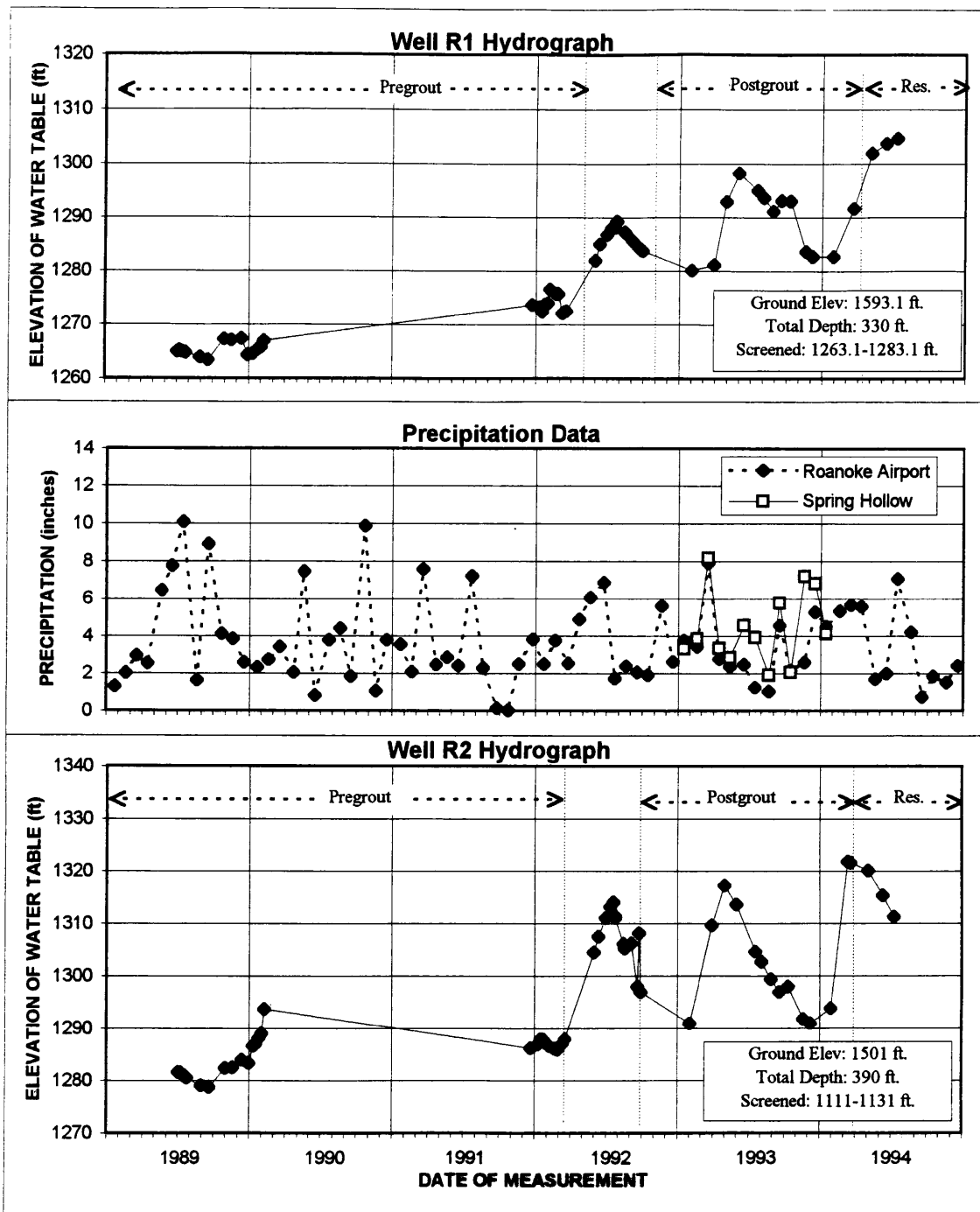


Figure 46

Hydrographs of Wells R1 and R2

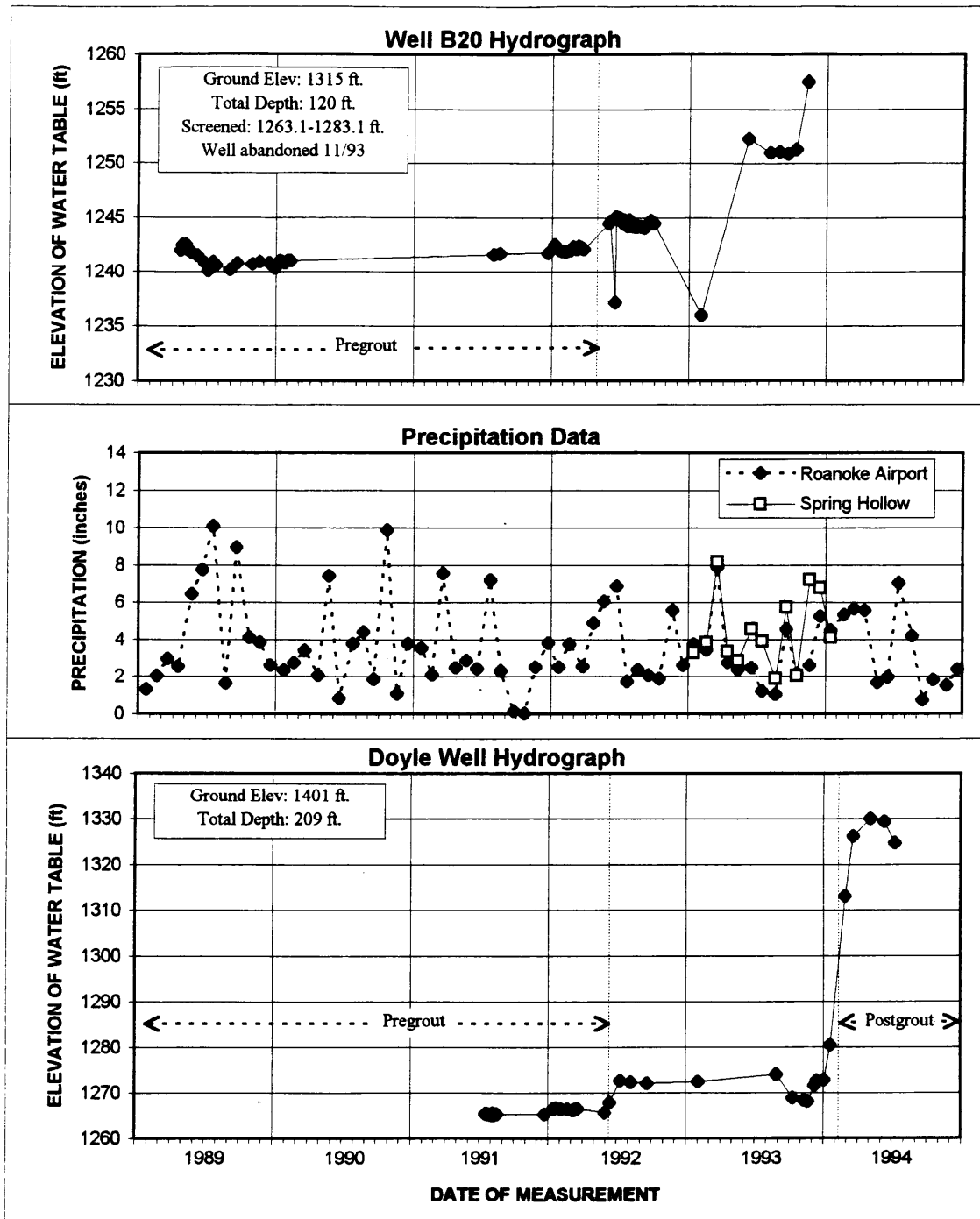


Figure 47

Hydrographs of Wells B20 and Doyle Well

hydrographs of these wells illustrate this response to grouting. Wells B14A, B19, B16D, B17A, and Q1 are located within the reservoir perimeter, and were not expected to respond. The hydrographs of these wells are presented in Appendix D.

#### 8.2.1.1.2 Post-Grout Monitoring Wells

Five monitoring wells, G4 through G8 (Table 1, Plate 1), were installed in January and February, 1992, immediately preceding reservoir-wide grouting. All of these, except Well G8, functioned properly as monitoring wells. The hydrographs of Wells G4 through G7 are presented in Figures 48 and 49. Although they were installed prior to grouting activities, and some correlation of a rise in water levels with continued grouting was expected, none was observed. Wells G4 and G5 are located behind Grout Zone 3. Their lack of response to grouting indicates either that grouting was unsuccessful, or that the zone is not significantly solutioned. Additional grouting in 1993 near the Pond Spring elicited a rise in the water level of Well G4. The response may be related to the presence of the colluvial/residual material, in that the laterally continuous layer provided a hydraulic conduit down the Dry Hollow valley. A rise in the water level of G7 in early 1994 was probably due to surface infiltration and was not related to grouting activities. This event rendered the well unsuitable for use in monitoring post-reservoir ground-water conditions. Grouting at the Pond Spring caused water levels to rise above the top of the Doyle Well/Well B20 carbonate and into the colluvial/residual layer, allowing flow to move in a down-valley direction as the water table rose.

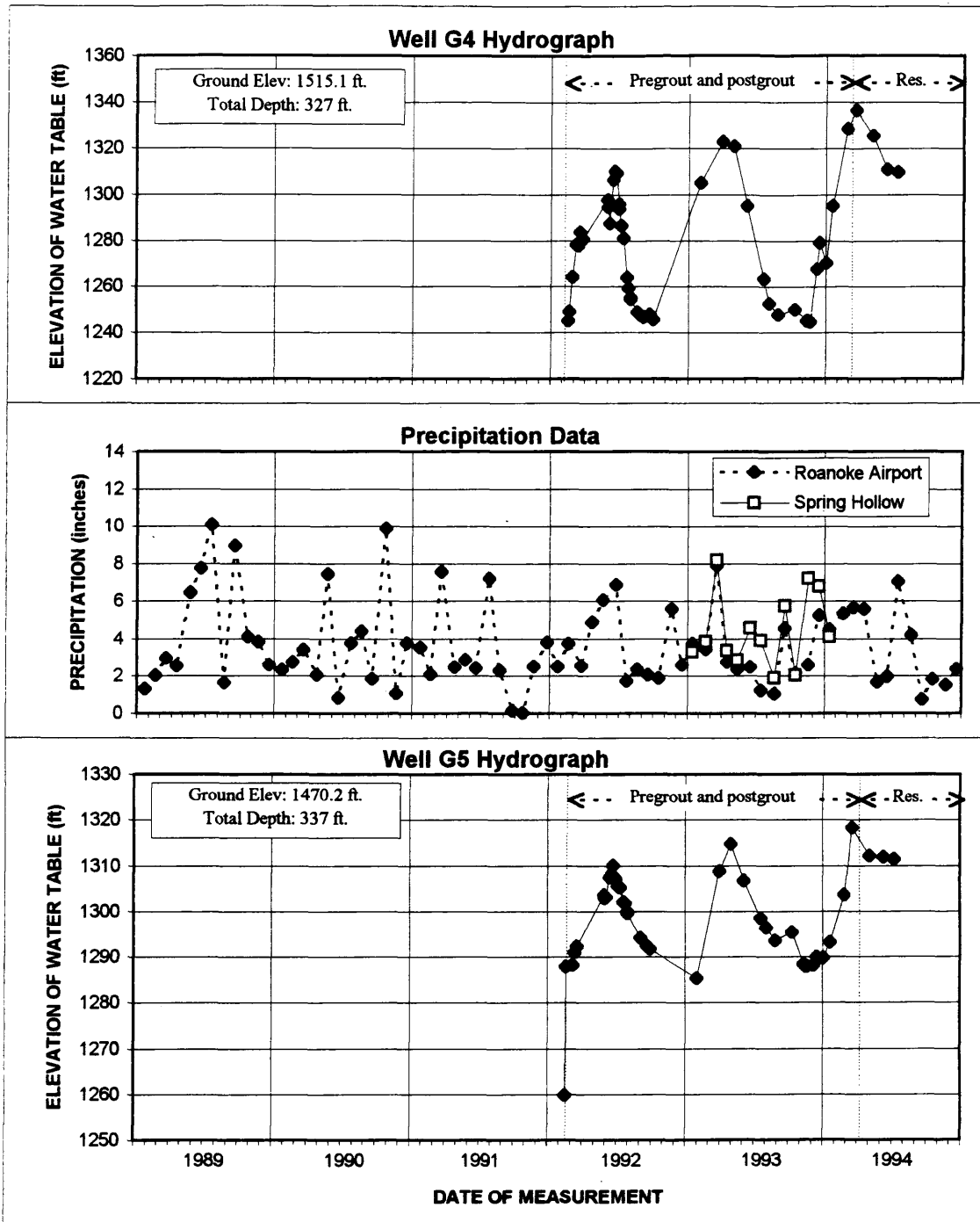


Figure 48

Hydrographs of Wells G4 and G5

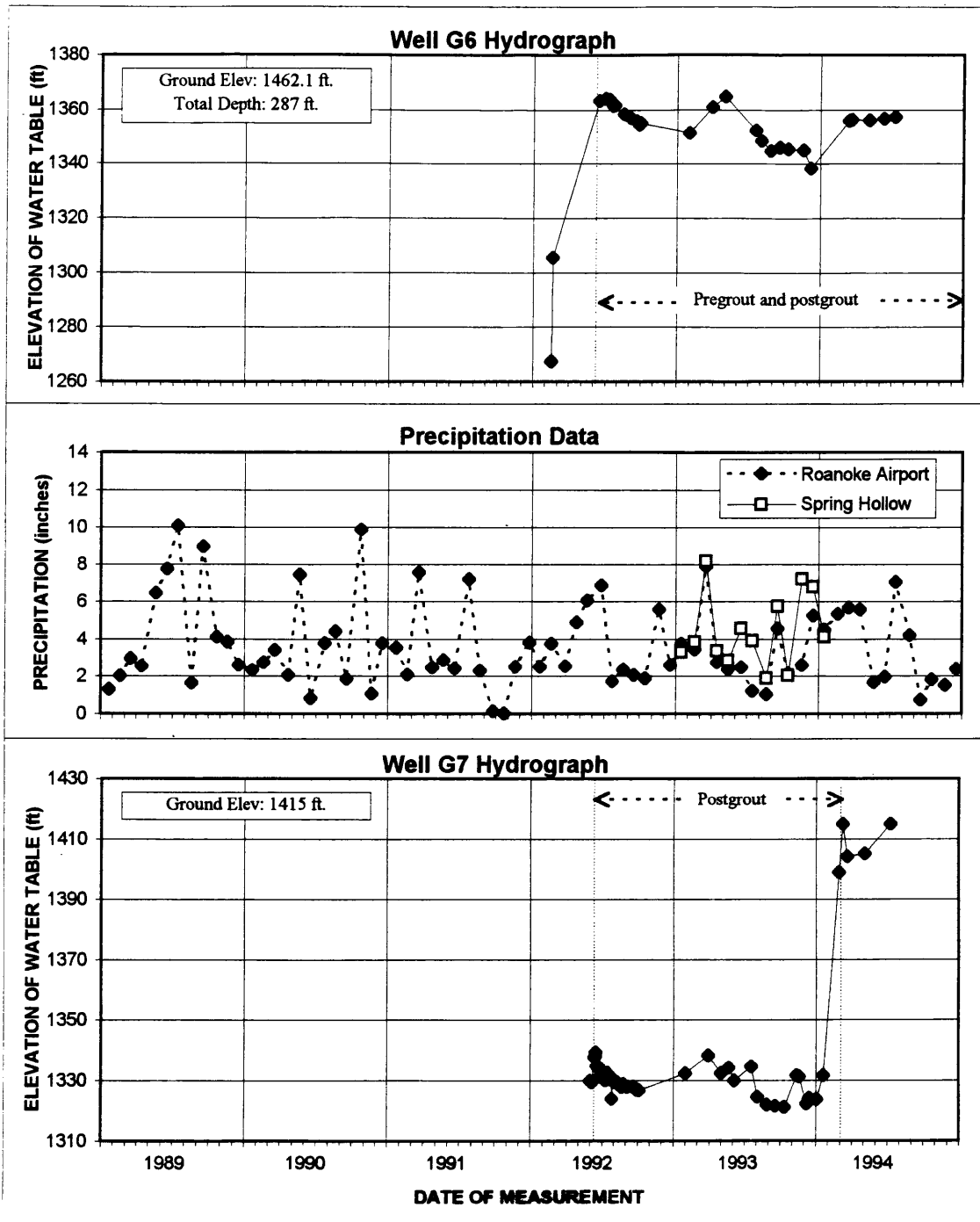


Figure 49

Hydrographs of Wells G6 and G7



Six more wells, P1 through P6, were installed in May and June, 1993 after the 1992 grouting program had been completed, and before the additional grouting along the Pond Spring in late 1993 (Table 1, Plate 1). The water level in Well P1 (Appendix D) does not reflect the general condition of the ground-water system, and may relate to a locally confined system. Well P6 was completed above the water table and is not used. Annotated hydrographs of Wells P2 through P5 are presented in Figures 50 and 51. With the exception of Wells P2 and P3, which are located in the southern reaches of the site beyond the influence of the grout curtain, responses were expected in Wells P4 and P5, which are located along the dry stretch of Dry Hollow. Neither of the wells responded to the 1992 grouting activity, however, Well P5 reacted strongly to the 1993 grouting of the Pond Spring area. This is consistent with the reaction of the Doyle, G4, and B20 wells. The lack of a response in Well G5, which contains only a thin colluvial/residual layer above the post-grout water table, serves to affirm the influence of the colluvial/residual layer on the hydraulics of the northern half of Dry Hollow. However, the hydrograph of Well P4 displays no evidence of an impact by grouting. The fact that Wells P5 and G4 were impacted and Well P4 did not may reflect the fact that both P5 and G4 lie upgradient of Grout Zone 3, whereas, Well P4 lies upgradient of an area that was not grouted.

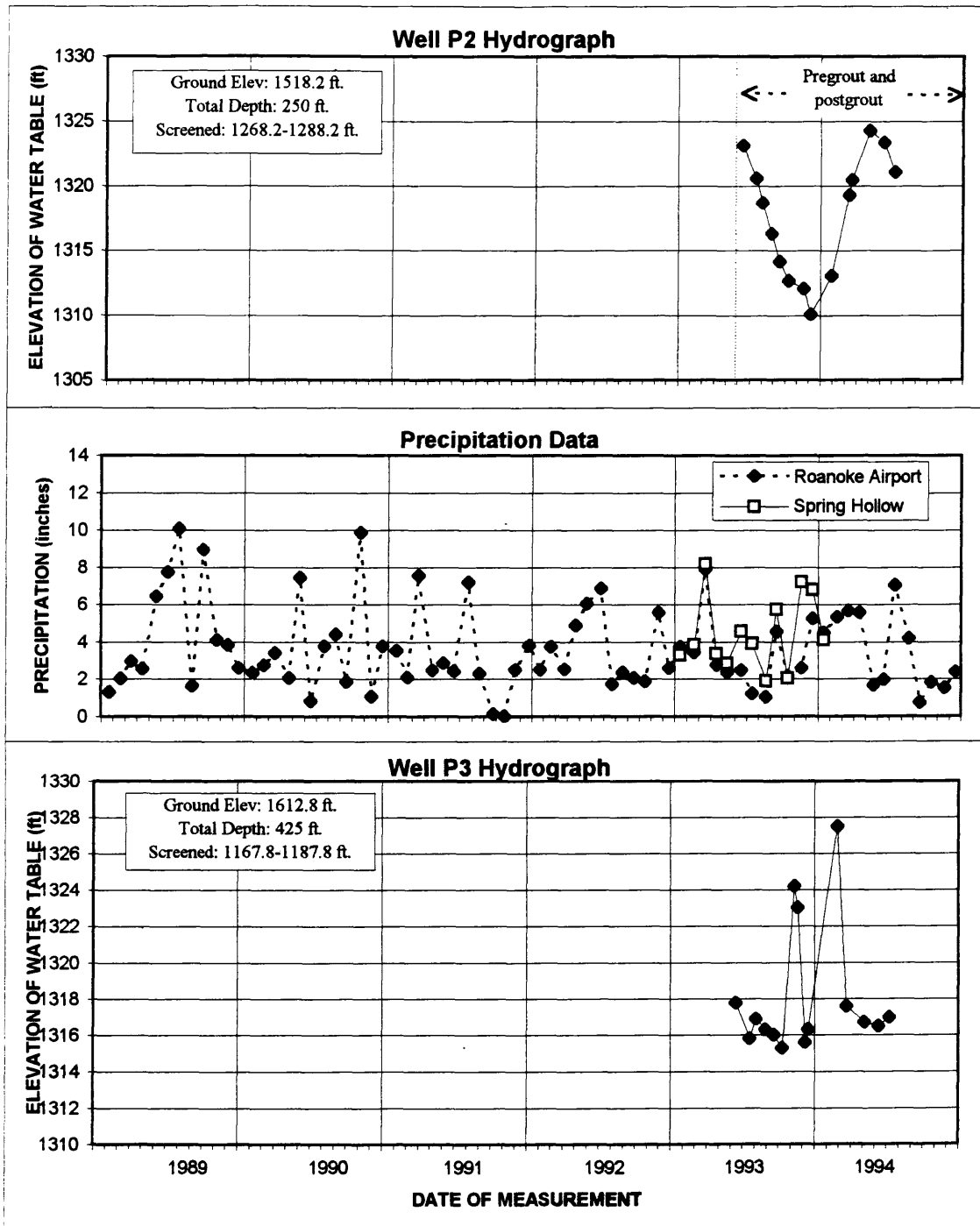


Figure 50

Hydrographs of Wells P2 and P3

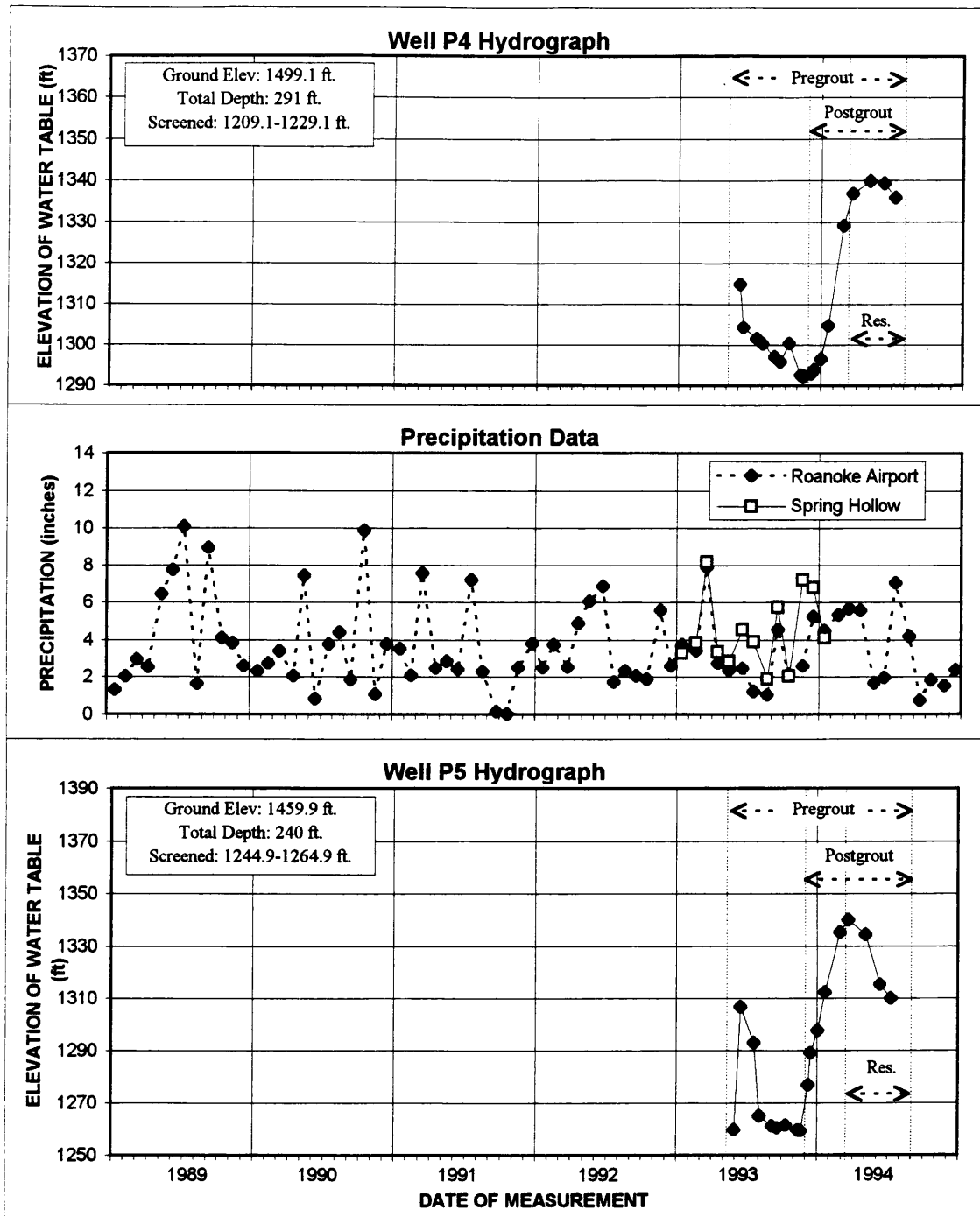


Figure 51

Hydrographs of Wells P4 and P5

### 8.2.1.2 Post-Grout Water Table

A post-grout water-table map, represented in Figure 52, was developed using water-level elevations in wells reflecting post-grout conditions. Water-level data were evaluated for each well to determine the appropriateness for use in the generation of the post-grout water table. Well hydrographs were examined for evidence of impacts on the wells by grouting. If no impacts were found, then all of the water-level elevations were used for an average water-table elevation. If grouting impacts were observed, then only post-impact data were used to find average water-table elevations. For some wells, only one or two observations qualified as post-grout, and these were used with reservation. This classification is annotated on the well hydrographs of Figures 45 through 51.

As is evident in Figure 52, grouting has impacted the ground-water flow system in the research area. The gradient has changed along the high-solution zone. The gradient is now toward Dry Hollow from Spring Hollow, indicating that the grout curtain is effective with water backing up behind the grout curtain. This is the desired effect of grouting. Also apparent is the effect of the colluvial/residual layer on the flow system. The water-table contours indicate that, as a result of grouting, the water table has risen into this material and is moving in a down-valley direction.

### 8.2.2 Quantitative Approach

The effectiveness of the grouting program was evaluated quantitatively through numerical simulation. The input for the simulation was based on the data collected

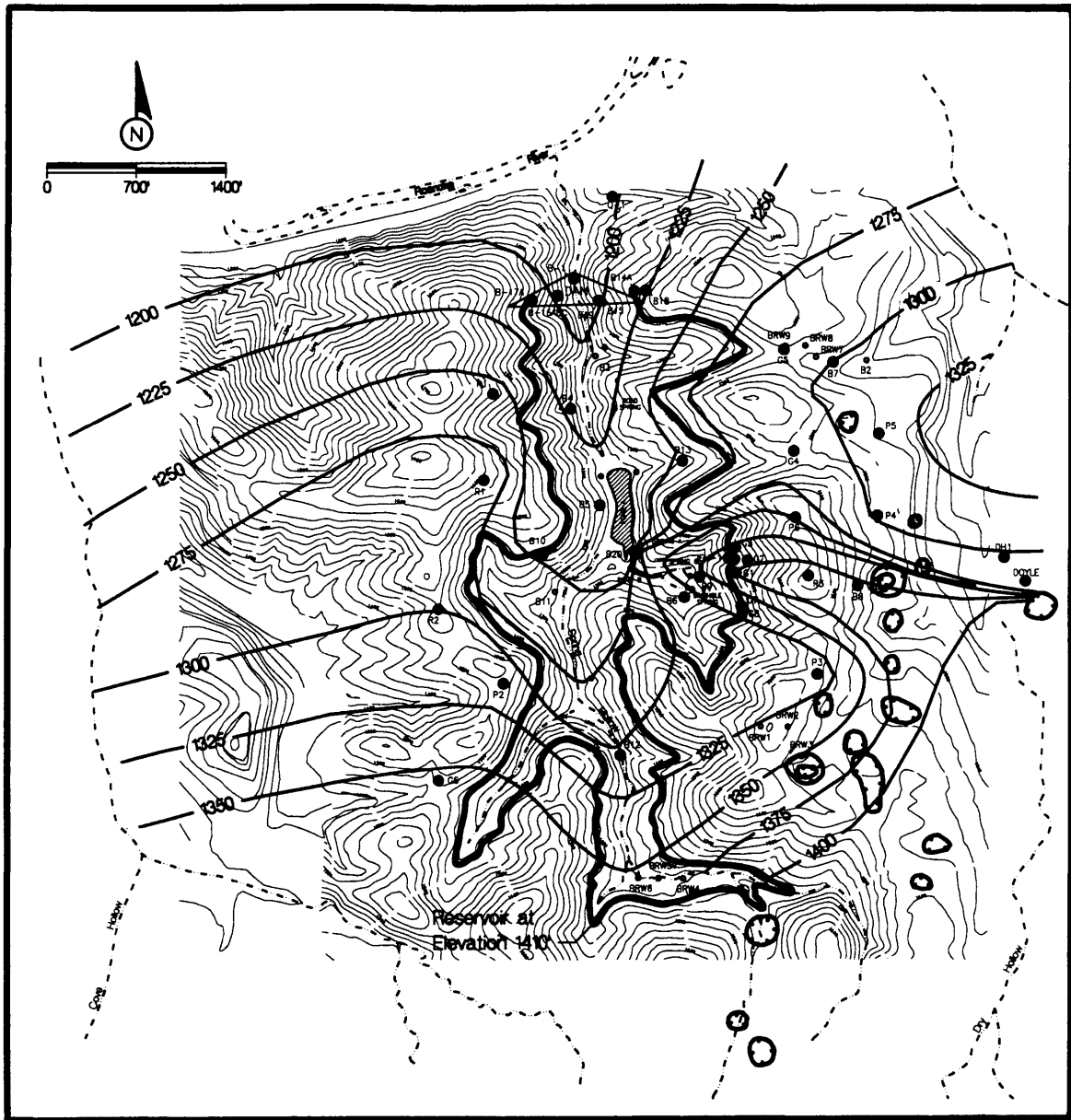


Figure 52

Water-Table Map Reflecting the Rise in Water Levels Related to the 1992 and 1993 Reservoir-Wide Grouting Activities

throughout the characterization and grouting programs. Input and output files for the models are listed in Appendix C. Seepage rates were predicted at staged rises in reservoir elevations to quantify effects of increasing head on seepage rates. The modeled area, as shown on Plate 1, extends from Dry Hollow on the east to Cove Hollow on the west. The Roanoke River bounds the site to the north and Poor Mountain forms the southern boundary.

#### 8.2.2.1 Assumptions, Limitations, and Simplifications

The numerical model MODFLOW was used for the simulations of ground-water flow. Limitations of the numerical model include those inherent in numerical modeling related to nonunique solutions as a result of trial-and-error calibration (Anderson and Woessner, 1992). Simplifications include those related to heterogeneities that cannot be accurately represented in a model. The assumptions in these simulations were steady state conditions and laminar flow. The possibility that turbulent flow is present in the high-solution zone is discussed in Section 8.3.2.

#### 8.2.2.2 Grid Size and Boundary Conditions

The grid is 44 columns by 56 rows, two layers, with active and inactive cells for Layers 1 and 2 as shown in Figures 53 and 54. Cell sizes are up to 400 feet wide in the areas farthest from the grout curtain and in areas where the geology has been extended. In the reservoir area cell sizes are smaller and decrease to forty feet wide along the grout curtain.

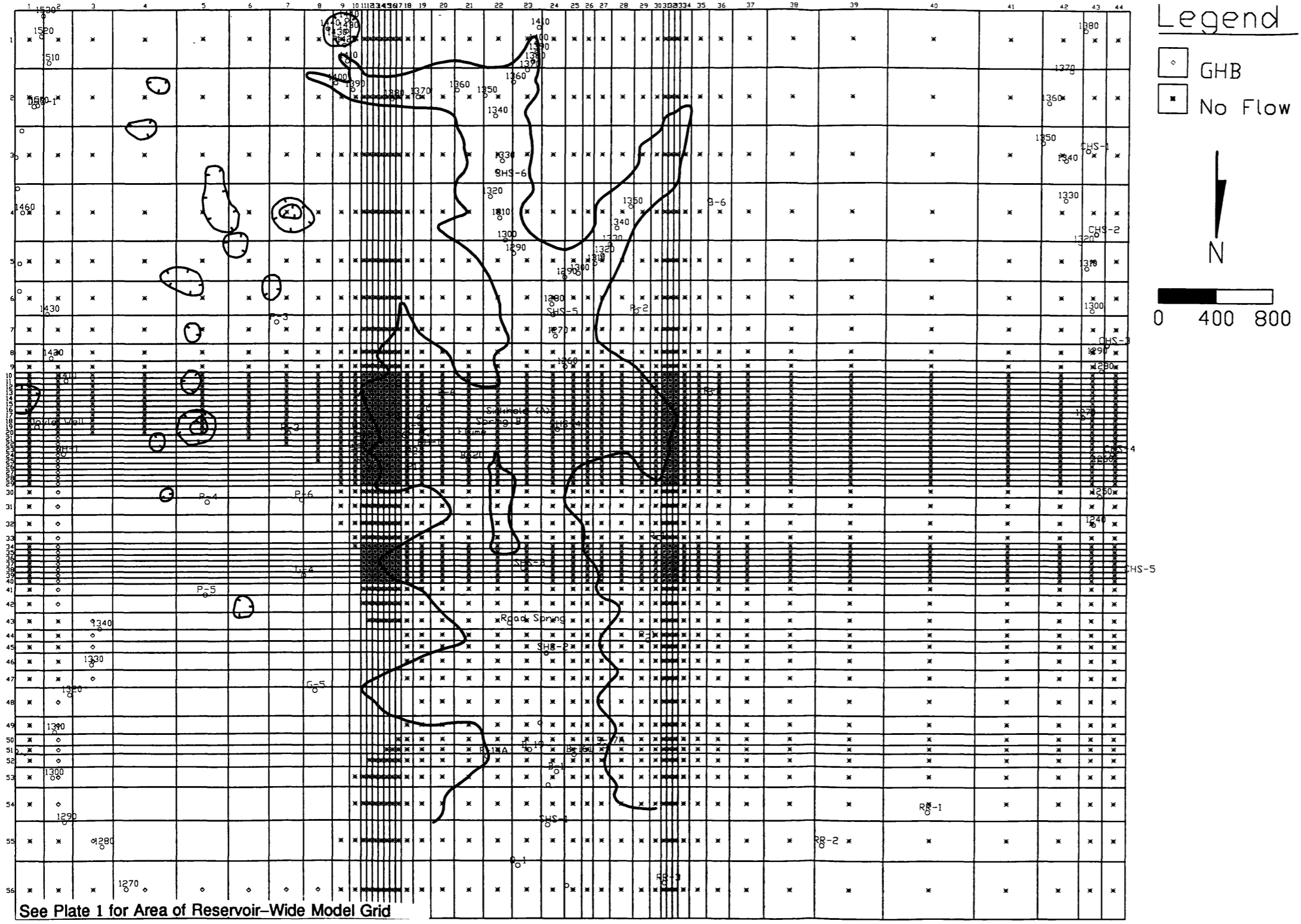


Figure 53

Reservoir-Wide Numerical Model Grid and Boundary Conditions for Layer 1

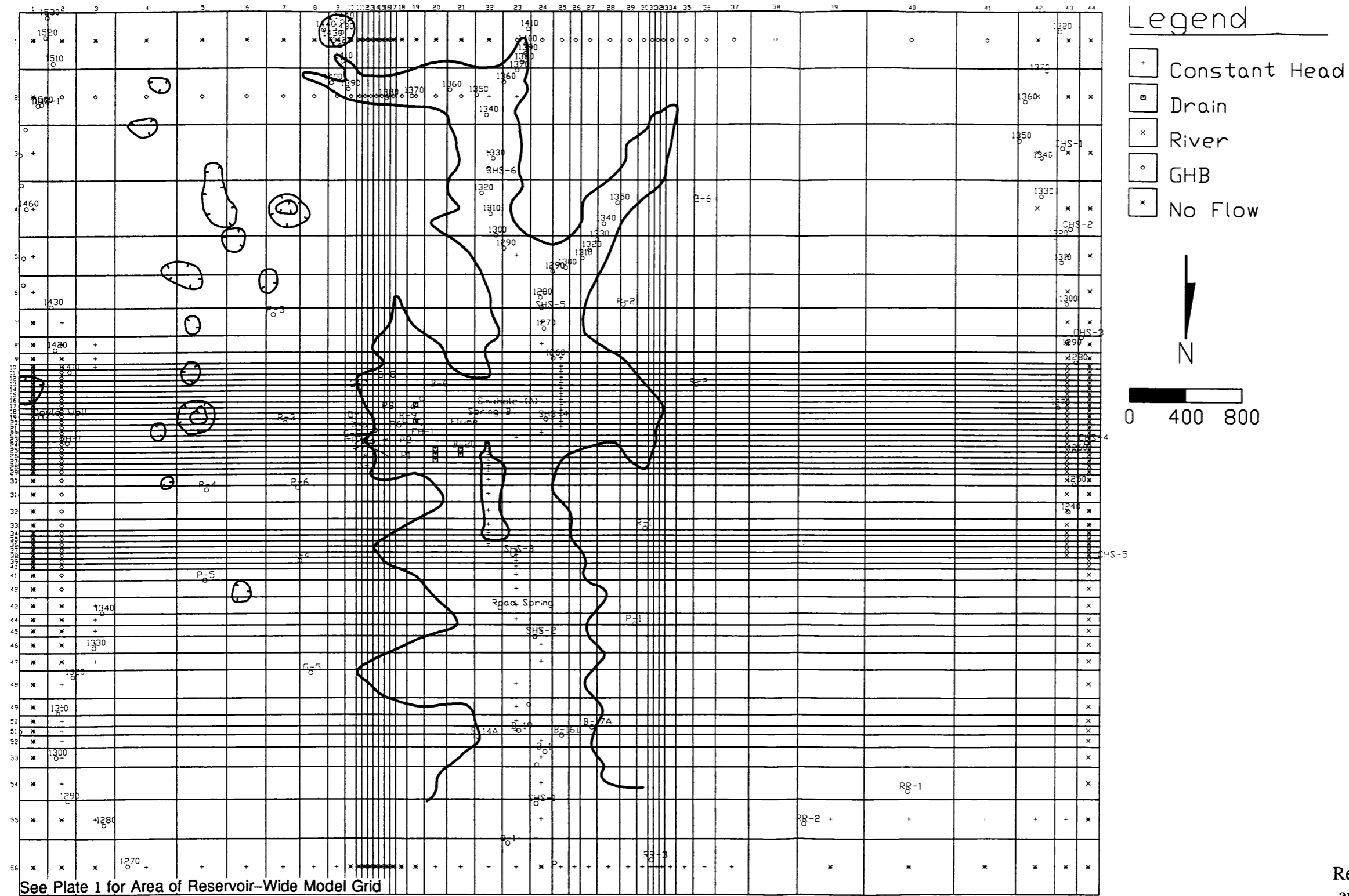


Figure 54

Reservoir-Wide Numerical Model Grid and Boundary Conditions for Layer 2



Layer 1 is comprised of the colluvial/residual material of Dry Hollow. Although there is some colluvial material in Cove Hollow, it is not known to be significant hydrogeologically, and was, therefore, not modeled. The area of active cells in this layer was modeled according to the extent of the colluvium/residuum (Figure 44). No-flow cells were used on the south and west edges of the active cells. General head boundaries were used on the east (Dry Hollow) and north (Roanoke River) edges to allow fluctuation of heads and movement of water out of the system.

Layer 2 consists of the bedrock as depicted in Figures 17 and 42. Active cells and boundary conditions are shown on Figure 54. Karst terrain and heavily solutioned areas exhibit flat gradients, sinking streams, caves, and faults and may not display ground-water divides for long distances. This is the case along the dry interval of Dry Hollow. Under pre-grout conditions there exists a gradient toward Spring Hollow, even along the dry stretches. Post-grout conditions will impact this boundary as the water table rises in response to grouting and the gradient from Dry Hollow to Spring Hollow reverses. Boundary conditions used for this simulation had to reflect an ability to absorb the stresses to the study area, while changing to minimize impacts by boundaries on the ground-water condition. Therefore, a general head boundary was used along the portion of Dry Hollow in which the water table is below the stream-bed elevation. This boundary type allows input of water from the general head cells in pre-grout conditions and also allows a rise in head in these cells under post-grout and post-reservoir conditions. Drains

were placed adjacent to and west of the general head cells and reflect stream-bed elevations, so that water levels were constrained to the stream-bed elevations. Constant heads were used in the southern and northern reaches of Dry Hollow where water flows in the stream (Figure 38).

Constant heads were used along the Roanoke River on the northern boundary of the model grid, except for a small area on the eastern half where no-flow cells were indicated by the water-table contours. Additionally, the southern boundary of the grid at the base of Poor Mountain, was modeled using general head boundaries. Although there is a ground-water divide between Cove and Spring Hollows, this divide may be impacted by reservoir conditions. Therefore, the model grid extends to Cove Hollow with the river package used to simulate the Cove Hollow stream, which is a gaining stream. River stages reflect stream-bed elevations derived from the topographic map of the site. River-bed conductances were represented with the hydraulic conductivity of the rock through which the stream runs, based on field observations that bedrock outcrops in the stream. The Spring Hollow stream was modeled using constant heads, as the fully-penetrating stream depicted on Figure 18.

### 8.2.2.3 Input Parameters

Most of the data for input parameters were derived from data collected during site investigation, characterization and grouting activities. Some data were based on values found in the literature, as discussed in the following sections.

#### 8.2.2.3.1 Aquifer Depth

The unconfined aquifer has developed in vertically dipping carbonates and shales. Since the carbonates have undergone significant development of secondary porosity through solutioning, the thickness of the aquifer is not known with certainty, but generally solution features in karst terrain do not extend over 200 feet below base level (Fetter, 1980) before solution porosity decreases exponentially with depth. Well and boring logs and grout hole logs were reviewed to find the deepest evidence of solution activity. The deepest solution feature in a well occurs in Well R2 which displays a large rock- and clay-filled void at elevation 1166 feet. This is about 84 feet below the on-strike 1250-foot stream-bed elevation of Spring Hollow. Well R2 is located near the deepest solution feature in a grout hole at elevation 1103 feet, which is 147 feet below the on-strike 1250-foot stream-bed elevation in Spring Hollow. Both are located in Grout Zone 2 on the west side of the reservoir. The deepest solution features for the other zones are as follows: elevation 1165 in Zone 1, elevation 1163 in Zone 3, and elevation 1159 in Zone 4, which correspond to 72, 57, and 81 feet below their respective on-strike Spring Hollow

stream-bed elevations. It is noted that at least two grout holes in Zone 4 end in solution features.

The deep solutioning in Zone 2 at 147 feet below the on-strike stream-bed elevation is an isolated feature. Based on the presence of a ground-water divide between Spring and Cove Hollows (Figure 17), this solutioning is considered irrelevant to a hydraulic connection between the hollows and may be related to an older karst base level.

The average depths in feet of the grout curtain below the average on-strike stream-bed elevations are 75, 85, 75, and 85, for Zones 1, 2, 3, and 4. In order to be consistent with the average depth of the grout curtain site-wide, the depth of the aquifer was modeled as 80 feet below the on-strike stream-bed elevation in Spring Hollow along each row of the grid.

In the northern half of Dry Hollow the unconfined aquifer includes the Layer 1 colluvial/residual layer. The base of Layer 1 extends to the base of the colluvial layer presented in Figure 44, which is also the top of Layer 2.

#### 8.2.2.3.2

No pressure-testing data were available for the colluvial/residual material of Layer 1, and the log descriptions varied widely from a clayey gravel and silty sand to a silty clay. Therefore, the material was modeled with a single hydraulic conductivity, with possible values consistent with the textural range,  $2.8 \times 10^{-4}$  to 2.8 fpd ( $1 \times 10^{-7}$  to  $1 \times 10^{-3}$  cm/sec) (Fetter, 1980).

Estimates of bedrock hydraulic conductivities were obtained through analysis of packer tests conducted during previous site characterizations (SEA, 1989) and during pressure testing of grout holes during the test program (SEA, 1991), summarized in Appendix B. The analyses provided a range of hydraulic conductivities from infinity (no pressure on testing) to  $2.8 \times 10^{-3}$  fpd ( $1 \times 10^{-6}$  cm/sec). Generally, the values were low, averaging  $2.8 \times 10^{-2}$  fpd.

Grout-take data provided a second method of estimating initial hydraulic conductivities. The grout holes in each zone along the 1410-foot topographic contour (Figures 33 through 36) were reviewed for volume of grout to reflect the degree of solutioning. Grout-take volumes per grout hole ranged from less than 200 cf to over 22,000 cf. Core logs of grout holes from the Test-Grout Program were used to correlate grout-take volumes to degree of solutioning and lithology site-wide. Grout takes along the lengths of grout holes were correlated to lithology based on core. Generally, in rocks with no solution porosity such as the vari-colored shales and siltstones, and unsolutioned dolomites, the grout take volume was less than 200 cf. Based on the results of the pressure tests, an average low hydraulic conductivity of  $2.8 \times 10^{-2}$  fpd was assigned to these rocks. The highest grout take volumes of 10,000-22,000 cf occurred in carbonate rocks with large solution features which were situated adjacent to maroon-colored fault breccia. These rocks were assigned an initial hydraulic conductivity of 2800 fpd. The remaining intermediate ranges were used in a qualitative manner to assign initial hydraulic conductivities along the grout curtains in each zone.

In areas outside the grout zones where no grout holes were drilled, the hydraulic conductivities were assigned each lithologic unit as mapped according to the grout-take correlation discussed above. The vari-colored shales and siltstones (Unit 1) and the carbonates (Unit 3) were given initial hydraulic conductivities of  $2.8 \times 10^{-2}$  fpd, the fault breccia and associated deformed shales (Unit 2),  $2.8 \times 10^{-1}$  fpd, and the shaley dolomites (Unit 4),  $2.8 \times 10^{+0}$  fpd. Where the Unit 3 carbonates and Unit 4 shaley dolomites occur next to the fault breccia, hydraulic conductivities of  $2.8 \times 10^{+3}$  fpd and  $2.8 \times 10^{+2}$  cm/sec respectively were assigned. The range in values theoretically for the carbonate units and the fault breccia can range from almost no conductivity to infinity. This range, particularly in vertical bedrock, requires lengthy trial-and-error calibration.

#### 8.2.2.3.3 Anisotropy

The multiple joint sets discussed previously have two strong trends that are subperpendicular and that strongly affect the ground-water flow regime. Although much of the ground-water flow is channeled through solutioned carbonates that run east-west, joint sets transect these beds and provide an interconnection between lithologies. To offset the strong control exerted by heterogeneities in the row direction (y-direction) (Figure 54), and allow more movement of water along the column direction, an anisotropy of 1.1 was used. This ratio reflects the column-to-row (y/x) anisotropy.

#### 8.2.2.3.4 Recharge

The maximum value of recharge, 12.2 inches per year, was calculated as the difference between the annual average precipitation of 41.1 inches and the estimated evapotranspiration rate of 28.9 inches determined in Section 6.1.2.2. This 12.2 inches per year is a maximum since the contribution of precipitation to surface runoff was not included.

Since most recharge takes place during the winter and early spring when evapotranspiration demands are virtually nonexistent, a check on the validity of this number is made. Average annual rainfall during the months of November, December, January and February are 3.19, 2.97, 2.62, and 3.04 inches summing to 11.82 inches (Table 5). Some of this recharge is taken up by wetting of the soil column, so that not all of the 11.82 inches can be expected to recharge the system. However, a water surplus is also expected during the months of March, April, September and October which would contribute additional ground-water recharge (Fetter, 1980).

A case for low surface runoff may be made on the basis of site-specific conditions, particularly in areas of highly fractured and solutioned rock, where recharge to the water table may occur through macropore flow instead of diffuse recharge. In this area specifically along Dry Hollow, where slope is minimal and ponding in sinkholes and solution features is likely, recharge may be much higher than that falling on residual material.

Recharge was applied to the model using the option of recharge to the highest active cell. Initial values of recharge ranged to 15.0 inches, with a higher value for Layer 1 (Dry Hollow) than for Layer 2.

### 8.2.3 Pre-Grout Simulation

For pre-grout simulations the stream of Spring Hollow was an important hydrogeologic boundary. With Spring Hollow modeled as a discharge zone, the stream was considered to be a point of upward gradient and therefore fully penetrating. For calibration purposes, flows into the constant heads and springs were summed to total the average flux in the stream. The two springs in the high-solution zone and the Pond Spring were modeled as drains.

The pre-grout simulation was performed to calibrate the system to pre-grout conditions. This simulation included input data as discussed in Section 8.2.2.3. Hydraulic conductivity was the primary calibration parameter, however, recharge was adjusted to build a ground-water divide between Cove and Spring Hollows. There is a trade-off between hydraulic conductivity and recharge. As recharge is increased, hydraulic conductivity must also be increased to achieve the same heads and flux. The result is a trial-and-error solution that is non-unique.

#### 8.2.3.1 Calibration Targets

Calibration targets for the pre-grout simulation included water levels in wells, and spring and stream flow data. The target flow for the section of Spring Hollow stream



above the high-solution zone (Weir A) was 0.23 to 0.36 cfs, for the Flume, 0.76 to 1.94 cfs, for the Pond Spring, 0.15 to 0.17 cfs, and for the total flow in Spring Hollow to the dam (Weir B), 1.30 to 2.77 cfs. These values reflect ranges discussed in Section 6.1.2.1. Although flows in Cove Hollow and Dry Hollow are relatively unknown, values obtained during the 1984-1985 field study (ASI, 1989) were used as target values. Flow above the sinking point in Dry Hollow ranged between 0.9 and 3.5 cfs and total flow in Cove Hollow was between 0.7 and 3.1 cfs. Calibration within reasonable range of these values was considered adequate.

Target heads were based on the data used to generate the water-table map (Figure 38). Point calibration to the water-level elevations of individual wells was performed. The point values shown in Table 8 are the average pre-grout water-table elevations. Calibration to the trends of the water-table map was also performed. Post-grout wells, G4 through G7, and P2 through P6, were used in a qualitative manner for both the trend calibration target and the point calibration targets.

#### 8.2.3.2 Calibration and Results

The calibration process consisted of point calibration and trend calibration. In the point calibration, the heads in cells containing the target wells were calibrated as closely as possible to the target value, the mean of the pre-grout water-table data, presented in Table 8. The simulated heads for the target wells, with the exception of Well B14A, fell within one standard deviation of the mean, indicating a Level 1 calibration (Anderson &

Table 8

## Comparison of Pre-Grout Target Heads with Simulated Heads

Target	Heads (ft), Flow (cfs)			Calibration Criterion
	Measured	Simulated	Residual	
Well R1	1269.1	1273.6	-4.4	4.4
Well R2	1285.3	1288.5	-3.3	3.5
Well R3	1275.2	1278.3	-3.1	8.2
Well G1	1265	1267.1	-2.1	12.6
Well G4 <sup>1</sup>	1273.6	1273.4	0.2	25.4
Well G5 <sup>1</sup>	1297.9	1292.7	5.2	8.1
Well G6 <sup>1</sup>	1355.1	1358.4	-3.3	7
Well G7 <sup>1</sup>	<<1331.3	1270.1	NA <sup>2</sup>	NA
Well P2 <sup>1</sup>	1317.8	1316.1	1.72	4.7
Well P3 <sup>1</sup>	1318.2	1320.5	-2.31	3.7
Well P4 <sup>1</sup>	1307.7	1312.8	-5.2	17.9
Well P5 <sup>1</sup>	1287.9	1294.1	-6.23	29.2
Well P6 <sup>1,3</sup>	Dry	Dry	NA	NA
Well B14A	1218.6	1214.3	4.3	2.7
Well B16D	1197.6	1197.8	-0.15	2
Well B17A	1210.1	1213.4	-3.34	9.4
Well B19	1194.2	1195	-0.8	1.2
Well B20	1241.5	1244.7	-3.2	0.73
Well DH1	Dry	Dry	NA	NA
Well Q1	1209.1	1208	1.1	1.1
Weir A (Rows 1-7)	0.23 - 0.36	0.3	NA	NA
High Solution Zone	NA	1.36	NA	NA
Flume	0.79 - 1.94	1.04	NA	NA
Pond Spring	0.27	0.26	NA	NA
Weir B (Rows 1-50)	1.3 - 2.77	1.9	NA	NA

<sup>1</sup> Secondary target, well installed post-grout.

<sup>2</sup> Not Applicable

<sup>3</sup> Well wets in post-reservoir scenario.

Woessner, 1991). Since the hydraulic conductivities, and therefore heads, varied substantially from row to row, interpolation to the target well location in each cell would have produced a value less realistic than a center of cell value. Trend calibration was also used, whereby the water-level contours based on field measurements was simulated as closely as possible.

The pre-grout simulated water-table map is shown in Figure 55. A calibration to trend is apparent in the comparison of the model-simulated water-table contours with the water-table map based on measured values (Figure 38).

Calibration also required some adjustment of the recharge value, with final values of 9.0 inches per year in Layer 1, and 6.0 inches per year in Layer 2. The springs and streams were also calibrated to within the calibration range. The target and simulated flows are presented on Table 8.

The unconsolidated material of Layer 1 was calibrated to 0.06 fpd. Calibration of Layer 2 bedrock resulted in 14 zones of hydraulic conductivity as depicted in Figure 56. The highest hydraulic conductivity, 1400 fpd, occurred within the high-solution zone. The lowest hydraulic conductivity, 0.02 fpd, was calibrated to the vari-colored shales and siltstones as expected. These results are the same orders of magnitude as previous simulations. Calibration also required the insertion of two thrust faults within the high-solution zone to simulate the effect of the carbonates behaving hydraulically like isolated pipes. The thrust faults were simulated with a hydraulic conductivity of  $2.8 \times 10^{-4}$  fpd, as

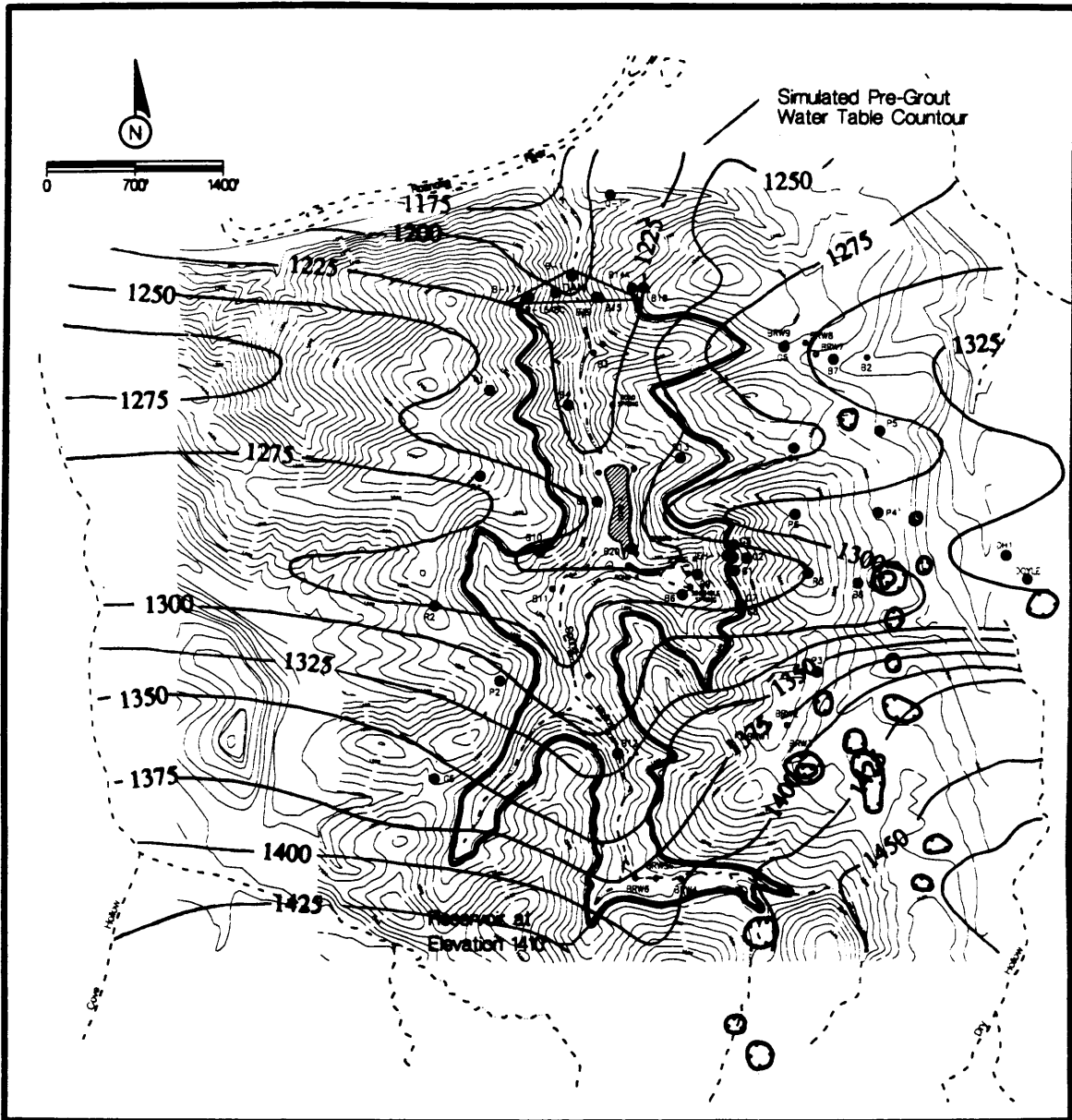
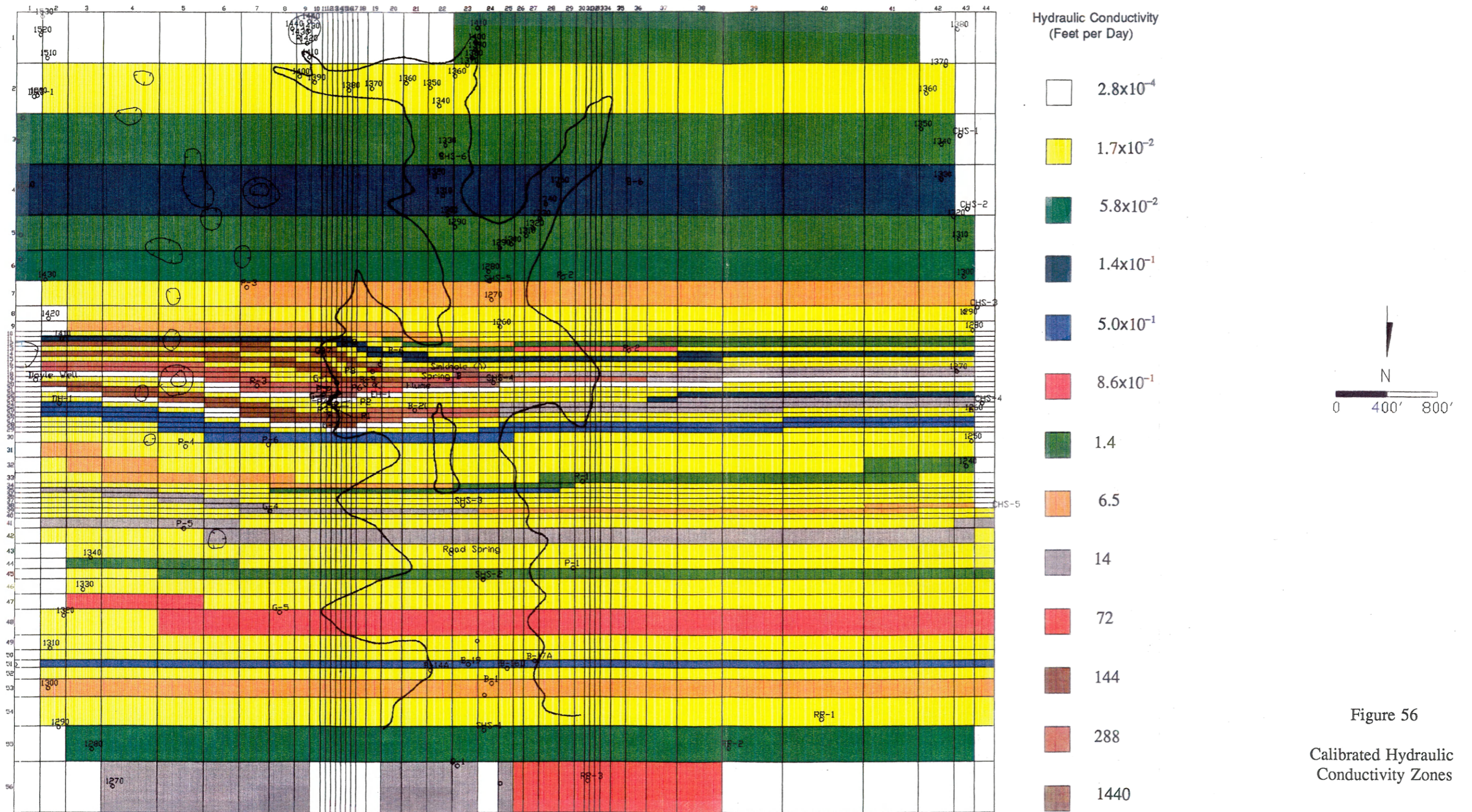


Figure 55

Pre-Grout Simulated Water-Table Map



shown in Figure 56. To avoid building unreasonably high heads on the thrust fault cells, recharge was removed.

Gaining and losing reaches along the three streams and the river were consistent with model simulations of gaining and losing reaches. The volumetric budget discrepancy was 0%.

#### 8.2.3.3 Violation of Darcy's Law

Of the three types of carbonate aquifers described by Fetter (1980), diffuse-flow, free-flow and confined flow, the aquifer of the research area behaves like a free-flow, but has many of the features of a confined flow aquifer. It is similar to a free-flow in that much of the flow is preferentially channeled by large solution features and much of the ground-water discharge is through springs. However, the aquifer is intensely influenced by the laterally interbedded low-permeability shales, siltstones and carbonates, lending characteristics of the confined flow aquifer in the striking relief of the water table. Flow in a free-flow aquifer, with much of the flow through 'pipes' may behave hydraulically like pipe flow and be subject to turbulent flow.

In order to evaluate the simulated ground-water system for non-laminar flow, cell-by-cell flows in the high-solution zone were reviewed for large values. The largest cell-by-cell flow, 0.59 cfs, was found in Layer 2, Row 19, Column 7. Flow in this cell is toward Spring Hollow from Cove Hollow in a very permeable carbonate. In order to determine whether the use of Darcy's Law was valid in the high-solution zone, the cell

by-cell flows ranging from 0.09 to 0.59 cfs were used to calculate Reynold's Numbers. The equation calls for pore or grain diameters. It is known, through exploration drilling at the site, that pore diameters range greatly, from microscopic to ten feet or more. Therefore, to give an indication of the possibilities, a range of diameters was used to calculate the Reynold's Numbers. The results of the calculations are shown in Table 9. As can be seen, Reynold's Numbers range from 0.01 to 46. Laminar flow is believed to occur in porous media in the Reynold's Number range of less than 1 to 10 (Fetter, 1980). Flow is laminar for pore diameters of 0.1 foot, however, for pore diameters of ten feet or more, turbulent flow is expected to occur.

Model simulation using Darcy's Law is valid in karst terrain if the solution features are small in comparison to the size of the grid. This is known as equivalent porous media. The smallest cell size is forty feet wide by eighty feet long. This is smaller than the size of the Blankenship Cave, which makes an equivalent porous media rationale inapplicable.

Although MODFLOW is a computer program based on Darcy's Law, a representation of the karst system of the research area can be made. This is confirmed by the results of the calibration effort. However, the most significant effect of representing turbulent flow as laminar flow is that higher flows than that which actually exist may be modeled. In this case, a seepage rate higher than that which actually exists would represent a conservative (worst-case) rate.

Table 9  
 Reynold's Number<sup>1</sup> Calculations for Determination of Flow Conditions

Cell	Flow (cfs)	Area (Ft <sup>2</sup> )	Velocity (V) V=Q/A (ft/sec)	Viscosity (v) (Ft <sup>2</sup> /sec)	Reynold's Number for 0.1-Foot Pore Diameter	Reynold's Number for 10-Foot Pore Diameter
2,19,14 <sup>2</sup>	0.09	3880	2.4x10 <sup>-5</sup>	1.1x10 <sup>-5</sup>	0.22	21.8
2,19,14	0.19	3760	5.1x10 <sup>-5</sup>	1.1x10 <sup>-5</sup>	0.46	46
2,22,4	0.26	5200	4.9x10 <sup>-5</sup>	1.1x10 <sup>-5</sup>	0.45	44.9
2,22,12	0.43	4000	1.1x10 <sup>-4</sup>	1.1x10 <sup>-5</sup>	1	100
2,19,24	0.49	3320	1.5x10 <sup>-4</sup>	1.1x10 <sup>-5</sup>	1.4	136
2,19,17	0.59	4360	1.3x10 <sup>-4</sup>	1.1x10 <sup>-5</sup>	1.18	118

<sup>1</sup> R=Vd/v

<sup>2</sup> Layer, Row, Column



#### 8.2.4 Post-Grout Simulation

The post-grout simulation achieved two goals. First, it provided a method of calibrating the effective hydraulic conductivity of the grout, and second, it acted as a verification simulation of the pre-grout calibration.

The post-grout model simulated the hydrogeologic regime after the 1992 and 1993 grouting programs. The constant heads representing the stream of Spring Hollow and the drains representing springs were retained. Boundary changes representative of the grout curtain were added as horizontal flow barriers (walls). The elevation of the grout curtain along the Pond Spring is at the 1315-foot topographic contour. Seepage at the 1315-foot elevation, at the top of the grout curtain, has been observed in the field (SEA, 1994a). There are no options in the horizontal flow barrier package to constrain height of the curtain, and without a height constraint, the effects of the grout curtain are consistent with the height of the water table. In order to account for this effect, three drains were placed directly upgradient of the grout wall, within the same cell. The drain elevation was set at 1315 feet, with the flow into the drains representing seepage of the ground water along the top of the grout curtain at the 1315-foot elevation. The conductances of the drains were the same as the hydraulic conductivities of the cells in which they were placed. The locations of Grout Zones 1, 2, 3, 4 and the Pond Spring Grout Zone are shown on Plate 1.

#### 8.2.4.1 Calibration Targets

Calibration targets for the post-grout simulation, presented in Table 10, included water levels in wells, and spring and stream flow data. Since grouting activities did not impact water levels in the southernmost reaches of the reservoir valley, the target flow for the section of Spring Hollow stream above the high-solution zone (Weir A) remained the same. Spring flow at the flume was considerably reduced as a result of grouting to an average of 0.4 cfs (SEA, Personal Communication). Although this number is greater than the flux of 0.05 at the end of the Test-Grout Program, the head behind the grout curtain has risen after the installation of the grout curtain with a concurrent increase in spring flow. The Pond Spring flows were reduced from approximately 0.27 cfs prior to grouting to approximately 0.06 cfs at the end of grouting (SEA, 1994b). Total flow in Spring Hollow after grouting was not measured, since Weir B had been badly weather-damaged prior to grouting. Calibration of that flow was based on reduction in spring flow and changes in water levels in wells.

Target heads were based on the post-grout water-table elevations generated for the post-grout water-table map (Figure 52) and as depicted in the hydrographs of Figures 45 through 51. Wells B20, B14A, B16D, B19, and Q1 were not used as targets for the post-grout simulation since they were abandoned during the grouting activities. Wells G4 through G6 and P2 through P5, along with the remaining pre-grout wells, R1, R2, R3, DH1 and G1 were used as calibration targets. Both point calibration to individual wells (Table 10), and trend calibration to pre-grout water-table map trends, were used. Post-

Table 10

## Comparison of Post-Grout Target Heads with Simulated Heads

Target	Heads (ft), Flow (cfs)			Calibration Criterion
	Measured	Simulated	Residual	
Well R1	1288.9	1282.6	6.3	6.4
Well R2	1300.8	1308.8	-8	8.9
Well R3	1387.1	1387	0.1	11.3
Well G1	1379.1	1386.9	-7.8	10.1
Well G4	1273.6	1282.9	-9.3	25.4
Well G5	1297.9	1293.3	4.6	8.1
Well G6	1355.1	1359	-3.9	7
Well G7	1331.3	1330.1	1.2	10.5
Well P2	1317.8	1316.9	0.9	4.7
Well P3	1318.2	1323	-4.8	3.7
Well P4	1318.8	1328	-9.2	21.6
Well P5	1312.3	1297.3	15	21.8
Well DH1	Dry	Dry	NA <sup>1</sup>	NA
Weir A (Rows 1-7)	0.23 - 0.36	0.3	NA	NA
High Solution Zone	NA	0.52	NA	NA
Flume	0.34	0.33	NA	NA
Pond Spring	0.05	0.12	NA	NA
Weir B (Rows 1-50)	NA	1	NA	NA

<sup>1</sup> Not Applicable or Not Available

grout wells were also used in a qualitative manner for both the trend calibration target and the point calibration targets.

#### 8.2.4.2 Results

Three parameters were adjusted to achieve the calibration, hydraulic conductivity, recharge, and the grout curtain hydraulic conductivity. Point calibration for the post-grout simulation required repeated adjustment of the pre-grout model in a trial-and-error manner in order to bring both models within the one standard deviation calibration criteria. The wells with significant colluvial/residual material proved the most difficult to calibrate. This was expected in a hydrogeologic regime as complicated as the research area. Heterogeneities on scales too small to map or model argue that calibration by trend is a more realistic and achievable approach than point calibration. However, the results of the point calibration were good with only Well P3 not calibrated to within one standard deviation of the mean (Table 10). The post-grout simulated water table is presented as a map in Figure 57. The trends compare well with those of the post-grout water-table map based on measured values (Figure 52). The simulated flume and Pond Spring flows are very close to the calibration targets and the volumetric budget discrepancy was less than 1%.

#### 8.2.5 Evaluation of Grout Effectiveness

The grout curtain of the post-grout simulation was calibrated to a range of hydraulic conductivities in an effort to reproduce the conditions of the ground-water

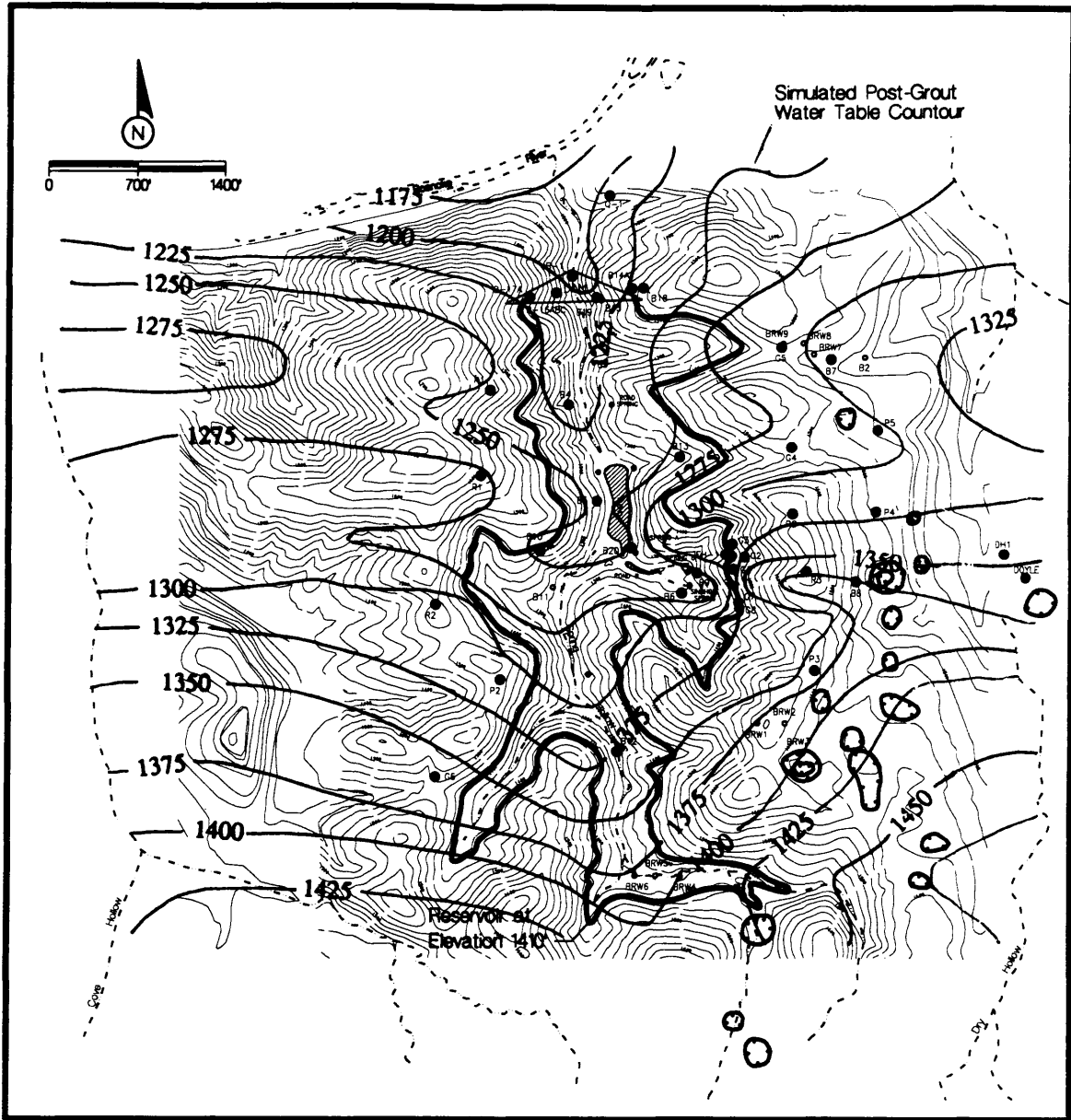


Figure 56

Post-Grout Simulated Water-Table Map

system at the site. Grout Zone 1 hydraulic conductivities ranged between 0.14 fpd ( $2 \times 10^{-4}$  cm/sec) and 0.0014 fpd ( $2 \times 10^{-6}$  cm/sec), Zone 2, between 0.017 to 0.0014 fpd, Zone 3, between 0.14 to 0.017 fpd and Zone 4, between 0.14 to 0.0029 fpd. In Zone 4, the high-solution zone, the most permeable lithologic unit corresponds to the carbonate in which Wells R3 and G1 are open. Grouting in this carbonate was highly successful with a calibrated grout-curtain hydraulic conductivity of 0.0029 fpd. This is reflected in their very high post-grout heads (Figure 45). The carbonate to which Well G7 of Zone 4 is open also is very permeable. However, the head is not nearly as high in this well as in Wells R3 and G1. This resulted in the calibration of a higher grout curtain hydraulic conductivity of 0.14 fpd, which is also the highest grout-curtain hydraulic conductivity in Zones 1 and 3. This value is comparable to the grout-curtain hydraulic conductivity of 0.28 fpd ( $1 \times 10^{-4}$  cm/sec) discussed in Section 7.3 as that which produced seepages below the acceptable rate of 1 to 2 mgd.

Reduction of the pre-grout seepage of 1,227,000 gpd to post-grout seepage of 646,000 gpd indicates that the grouting program was successful. Based on the results of the modeling, a 47% reduction in pre-reservoir seepage was achieved as a result of the reservoir-wide grouting program. This seepage reduction, however, cannot be extrapolated to post-reservoir seepage reduction because of the change in the hydrogeologic regime associated with filling the reservoir, particularly the change in gradient from Spring Hollow to Dry Hollow.

## Chapter 9

## PREDICTION OF POST-RESERVOIR SEEPAGE

In order to predict reservoir seepage rates, the calibrated model was run under reservoir conditions. Elevations of the grouted reservoir were simulated at 1350 feet and at 1410 feet.

The grid and boundary conditions were similar to those used for the post-grout scenario. The reservoir elevations were simulated with constant heads approximately along the respective topographic contours. The drains representing the springs were removed. The drains representing the height of the grout curtain at the Pond Spring were retained. Additionally, drains were added to represent the stream in the dry interval of Dry Hollow. Elevations used in the drains were equivalent to the stream-bed elevation along the stream at the location of the drain cell. This approach achieved the simulation of surface water drainage when the water table rose to the level of the stream bed. The dam was modeled with a permeability of  $2.8 \times 10^{-4}$  fpd.

The model was executed for each simulation of the reservoir elevations. Volumetric budget discrepancies were 0.07% for the 1350-foot simulation, and 0.3% for the 1410-foot simulation. Flow through the faces of the constant heads were summed to find seepages from the reservoir. Under the 1410-foot reservoir simulation, the southern

third of the reservoir did not lose water. The gradient remained toward Dry Hollow as predicted. The seepage at the reservoir elevation of 1350 feet was 150,000 gpd. As expected, seepage rates increase with each rise in the elevation of the reservoir. The seepage rate at the reservoir elevation of 1410 feet was 443,000 gpd, well within the acceptable range. A review of constant head fluxes revealed that most of this seepage occurred in the high-solution zone and in the carbonate beds near the dam.



## Chapter 10

### PERFORMANCE ASSESSMENT

Although the reservoir had not been completely filled by July, 1994, some data were available with which to assess the performance of the grout curtain and to test the predictive ability of the model. From the end of 1993 through July, 1994, the reservoir underwent a fluctuating but gradual rise in elevation. The fluctuations were due to manual raising and lowering of the reservoir. Although the conditions were not steady, the reservoir elevations were averaged over the time period to represent a single elevation of 1275 feet. The well heads were averaged over the same time period to provide a baseline against which an assessment could be made. These heads are presented in Table 11.

A comparison of post-grout target well heads with post-reservoir heads (Tables 10 and 11) provides confirmation of the effectiveness of the grout curtain in serving as a permeability barrier. With the exceptions of Wells P2, P3, and G6, the heads in the wells have undergone substantial increases. Wells P2, P3, and G6 are outside the southernmost portion of the reservoir, where the higher water table was not expected to have an effect. The pre-reservoir elevations are greater than the average reservoir elevation of 1275 feet.

Table 11  
 Comparison of 1275-Foot Reservoir Target  
 Heads With Simulated Heads

Target	Heads		Residual	Calibration Criterion
	Measured	Simulated		
Well R1	1300.6	1307.4	-6.8	6
Well R2	1318	1310.6	7.4	4.6
Well R3	1391.9	1387.5	4.4	3.5
Well G1	1386.5	1387.3	-0.81	3.3
Well G4	1320.7	1307.9	12.8	12.9
Well G5	1313.41	1315.3	-1.9	3.3
Well G6	1355.1	1359.7	-4.6	7
Well G7	1331.3	1331.9	-0.61	10.5
Well P2	1317.8	1318.8	-0.9	4.7
Well P3	1318.2	1321.5	-3.4	3.7
Well P4	1338	1333.1	4.93	1.6
Well P5	1325	1317.5	7.44	14.4
Well P6	1331.1	1335.7	-4.5	1.4
Well DH1	Dry	Dry	NA <sup>1</sup>	NA

<sup>1</sup> Not Applicable or Not Available

In order to test the model as to its predictive ability, a numerical simulation of the reservoir at elevation 1275 feet was conducted. The reservoir elevation was represented in the model through the use of constant heads. The model was run as a steady-state simulation using the recharge, hydraulic conductivity and grout curtain parameters obtained through the pre-grout and post-grout calibrations. The target heads and the simulated heads are presented for comparison in Table 11. Only three simulated heads did not fall within one standard deviation of the mean, however, these wells, R3, R2, and R1, were very close to their targets. The simulated head in Wells R2 was 7.4 feet low, in R1, 6.8 feet high, and in R3, 4.4 feet low. The water table rose with the filling of the reservoir, and as a result, the water table rose above the base of Well P6, which had been dry (Appendix D). The model predicted a head that was only 4.5 feet higher than that actually observed. Additionally, there are no patterns or trends in the residuals. The volumetric budget discrepancy was only -0.15%.

Performance assessments of the effectiveness of the grout curtain both by analysis of well data and by numerical simulation, provide confirmation of the effectiveness of the curtain. Additionally, the ability of the model to represent a complicated hydrogeologic regime and provide heads comparable to those measured in the field allows confidence in the model to accurately predict seepage from the reservoir. This is critical to the effective use of numerical modeling as a tool in grout optimization, seepage prediction, and remedial design evaluation.

As of August 1, 1995, the reservoir was at elevation 1385 feet. The estimated seepage losses from the reservoir using a water budget approach were estimated between 250,000 gpd and 500,000 gpd (Personal Communication, SEA). This is in good agreement with order of magnitude of reservoir seepage losses predicted by the model.

## Chapter 11

### SUMMARY OF METHODOLOGY

Optimization of a grouting plan lies in the ability of the planner to correctly identify zones of potential seepage, and selectively grout the zones, thereby limiting the expense of field time and grout. The methodology implemented in the research area utilizes numerical modeling as a tool for grout optimization and seepage minimization. The activities related to the design and construction of the Spring Hollow Dam and Reservoir provided a vehicle for testing this methodology.

The methodology includes the following: evaluation of seepage potential; evaluation of grouting alternatives; evaluation of grout effectiveness; prediction of seepage; and, performance assessment and evaluation of remedial design.

#### 11.1 Evaluation of Seepage Potential

Prior to the development of a grouting program is the assessment of the potential for seepage. Key to evaluating seepage potential is an understanding of the hydrogeological setting. This understanding is gained through the development of a hydrogeological conceptual model of the site. For the research area this was based on the characterization of the site geologically, hydrologically, and geomorphologically. The data base for this characterization was collected through drilling of boreholes, installation

of piezometers and surface-water monitoring equipment, field mapping, tracer testing, and a review of the literature, including air photos and the topographic map of the site. The site characterization provided a basis upon which the area of the reservoir was zoned through a series of map overlays according to potential for seepage. These overlays used geologic, hydrologic and geomorphologic characteristics of the site related to solution features and fractures. The overlays were compiled to produce a seepage potential map that classified the reservoir perimeter according to seepage potential. The map provided a qualitative assessment of the seepage. In order to evaluate the need for grouting, an estimate of seepage was obtained.

A zone of maximum seepage was identified, and the hydrogeology of the zone was conceptualized. A quantitative estimate of seepage through the zone of highest seepage potential under the conditions of a full reservoir, was obtained numerically and analytically. The model for each of these solutions was based on the hydrogeological conceptual model. The result of the evaluation of seepage potential, was that the potential for a large magnitude of seepage existed, and that a grout plan was necessary.

### 11.2 Evaluation of Grouting Alternatives

Various grouting alternatives to reduce reservoir seepage were evaluated. The evaluation of grouting alternatives relied on the results of a test-grout program, and included a numerical simulation of part of the reservoir valley. The object was to compare the impact of the grout at different effective hydraulic conductivities of the grout

curtain with percent reduction in seepage. The model was based on field data and the site-wide conceptual model. The results of this effort provided a basis for the development of a site-wide selective grouting plan.

### 11.3 Evaluation of Grout Effectiveness

An integral component of the site-wide grout program was the evaluation of the effectiveness of the grout through both a quantitative and qualitative approach. A qualitative determination of the effectiveness of the selectively grouted curtain was achieved through analysis of well hydrographs and surface-water data to find a correlation between grouting activities and a change in the hydrogeologic regime. Climbing well heads and reduced spring flow provided evidence of the positive effect of the grout curtain. In order to evaluate, in quantitative terms, the reduction in total seepage into the reservoir as a result of grouting activities, a numerical simulation of pre-grout and post-grout conditions was conducted. The numerical model provided not only provided a value for the reduction in seepage, it also provided an effective hydraulic conductivity for the grout curtain which allowed a prediction of post-reservoir seepage rates and an assessment of the performance of the grout curtain.

### 11.4 Prediction of Post-Reservoir Seepage

The success of a grouting program is the reduction in seepage to an acceptable level. In order to determine whether grouting was sufficient to do so under post-reservoir conditions, a prediction of seepage was conducted using the numerical model. Seepage

predictions were made for the reservoir at 1350 feet and at the maximum elevation of 1410 feet. The predictions were consistent with the results of the evaluation of grouting alternatives.

#### 11.5 Performance Assessment and Evaluation of Remedial Designs

The performance of the grout curtain under real conditions was evaluated through numerical modeling of the reservoir under real field conditions, at an average elevation of 1275 feet. This procedure resulted in an assessment not only of the grout curtain, but also of the ability of the model to accurately simulate the conditions of the reservoir. This is key to its ability to predict seepages at various reservoirs elevation and to evaluate remedial designs as they may become necessary.



## Chapter 12

### CONCLUSIONS

A grouting methodology using numerical modeling as a tool, can be effectively implemented to reduce time-in-the-field costs related to total grout volumes, test borings, and numbers of grout holes, through selective grouting. The applicability of the numerical modeling methodology has been demonstrated in the karst terrain of the Spring Hollow Dam and Reservoir. This study has demonstrated that a numerical model, based on a thorough understanding of the hydrogeological setting, can be an effective approach to a grouting program

As demonstrated with the post-reservoir data from Spring Hollow, the method was effective at identifying potential seepage zones, estimating seepage rates, predicting grout curtain effectiveness, and evaluating grout curtain performance. The reliability, not only of the model, but also of the method is borne out by the ability of the model to accurately simulate post-reservoir conditions at the 1275-foot elevation. The accuracy of this simulation lends credence to the ability of the model to accurately predict order of magnitude seepage rates at higher elevations of the reservoir, and the ability of the model to effectively evaluate remedial designs if and when necessary. In addition, the grout

optimization and seepage reduction objectives of the methodology are validated in the success of the selective grout program in producing seepage at an acceptable level.

## Chapter 13

## REFERENCES

- Amato, Roger, 1974. Geology of the Salem Quadrangle, Virginia. Reports of Investigations No. 37. Charlottesville: Virginia Division of Mineral Resources, Department of Conservation and Economic Development. 1-40.
- Anderson, Mary P., and William W. Woessner, 1992. Applied Groundwater Modeling, Simulation of Flow and Advective Transport. San Diego, Calif.: Academic Press, Inc.
- Bowen, Robert, 1981. Grouting in Engineering Practice, 2nd ed. New York: John Wiley & Sons.
- Breeding, N. K., and J. W. Dawson, 1976. Roanoke County groundwater: present conditions and prospects. Planning Bulletin 301. Richmond: Virginia State Water Control Board Bureau of Water Control Management.
- Edwards, Jonathan, Jr., 1959. The Geology of the Upper Roanoke River Valley Area, Montgomery and Roanoke Counties, Virginia. Master of Science Thesis, Virginia Polytechnic Institute, Blacksburg, Virginia. 1-92.
- Fetter, C. W., Jr., 1980. Applied Hydrogeology. Columbus: Charles E. Merrill Publishing Co.
- Freeze, R. Allan, and John A. Cherry, 1979. Groundwater. Englewood Cliffs, N.J.: Prentice-Hall, Inc.
- Holsinger, John R., 1975. Description of Virginia Caves. Bulletin 85. Charlottesville: Virginia Division of Mineral Resources, Department of Conservation and Economic Development. 197.
- Kipko, Eh. Ya., Yu A. Polozov, O. Yu. Lushinkova, V. A. Lagunov, and Yu. I. Svirskiy, 1993. Integrated Grouting and Hydrogeology of Fractured Rocks in the Former

- USSR. Converted into Technical English by Roy E. Williams, Society for Mining, Metallurgy, and Exploration, Inc., Littleton, Colorado.
- Martin, Ray E., and Milner, Brian, 1988. Evaluation of Reservoir Seepage in Karst Topography. Proceedings of Geotechnical Aspects of Karst Terrains, GT Div/ASCE, May 10-11, Nashville, TN.
- McDonald, M.G., and A.W. Harbaugh, 1991. MODFLOW, A Modular Three-Dimensional Finite Difference Flow Model. Golden, Colorado: International Ground Water Modeling Center (March).
- Palmer, W.C., and A. V. Havens, 1957. A Graphical Method for the Determination of Evapotranspiration Adapted from the Thornwaite Method. Prepared for the Weather Bureau Short Course in Agricultural Meteorology, July, 1956.
- Schnabel Engineering Associates, P.C., 1985. Preliminary Geotechnical Engineering Study, West County Reservoir, Roanoke County, Virginia.
- Schnabel Engineering Associates, P.C., 1987. Technical Memorandum, Expanded Phase A2 Program, Proposed West County Dam, Roanoke County, Virginia.
- Schnabel Engineering Associates, P.C., 1989. Schnabel Engineering Associates, Design Phase Geotechnical Engineering Report Spring Hollow Dam and Reservoir, Roanoke County, Virginia, August 17.
- Schnabel Engineering Associates, P.C., 1991a. Engineering Analysis Report, Test Grouting Program, Spring Hollow Reservoir, Roanoke County, Virginia.
- Schnabel Engineering Associates, P.C., 1991b. Evaluation of Predicted Reservoir Seepage, Spring Hollow Dam Reservoir, Roanoke County, Virginia.
- Schnabel Engineering Associates, P.C., 1992a. Monthly Report for February, Spring Hollow Dam Construction Monitoring, Roanoke County, Virginia.
- Schnabel Engineering Associates, P.C., 1992b. Monthly Report for April, Spring Hollow Dam Construction Monitoring, Roanoke County, Virginia.
- Schnabel Engineering Associates, P.C., 1992c. Monthly Report for July, Spring Hollow Dam Construction Monitoring, Roanoke County, Virginia.

- Schnabel Engineering Associates, P.C., 1992d. Monthly Report for August, Spring Hollow Dam Construction Monitoring, Roanoke County, Virginia.
- Schnabel Engineering Associates, P.C., 1992e. Monthly Report for September, Spring Hollow Dam Construction Monitoring, Roanoke County, Virginia.
- Schnabel Engineering Associates, P.C., 1992f. Geologic Map of the Spring Hollow Dam and Reservoir.
- Schnabel Engineering Associates, P.C., 1994a. Spring Hollow Pond Drilling and Grouting Activities, Spring Hollow Reservoir, Roanoke County, Virginia.
- Schnabel Engineering Associates, P.C., 1994b. Memorandum from John Pappas to File, Subject: Changes in water flow after grouting the Pond Spring Area, March 4, 3 pages.
- Sherard, James L., Richard J. Woodward, Stanley F. Gizienski, William A. Clevenger, 1963. Earth and Earth Rock Dams. John Wiley & Sons, Inc.
- State of Virginia, 1972. Aerial Photos 2-80-416-213, 2-80-416-213, and 2-80-416-239, 1-31-72. Virginia Department of Highways and Transportation.
- State of Virginia, 1995. Normals, Means, and Extremes for Roanoke, Virginia. Charlottesville: Virginia State Climatology Center, University of Virginia, Environmental Sciences, Charlottesville, Virginia, By Facsimile, May 22, 1995.
- United States Geological Survey, 1972. Elliston Quadrangle, Virginia.

**APPENDIX A**  
**STRUCTURAL DATA**

Table A-1

Spring Hollow Valley Bedding and  
Joint Orientation Data

Strike	Dip	Strike	Dip
N 08 W	90 NE	N 37 E	86 SE
N 17 E	83 SE	N 21 W	58 SW
N 13 W	36 SW	N 42 E	62 SE
N 04 W	11 NE	N 20 W	78 SW
N 04 W	79 SW	N 40 E	49 SE
N 67 W	64 NE	N 04 W	79 SW
N 28 W	75 SW	N 22 W	76 NE
N 03 E	90 NW	N 78 E	60 SE
N 06 W	90 NE	N 22 E	80 NW
N 06 E	73 NW	N 02 E	80 NW
N 44 E	88 SE	N 41 E	45 NW
N 08 W	63 NE	N 00 W	80 SW
N 15 E	73 NW	N 19 E	90 SE
N 46 E	68 SE	N 12 W	90 SW
N 22 E	69 SE	N 88 E	76 NW
N 20 W	75 SW	N 90 E	78 NW
N 20 E	76 SE	N 89 W	62 NE
N 21 W	27 SW	N 89 W	66 NE
N 01 E	84 NW	N 89 W	62 NE
N 11 W	65 SW	N 82 W	56 NE
N 43 E	44 NW	N 80 W	45 NE
N 04 W	67 SW	N 83 W	62 NE
N 44 W	24 NE	N 78 W	65 NE
N 05 E	74 NW	N 82 E	83 NW
N 11 W	78 SW		
N 17 W	83 SW		
N 03 E	89 NW		
N 79 E	82 SE		
N 71 W	52 SW		
N 05 W	62 SW		
N 24 W	58 SW		
N 20 W	78 SW		
N 08 E	82 NW		
N 88 E	48 NW		
N 15 W	25 SW		
N 08 E	87 NW		
N 88 E	41 SE		
N 08 E	66 SE		
N 01 E	71 NW		
N 13 W	84 SW		
N 00 W	84 SW		
N 05 E	44 SE		
N 08 W	80 SW		
N 25 E	77 SE		
N 75 E	44 SE		
N 06 W	68 SW		

From SEA, 1989

Table A-2  
 Dominant Geologic Structural Trends  
 Spring Hollow Reservoir Valley

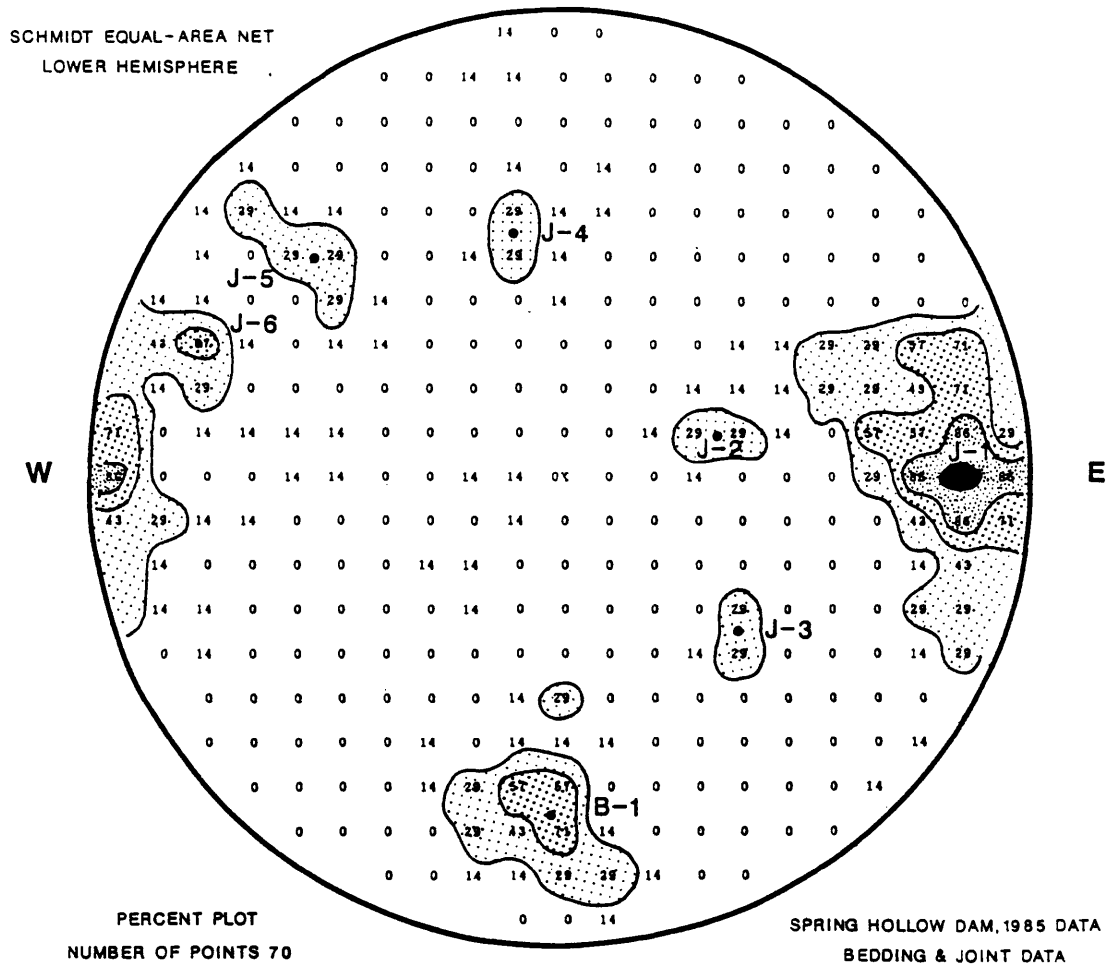
Trends	Feature Type	Modal Strike	Modal Dip	Approx. Strike Range	Approx. Dip Range
B-1	BEDDING	N88°W	65°NE	N80°E TO N70°W	40° TO 85°N
J-1	JOINTS	N - S	78°W	N20°W TO N25°E	55°W TO 80°E
J-2	JOINTS	N10°W	30°SW	N00°W TO N20°W	20° TO 40°SW
J-3	JOINTS	N40°E	45°NW	N30°E TO N50°E	40° TO 50°NW
J-4	JOINTS	N80°E	45°SE	N75°E TO N90°E	40° TO 55°SE
J-5	JOINTS	N42°E	60°SE	N35°E TO N50°E	45° TO 85°SE
J-6	JOINTS	N24°E	72°SE	N15°E TO N28°E	60° TO 90°SE



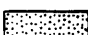

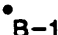
From SEA, 1989



Figure A-1

Geologic Structure Data From  
Spring Hollow Dam Reservoir Area



-  2 to 5 Percent of Poles
-  5 to 8 Percent of Poles
-  8 to 10 Percent of Poles
-  Greater than 10 Percent of Poles
-  Modal Point for Fracture Trend

From SEA, 1989

**APPENDIX B**  
**DATA**

Table B-1

Summary of Packer Permeability Tests  
1989 Field Investigation

<u>BORING NO.</u>	<u>TEST INTERVAL(ft)</u>	<u>WATER PRESSURE, psi</u>	<u>MEASURED FLOW, gpm</u>	<u>CALCULATED PERMEABILITY k, cm/sec</u>
B-1	20-110.3 ft	35	11.75	$3.1 \times 10^{-4}$
	26.3-31.3 ft	45	11.6	$1.3 \times 10^{-4}$
	21.3-26.3 ft	50	0.1	$6.6 \times 10^{-6}$
	16.3-21.3 ft	50	0.05	$3.3 \times 10^{-5}$
		80	0.08	$3.1 \times 10^{-6}$
	11.3-16.3 ft	100	0.4	$1.3 \times 10^{-5}$
		50	4.25	$2.8 \times 10^{-4}$
	50-110.9 ft	100	12.25	$4.1 \times 10^{-4}$
		60	11.0	$8.4 \times 10^{-5}$
	B-1A	7.8 - 14.9 SINGLE PACKER	25	2.7
50			7.4	$3.76 \times 10^{-4}$
75			10.1	$3.48 \times 10^{-4}$
75			9.9	$3.41 \times 10^{-4}$
50			7.0	$3.56 \times 10^{-4}$
14.9-24.9 SINGLE PACKER		25	1.8	$1.74 \times 10^{-4}$
		25	.2	$1.48 \times 10^{-5}$
		50	2.8	$1.09 \times 10^{-4}$
		75	4.3	$1.13 \times 10^{-4}$
		75	3.7	$9.76 \times 10^{-5}$
25-30 DOUBLE PACKER		50	3.6	$1.40 \times 10^{-4}$
		25	NO FLOW	IMPERMEABLE
		25	NO FLOW	IMPERMEABLE
		50	NO FLOW	IMPERMEABLE
		75	NO FLOW	IMPERMEABLE
30-35 DOUBLE PACKER		100	NO FLOW	IMPERMEABLE
		25	NO FLOW	IMPERMEABLE
		50	NO FLOW	IMPERMEABLE
		75	NO FLOW	IMPERMEABLE
		100	NO FLOW	IMPERMEABLE
13.6-18.6		25	.04	$6.01 \times 10^{-6}$
		50	.20	$1.43 \times 10^{-5}$
		75	.3	$1.41 \times 10^{-5}$
		100	.34	$1.91 \times 10^{-5}$
		75	.26	$1.22 \times 10^{-5}$
		50	.16	$1.15 \times 10^{-5}$
		25	.03	$4.51 \times 10^{-6}$
		18.6-23.6	25	NO FLOW
18.6-23.6		50	.10	$7.53 \times 10^{-6}$
		75	.22	$1.07 \times 10^{-5}$
		100	.36	$1.29 \times 10^{-5}$
		75	.23	$1.12 \times 10^{-5}$
		50	.10	$7.53 \times 10^{-6}$
24.3-29.3		25	NO FLOW	IMPERMEABLE
		50	NO FLOW	IMPERMEABLE
		75	NO FLOW	IMPERMEABLE
		100	NO FLOW	IMPERMEABLE
		75	NO FLOW	IMPERMEABLE
29.3-34.4		50	NO FLOW	IMPERMEABLE
		25	NO FLOW	IMPERMEABLE
	50	.04	$3.02 \times 10^{-6}$	
	75	.02	$9.73 \times 10^{-7}$	
	100	.06	$2.16 \times 10^{-6}$	
	75	.02	$9.73 \times 10^{-7}$	
	50	.02	$1.51 \times 10^{-6}$	

(continued)

Table B-1 (continued)

BORING NO.	TEST INTERVAL (FT)	WATER PRESSURE, psi	MEASURED FLOW, gpm	CALCULATED PERMEABILITY k, cm/sec
B-1A con't	34.3-39.3	25	NO FLOW	IMPERMEABLE
		25	NO FLOW	IMPERMEABLE
		50	NO FLOW	IMPERMEABLE
		75	NO FLOW	IMPERMEABLE
		100	NO FLOW	IMPERMEABLE
		75	NO FLOW	IMPERMEABLE
	39.0-44.0	50	NO FLOW	IMPERMEABLE
		25	NO FLOW	IMPERMEABLE
		25	NO FLOW	IMPERMEABLE
		50	NO FLOW	IMPERMEABLE
		75	.02	$9.76 \times 10^{-7}$
		100	.06	$2.16 \times 10^{-6}$
	44.0-49.0	75	NO FLOW	IMPERMEABLE
		50	NO FLOW	IMPERMEABLE
		25	NO FLOW	IMPERMEABLE
		25	NO FLOW	IMPERMEABLE
		50	.02	$1.43 \times 10^{-6}$
		75	.02	$9.40 \times 10^{-7}$
	49.3-54.3	100	.14	$4.90 \times 10^{-6}$
		75	.02	$9.40 \times 10^{-7}$
		50	.02	$1.43 \times 10^{-6}$
		25	NO FLOW	IMPERMEABLE
		25	NO FLOW	IMPERMEABLE
		50	.02	$1.51 \times 10^{-6}$
	54.3-59.3	75	.04	$1.95 \times 10^{-6}$
		100	NO FLOW	IMPERMEABLE
		75	NO FLOW	IMPERMEABLE
		50	NO FLOW	IMPERMEABLE
		25	NO FLOW	IMPERMEABLE
		25	NO FLOW	IMPERMEABLE
	59.5-64.5	50	.06	$4.35 \times 10^{-6}$
		75	.01	$4.74 \times 10^{-7}$
		100	.06	$2.12 \times 10^{-6}$
75		.06	$2.85 \times 10^{-6}$	
50		NO FLOW	IMPERMEABLE	
25		NO FLOW	IMPERMEABLE	
64.6-69.6	59.5-64.5	.02	$3.25 \times 10^{-6}$	
	50	.08	$5.95 \times 10^{-6}$	
	75	.04	$1.93 \times 10^{-6}$	
	100	.14	$5.00 \times 10^{-6}$	
	75	.14	$6.76 \times 10^{-6}$	
	50	.04	$2.98 \times 10^{-6}$	
B-3	64.6-69.6	25	NO FLOW	IMPERMEABLE
		50	1.1	$7.93 \times 10^{-5}$
		75	1.6	$7.56 \times 10^{-5}$
		100	5.7	$2.00 \times 10^{-4}$
		75	2.4	$1.13 \times 10^{-4}$
		50	1.4	$1.02 \times 10^{-4}$
B-3B	8.0-54.6	75	.01	$1.52 \times 10^{-5}$
		25	13.0	$1.06 \times 10^{-4}$
		50	18.0	$1.04 \times 10^{-4}$
		75	18.25	$1.02 \times 10^{-4}$
		80	17.75	$1.01 \times 10^{-4}$
		30	12.0	$2.50 \times 10^{-4}$

(continued)

Table B-1 (continued)

<u>BORING NO.</u>	<u>TEST INTERVAL (FT)</u>	<u>WATER PRESSURE, psi</u>	<u>MEASURED FLOW, gpm</u>	<u>CALCULATED PERMEABILITY k, cm/sec</u>	
B-4	17-50	80	0.24	$2.02 \times 10^{-5}$	
		95	0.32	$2.05 \times 10^{-6}$	
	10-50	80	0.41	$2.07 \times 10^{-6}$	
		100	0.27	$1.04 \times 10^{-6}$	
B-6	7.5-12.5	50	NO FLOW	IMPERMEABLE	
	12.5-17.5	100	12.5	$4.0 \times 10^{-4}$	
	17.5-47.5	50	NO FLOW	IMPERMEABLE	
		100	NO FLOW	IMPERMEABLE	
B-6A	5-15 SINGLE PACKER	25	2.9	$1.97 \times 10^{-4}$	
		50	8.2	$3.05 \times 10^{-4}$	
		25	8.0	$5.43 \times 10^{-4}$	
	15-25	25	.24	$1.58 \times 10^{-5}$	
		50	6.4	$2.34 \times 10^{-4}$	
		50	6.6	$2.41 \times 10^{-4}$	
		25	.18	$1.19 \times 10^{-5}$	
		25-35	25	2.1	$1.39 \times 10^{-4}$
			50	4.4	$1.61 \times 10^{-4}$
	75		6.9	$1.75 \times 10^{-4}$	
	50		4.4	$1.61 \times 10^{-4}$	
	35-45	25	1.7	$1.12 \times 10^{-4}$	
		25	NO FLOW	IMPERMEABLE	
		50	.2	$7.32 \times 10^{-6}$	
		75	.2	$5.06 \times 10^{-6}$	
		50	.2	$7.32 \times 10^{-6}$	
		25	.02	$1.32 \times 10^{-6}$	
	45-55	25	NO FLOW	IMPERMEABLE	
		50	NO FLOW	IMPERMEABLE	
		75	NO FLOW	IMPERMEABLE	
		50	NO FLOW	IMPERMEABLE	
		25	NO FLOW	IMPERMEABLE	
		25	NO FLOW	IMPERMEABLE	
	55-65	25	NO FLOW	IMPERMEABLE	
		50	NO FLOW	IMPERMEABLE	
		75	NO FLOW	IMPERMEABLE	
		50	NO FLOW	IMPERMEABLE	
		25	NO FLOW	IMPERMEABLE	
		25	NO FLOW	IMPERMEABLE	
	65-75	25	NO FLOW	IMPERMEABLE	
		50	.1	$3.66 \times 10^{-6}$	
		50	NO FLOW	IMPERMEABLE	
		25	NO FLOW	IMPERMEABLE	
		25	NO FLOW	IMPERMEABLE	
		50	NO FLOW	IMPERMEABLE	
	75-85	25	NO FLOW	IMPERMEABLE	
		50	NO FLOW	IMPERMEABLE	
		75	NO FLOW	IMPERMEABLE	
		50	NO FLOW	IMPERMEABLE	
		25	NO FLOW	IMPERMEABLE	
		25	NO FLOW	IMPERMEABLE	
	85-100	25	NO FLOW	IMPERMEABLE	
50		NO FLOW	IMPERMEABLE		
50		NO FLOW	IMPERMEABLE		
25		NO FLOW	IMPERMEABLE		
89.2-100		25	NO FLOW	IMPERMEABLE	
		50	.1	$3.47 \times 10^{-7}$	
	75	1.1	$2.64 \times 10^{-5}$		
	50	NO FLOW	IMPERMEABLE		
25	NO FLOW	IMPERMEABLE			
B-9	8-40	55	2.0	$2.9 \times 10^{-5}$	
B-10	9-48.6	25	11.4	$2.4 \times 10^{-4}$	
		50	16.8	$2.0 \times 10^{-4}$	

(continued)

Table B-1 (continued)

<u>BORING NO.</u>	<u>TEST INTERVAL (FT)</u>	<u>WATER PRESSURE, psi</u>	<u>MEASURED FLOW, gpm</u>	<u>CALCULATED PERMEABILITY k, cm/sec</u>
B-11	9.8-50	25	NO FLOW	IMPERMEABLE
		40	NO FLOW	IMPERMEABLE
		25	NO FLOW	IMPERMEABLE
B-12	8-30	34	12.15	$6.2 \times 10^{-4}$
		46	16.0	$5.2 \times 10^{-4}$
		28	4.0	$2.9 \times 10^{-4}$
B-13	20.0-99.9	0	10.5	WATER LOSS
B-14	12.8-17.8	20	4.9	$5.4 \times 10^{-4}$
		40	11.65	$7.8 \times 10^{-4}$
		20	6.0	$6.6 \times 10^{-4}$
	17.8-22.8	20	12.25	$1.3 \times 10^{-3}$
		26	8.0	$6.6 \times 10^{-4}$
	22.8-27.8	20	12.25	$1.2 \times 10^{-3}$
		29	14.5	$7.9 \times 10^{-3}$
	6.7-55.2	15	15.0	$3.4 \times 10^{-4}$
		30	18.0	$2.6 \times 10^{-4}$
		54	21.25	$1.9 \times 10^{-4}$
6.7-55.2	72	25.33	$1.8 \times 10^{-4}$	
	54	24.0	$2.1 \times 10^{-4}$	
	30	18.5	$2.6 \times 10^{-4}$	
B-16	20.0-100.0	70	1.3	$5.1 \times 10^{-6}$
B-16B	55.4-133.0	25	12.5	$1.54 \times 10^{-4}$
		50	15.0	$1.24 \times 10^{-4}$
		75	17.5	$1.09 \times 10^{-4}$
		50	15.0	$1.24 \times 10^{-4}$
		25	10.0	$1.23 \times 10^{-4}$
	11.7-133.0	25	18.0	$1.48 \times 10^{-4}$
		50	24.5	$1.35 \times 10^{-4}$
		25	18.0	$1.48 \times 10^{-4}$
B-17	14.3-50	25	15.0	$2.6 \times 10^{-4}$
		50	22.0	$2.4 \times 10^{-4}$
		60	24.0	$2.3 \times 10^{-4}$
		50	21.0	$2.3 \times 10^{-4}$
		25	13.0	$2.2 \times 10^{-4}$

From SEA, 1989  
 ARTHUR LAKES LIBRARY  
 COLORADO SCHOOL OF MINES  
 GOLDEN, CO 80401

Table B-2

## Test-Grout Program Pressure Test Results

Hole	Packer Depth Feet	Hydraulic Conductivity	
		Feet/Minute (x10-5)	Centimeter/Second (x10-5)
P1	10	33.22	16.87576
	30	11.84	6.01472
	50	3.305	1.67894
	100	1.521	0.772668
	150	0.2656	0.1349248
S1	20	17.75	9.017
	30	0.664	0.337312
	40	0.638	0.324104
P2	10	21.91	11.13028
	10	22.59	11.47572
	20	15.35	7.7978
	30	9.233	4.690364
	50	0.6785	0.344678
	100	0.2925	0.14859
	150	0.1992	0.1011936
P3	20	17.56	8.92048
	50	14.96	7.59968
	80	9.792	4.974336
	100	2.047	1.039876
	150	1.128	0.573024
S3	50	1.394	0.708152
	100	1.141	0.579628
P4	20	59.32	30.13456
	30	22.02	11.18616
	50	7.512	3.816096
	100	4.797	2.436876
	150	4.514	2.293112
S4	10-30	21.22	10.77976
	30-50	117.45	59.6646
	50-70	82.4	41.8592
	70-90	1.946	0.988568
	90-110	0.9216	0.4681728
	110-130	0.6437	0.3269996

(continued)

Table B-2 (continued)

	130	0.6919	0.3514852
S5	30	42.5	21.59
	50	26.22	13.31976
	100	9.878	5.018024
	150	13.1	6.6548
	200	16.12	8.18896
T6A	10-30	92.61	47.04588
	30-50	82.98	42.15384
	50-70	77.06	39.14648
	70-90	179.6	91.2368
	130	23.23	11.80084
T6B	10-30	195.8	99.4664
	30-50	52.53	26.68524
	50-70	10.6	5.3848
S2	20	9.029	4.586732
	30	3.541	1.798828
	40	3.619	1.838452
	50	1.952	0.991616
P4	20	8.846	4.493768
	30	4.735	2.40538
	40	18.28	9.28624
	50	1.052	0.534416
	100	0.81895	0.4160266
	150	0.6639	0.3372612
T4B	10-30	95.51	48.51908
	30-50	54.81	27.84348
	50-70	52.53	26.68524
	70-90	35.8	18.1864
	130-150	1.108	0.562864
	150-170	1.924	0.977392
	170-190	0.8583	0.4360164
	190-210	1.085	0.55118
	210-230	4.388	2.229104
P5	30-50	0.7613	0.3867404
	50-70	76.04	38.62832
	90-110	7.373	3.745484
T5B	10-30	52.06	26.44648
	30-50	202.1	102.6668

(continued)



Table B-2 (continued)

	50-70	67.76	34.42208
	70-90	92.64	47.06112
	90-110	69.82	35.46856
	110-130	64.37	32.69996
	130-150	32.12	16.31696
	150-170	25.1	12.7508
	160-180	4.952	2.515616
P6	30-50	59.38	30.16504
	50-70	37.08	18.83664
	80-100	114	57.912
	100-120	85.29	43.32732
	120-140	134.2	68.1736
P7	10-30	628.1	319.0748
	30-50	>295.1	>149.9
	50-70	150	76.2

Note: Does not include intervals which failed to pressurize.

(From SEA, 1989)

**APPENDIX C**  
**INPUT FILES FOR NUMERICAL MODELS**

Electronic copies of the files listed below are included in the cover pocket. The program Pkzip.exe was used to compress the data. Pkunzip.exe is included with the electronic files for use in decompressing the files.

- I: MODFLOW input and output files for the pre-grout simulation of Test-Grout Program Model include input files testpre.bas, testpre.bcf, testpre.sip, testpre.oc, the output file testpre.out, and the Modelcad grid file testpre.grd. These files have been compressed into one file, testpre.zip. The postgrout and reservoir scenario files are the same as those listed for the pregrout scenario and have been compressed into testpst.zip and testres.zip respectively.

Note: Testres.bcf is the file used to simulate various hydraulic conductivities of the grout curtain. Rows 32 and 33, Column 10, Rows 31 and 32, Column 13, and Rows 25 through 29, Column 9 represent the grout curtains of Carbonates A, B, and C respectively. Rwell.map is the base map used with the preprocessor, Modelcad, and is included here as Rwell1.zip. A 1989 version of MODFLOW was used to execute these runs.

- II. MODFLOW input and output files for simulation of the Reservoir-Wide Models:

Simulations of Pregrout, Postgrout, and the Reservoir at elevations 1275-, 1350-, and 1410-foot elevations are presented as Pregrout.zip, Postgrt.zip, Res1275.zip, Res1350.zip, and Res1410.zip respectively. All simulations include the same input and output files as those listed below for the Pregrout simulation. The MODFLOW/EM version (Maximal Engineering Software, Inc.) was used.

Input files pregrout.bas, pregrout.bcf, pregrout.ghb, pregrout.sip, pregrout.hfb, pregrout.rch, pregrout.drn, pregrout.riv, pregrout.oc, pregrout (batch file), and output files pregrout.out, pregrout.bin (binary heads), prel1.dat (Layer 1 heads), prel2.dat (Layer 2 heads), pregrout.cbc (cell-by-cell fluxes), prech.dat (constant head fluxes), prerf.dat (right-face cell fluxes), and preff.dat (front-face cell fluxes). The Modelcad input file, pregrout.grd, and the Modelcad binary head, target and calibration-statistics files (pregrout.hds, pregrout.trg and pregrt.cal) are also included in the zip file. Rwell.map, the base map used with Modelcad is included as Rwell2.zip.

**APPENDIX D**  
**HYDROGRAPHS OF SELECTED WELLS**

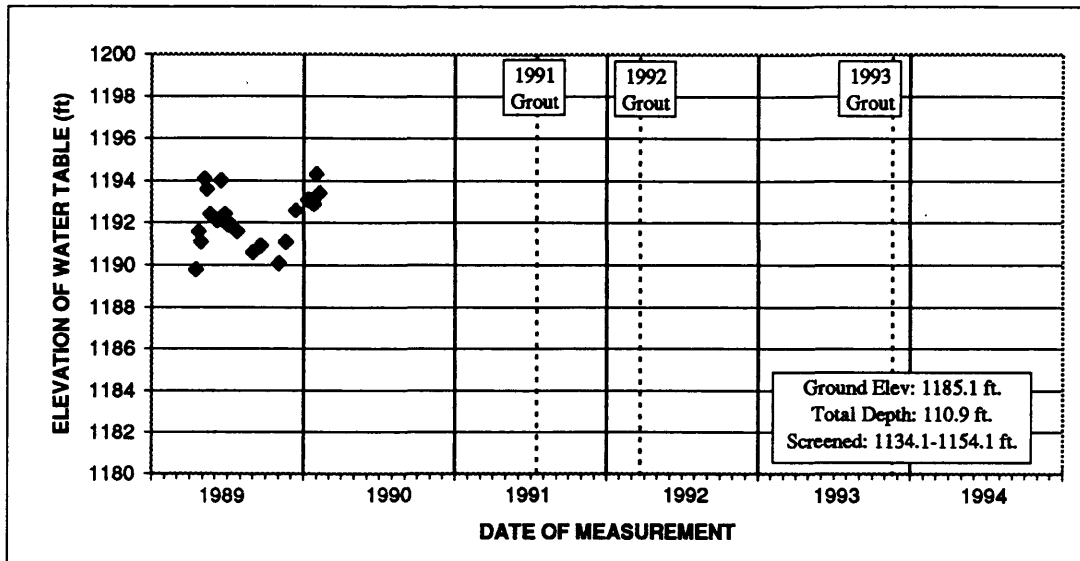


Figure D-1  
Hydrograph of Well B1

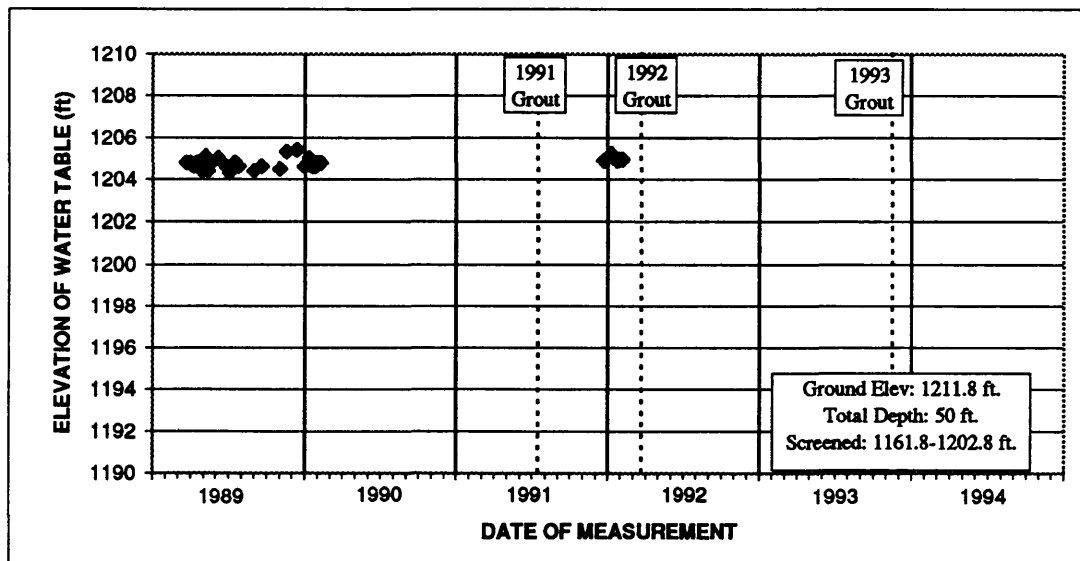


Figure D-2  
Hydrograph of Well B4

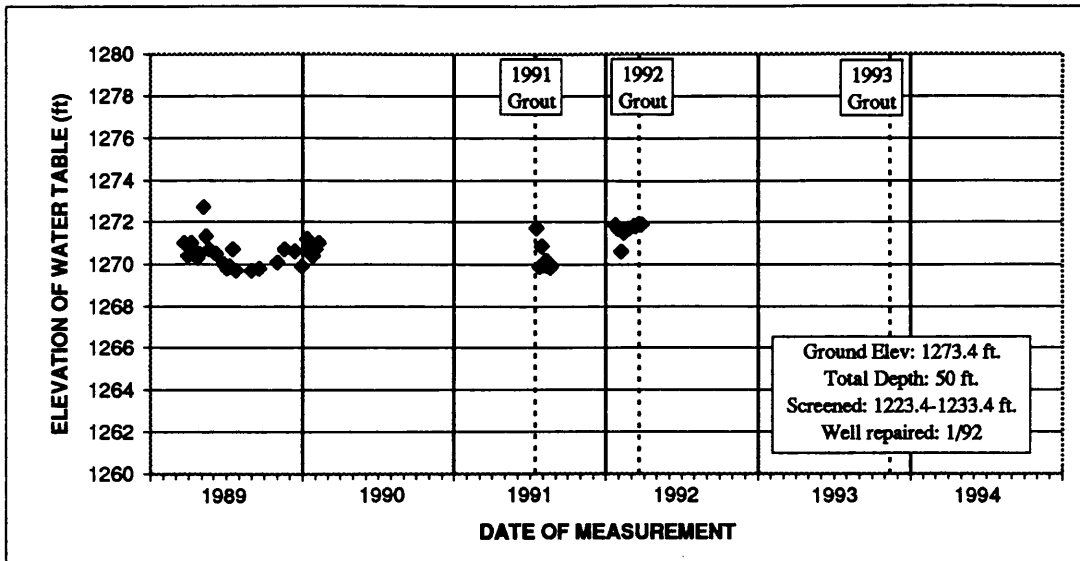


Figure D-3  
 Hydrograph of Well B6

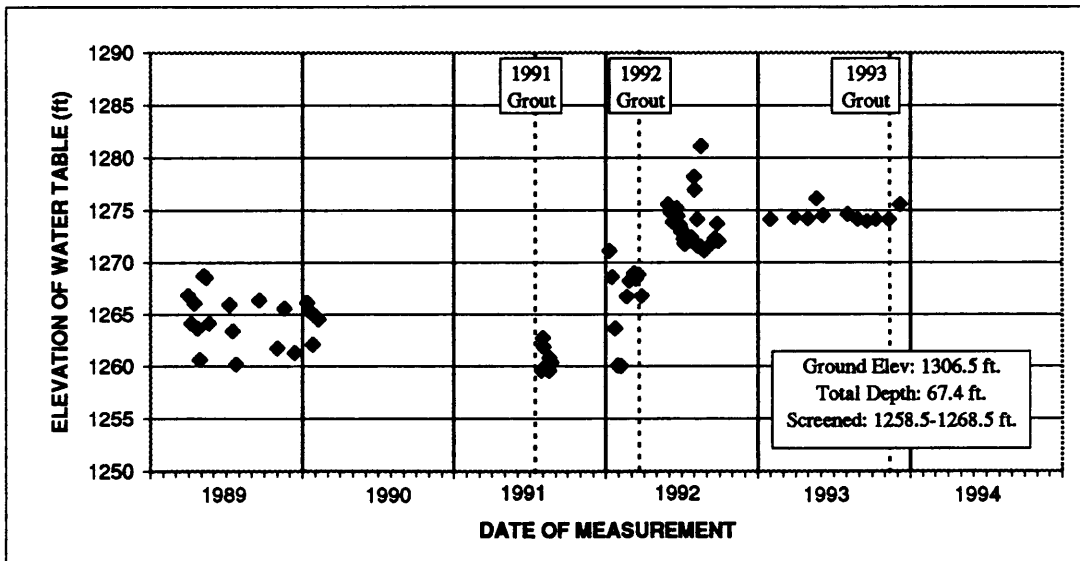


Figure D-4  
 Hydrograph of Well B9

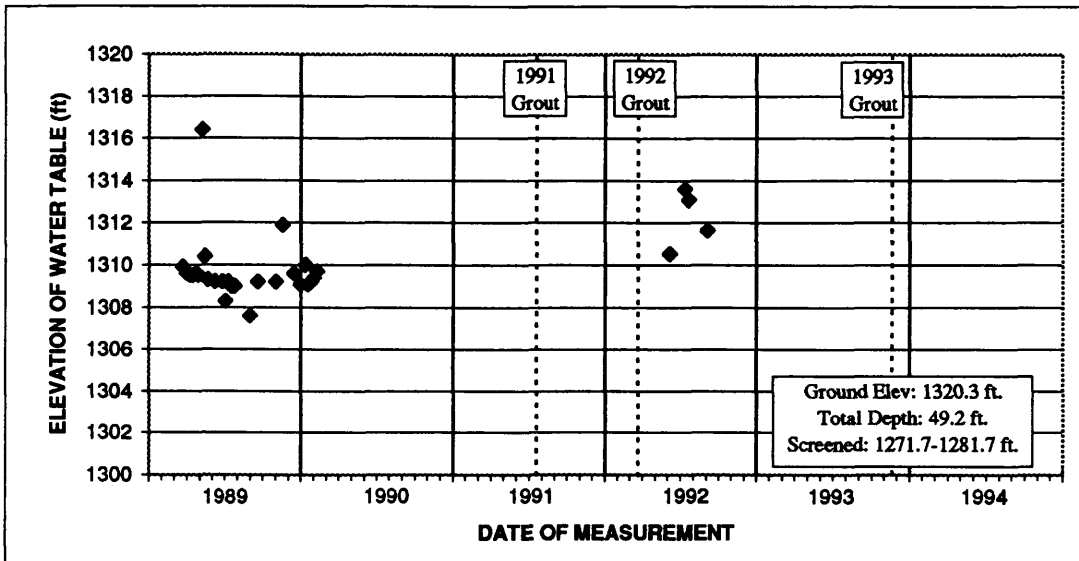


Figure D-5  
Hydrograph of Well B10

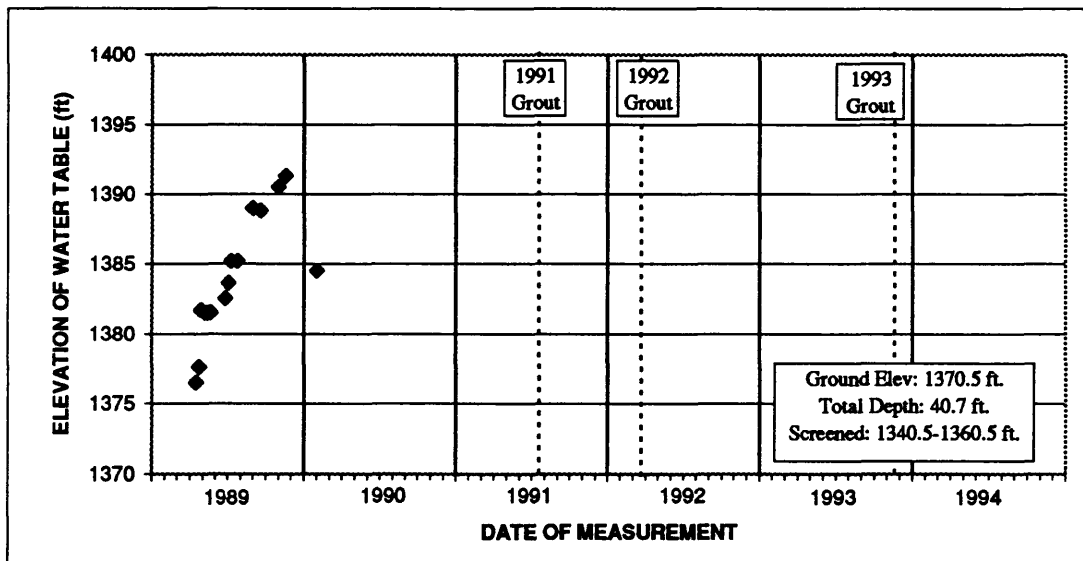


Figure D-6  
Hydrograph of Well B12

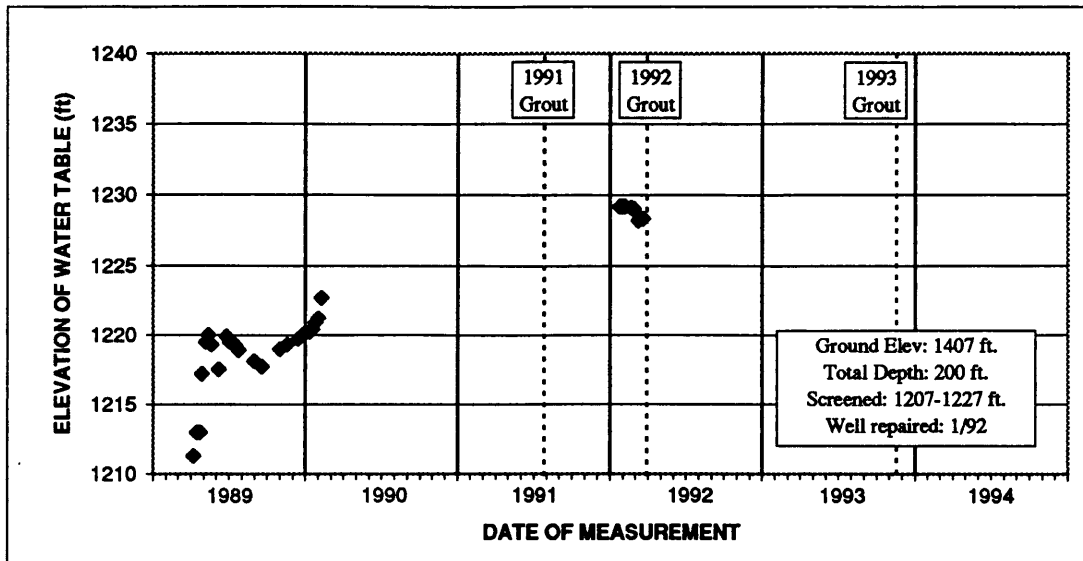


Figure D-7  
Hydrograph of Well B14A

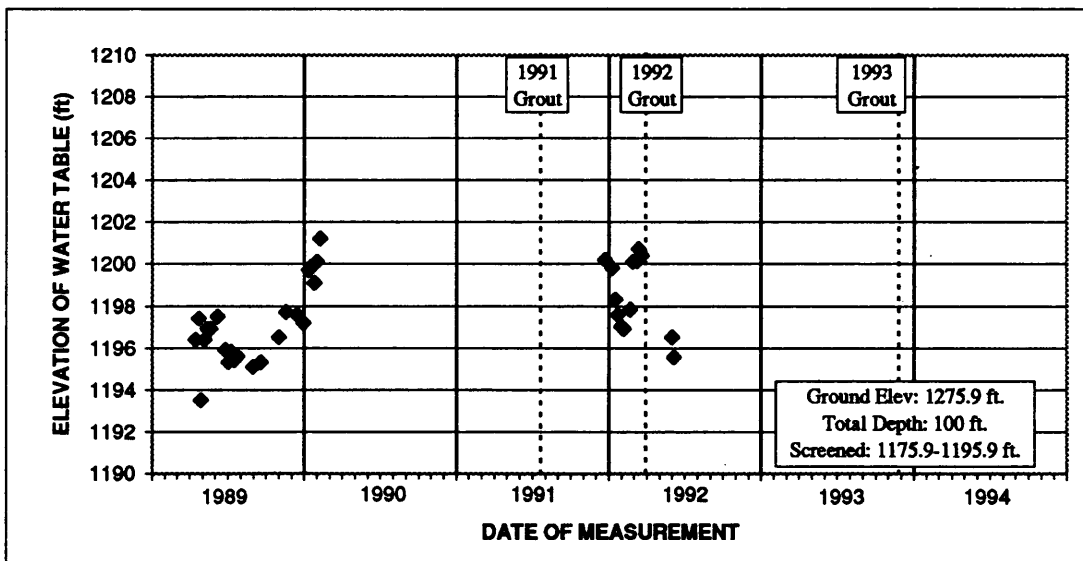


Figure D-8  
Hydrograph of Well B16D



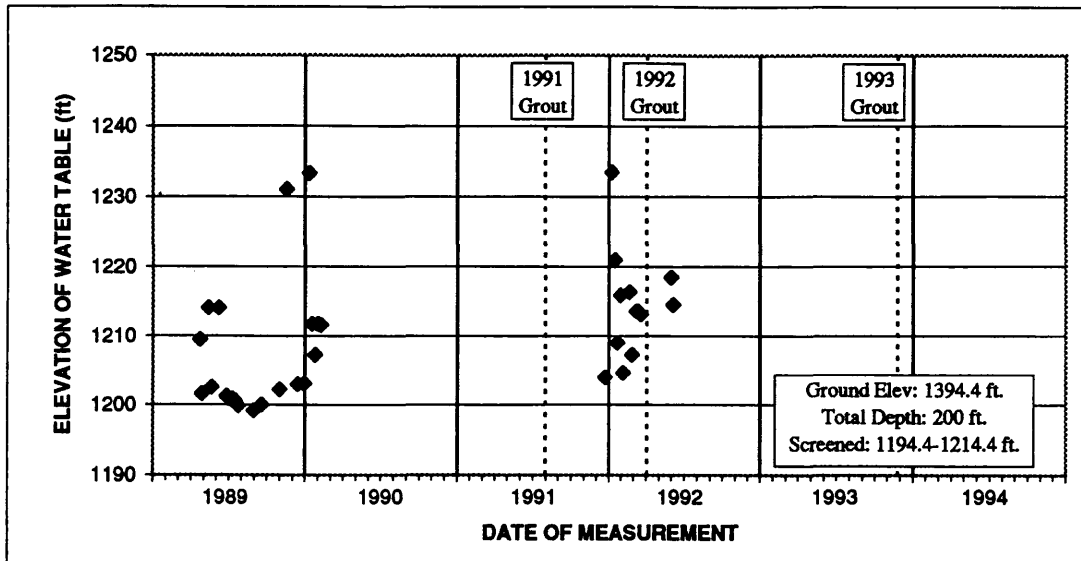


Figure D-9  
Hydrograph of Well B17A

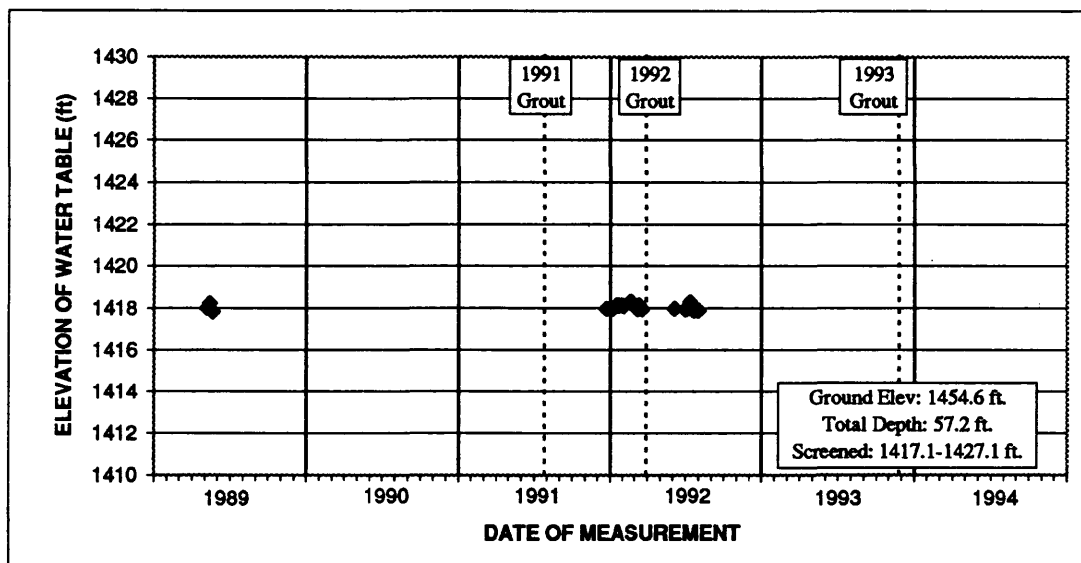


Figure D-10  
Hydrograph of Well B18

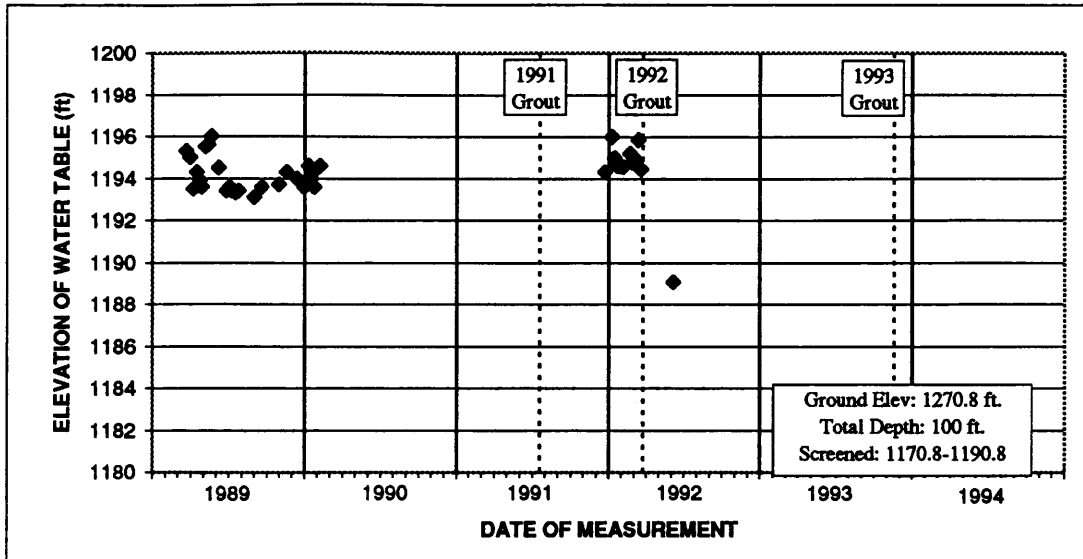


Figure D-11  
Hydrograph of Well B19

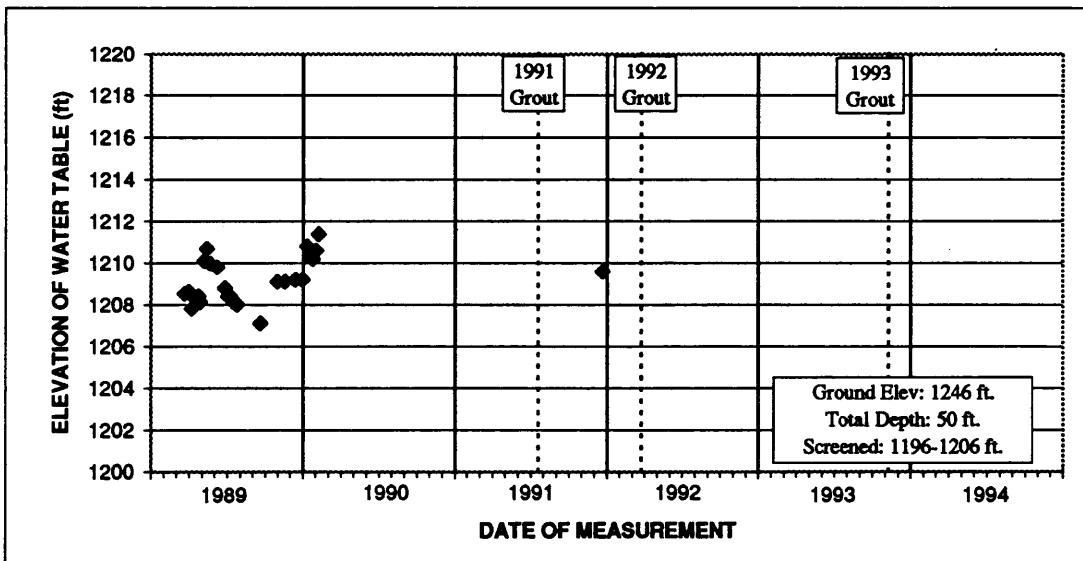


Figure D-12  
Hydrograph of Well Q1

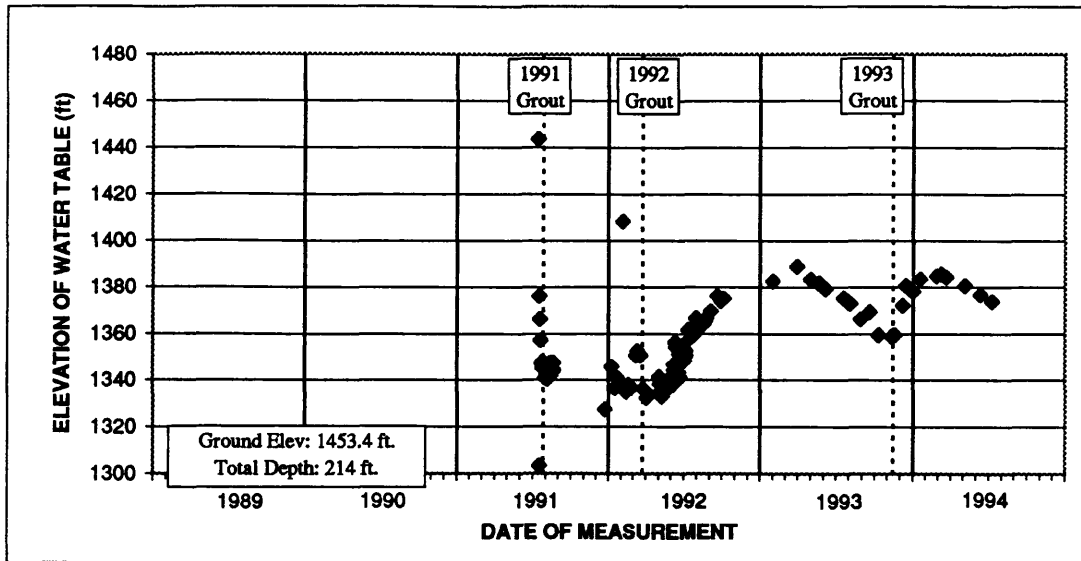


Figure D-13  
Hydrograph of Well G2

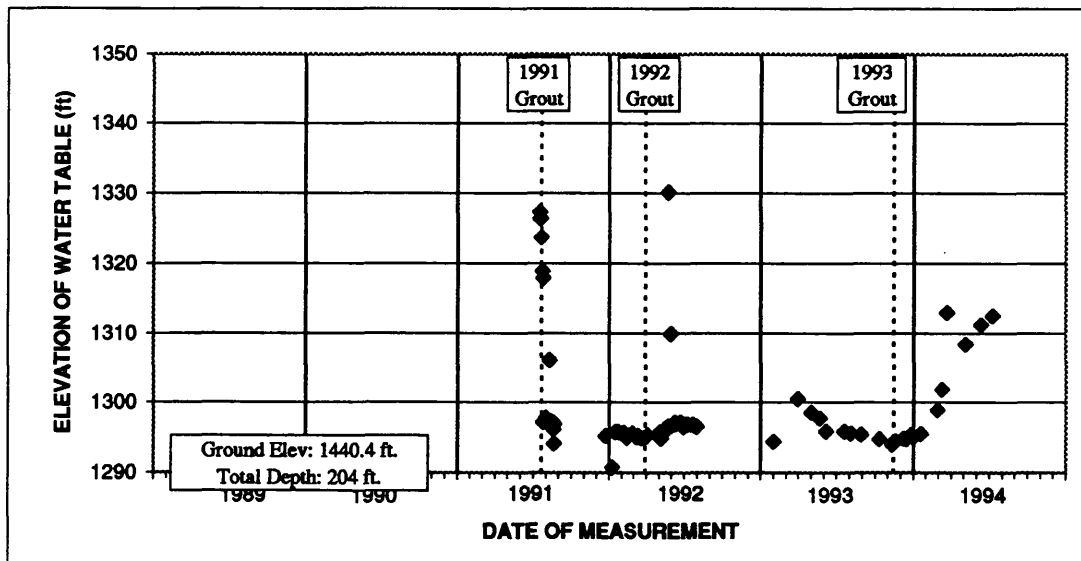


Figure D-14  
Hydrograph of Well G3

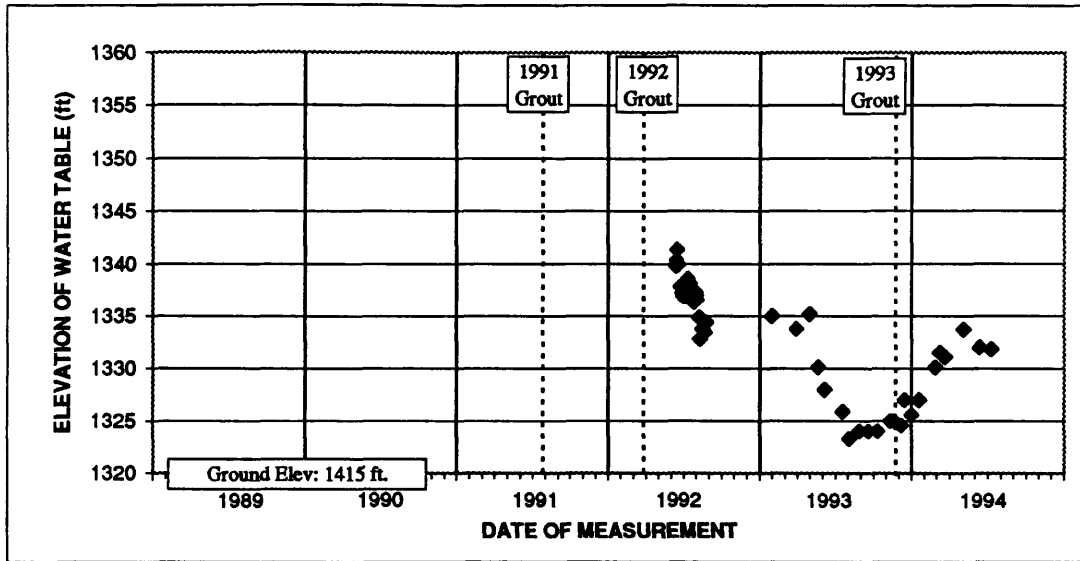


Figure D-15  
Hydrograph of Well G8

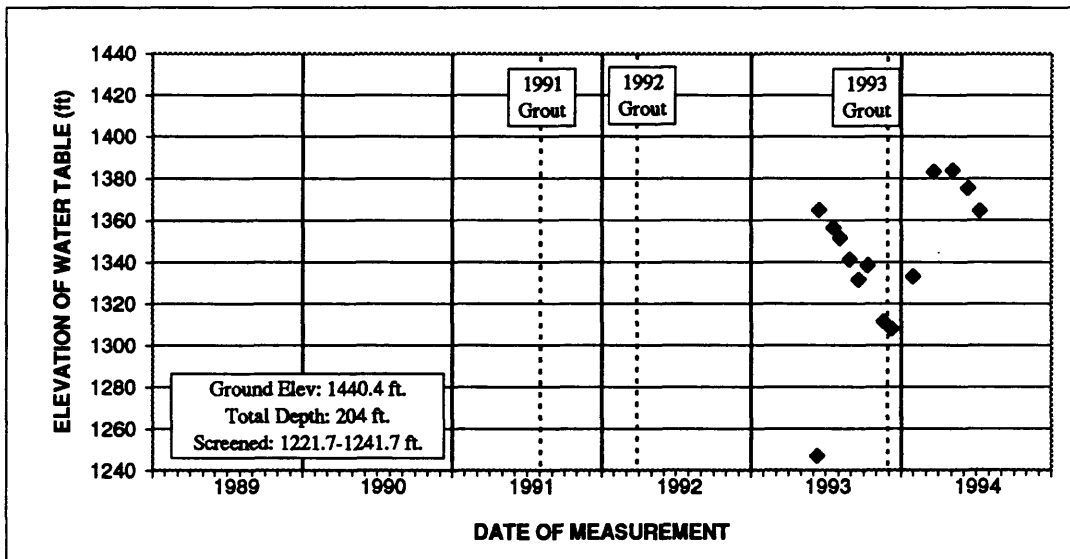


Figure D-16  
Hydrograph of Well P1

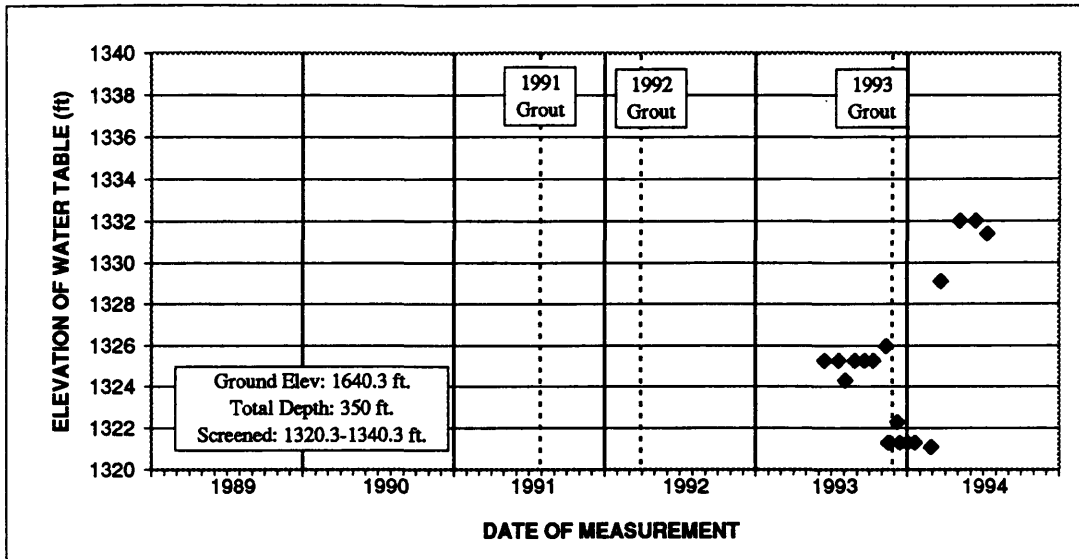
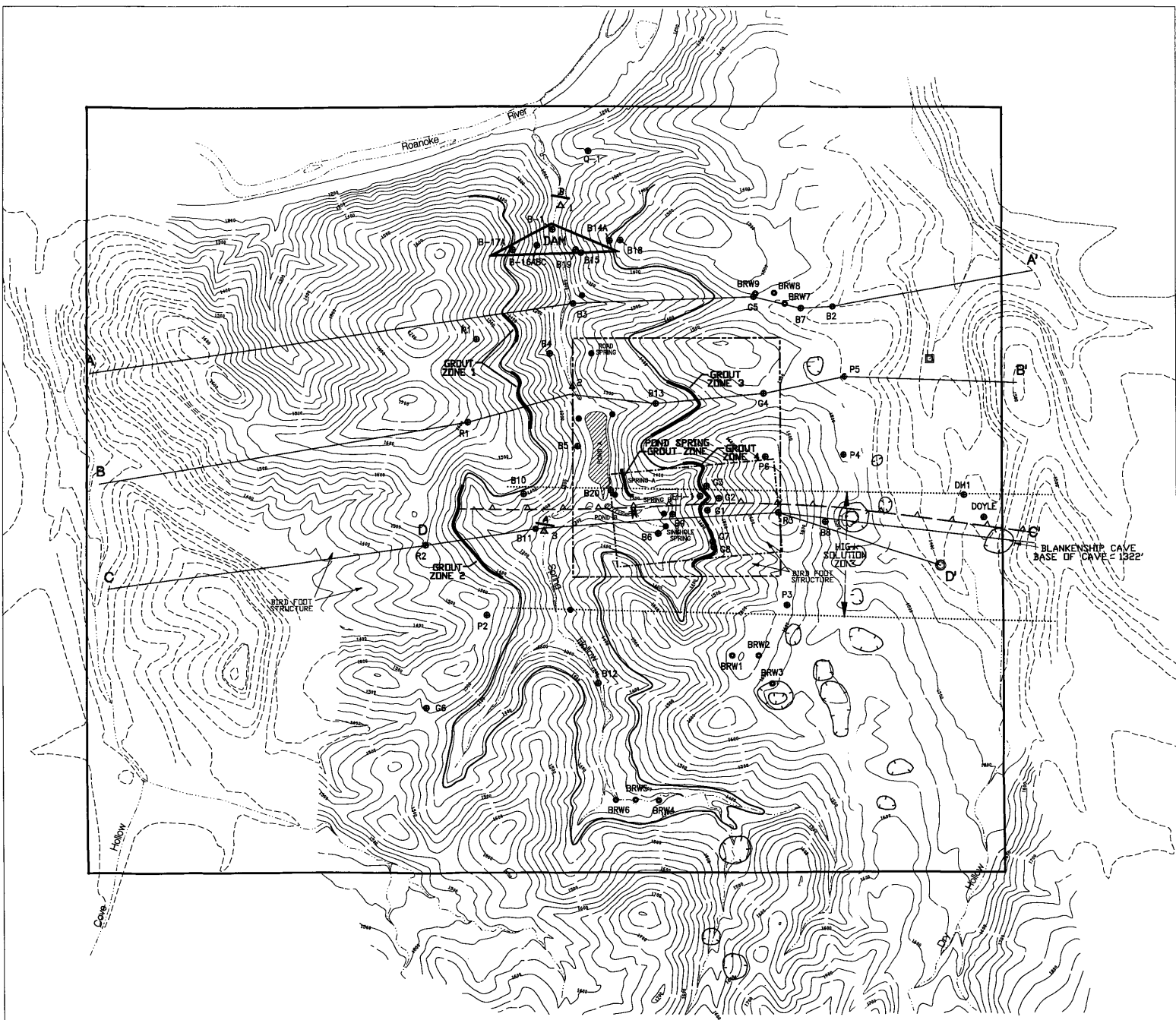


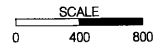
Figure D-17  
Hydrograph of Well P6



- Spring
- B6 ● Monitoring well
- Boring
- BRW5
- △<sub>1</sub> Stream flow station SEA, 1988
- Sinking point at 1405'
- Emergence point at 1340'

- ▲—▲— Thrust fault
- ⎵ Grout curtain
- Section line
- Sinkhole
- ⎵ Weir B
- ⎵ Flume

- - - - - Model area of numerical estimate of seepage
- - - - - Model area of test grout program
- Perimeter of reservoir at elevation 1410'
- Ground surface contour line (SEA, 1992)
- - - - - Ground surface contour line (USGS, 1979)
- Area of Reservoir-Wide Model



**PLATE 1**  
**FEATURES MAP OF RESEARCH**  
**SITE, SPRING HOLLOW DAM**  
**AND RESERVOIR**

036800 426033